ORE GENESIS OF PGE MINERALIZATION IN THE SUKINDA CHROMITE DEPOSIT, ORISSA, INDIA

A THESIS

Submitted in partial fulfilment of the requirements for the award of the degree

of

DOCTOR OF PHILOSOPHY

in

EARTH SCIENCES

by

DEBADUTTA MOHANTY

DEPARTMENT OF EARTH SCIENCES
INDIAN INSTITUTE OF TECHNOLOGY ROORKEE
ROORKEE-247 667 (INDIA)

JUNE, 2007

INDIAN INSTITUTE OF TECHNOLOGY ROORKEE

ROORKEE

CANDIDATE'S DECLARATION

I hereby certify that the work which is being presented in the thesis entitled **ORE GENESIS OF PGE MINERALIZATION IN THE SUKINDA CHROMITE DEPOSIT, ORISSA, INDIA** in partial fulfilment of the requirements for the award of the degree of Doctor of Philosophy and submitted in the Department of Earth Sciences, Indian Institute of Technology Roorkee, Roorkee, is an authentic record of my own work carried out during a period from July 2003 to June 2007 under the supervision of Dr. A. K. Sen, Associate Professor, Department of Earth Sciences, Indian Institute of Technology Roorkee, Roorkee.

The matter in this thesis has not been submitted by me for the award of any other degree of this or any other Institute.

(DEBADUTTA MOHANTY)

This is to certify that the above statement made by the candidate is correct to the best of my knowledge.

(A. K. Sen)
Associate Professor

Date: 17.06.2007

The Ph.D. Viva Voce Examination of **Mr. DEBADUTTA MOHANTY**, Research Scholar, has been held on _____

Signature of Supervisor

Signature of External Examiner

ABSTRACT

Platinum Group of Elements *(PGE)*, Os, Ir, Ru, Pt, Pd and Rh, along with gold (Au) and silver (Ag) are collectively known as *noble/precious* metals sub-grouped into: i. IPGE (Os, Ir, Ru) and PPGE (Rh, Pt, Pd). PGE behaves as a coherent group of siderophiles but behaves as chalcophiles under upper mantle and crustal conditions of fS_2. PGE occur in nature as *native state*, *alloys* (with other members of the group and/or with base metals) or as *discrete mineral* phases *i.e., Platinum Group Minerals (PGM)* of sulfides, sulfo-arsenides, arsenides, oxides and silicates.

Economic concentrations of PGE mainly occur in association with two major kinds of deposits *i.e.* Layered Ultramafic Complexes and Base Metal Sulfide (BMS) deposits. Former is further subdivided as *'Reef'* type (*e.g.* Merensky reef, Bushveld complex) deposits and PGE mineralization associated with *chromitites* (*e.g.* UG-2 chromitite, Bushveld complex).

Unlike PGE mineralizations associated with sulfide deposits, those associated with chromite deposits especially with the layered complex are confined to specific stratigraphic horizons with remarkable persistent in tenor and thickness and are economically attractive. Owing to the anomalous concentrations of PGE in chromites and associated mafic/ultramafics, different ophiolitic complexes are also worked out by researchers for their PGE potentialities. But ophiolitic complexes are found to be discouraging for

economic exploitation of PGE because of smaller size and erratic orientation of the host chromite lenses and, the lower whole rock concentration of total PGE with a dominance of IPGE those are relatively more difficult to beneficiate.

Prerequisites for the **formation of PGE** deposits are: i. a melt enriched in terms of PGE compared to the mantle source to give rise to PGE deposits and requires their partitioning to the melt by suitable carrier phases *i.e.*, sulfides; ii. Ascend of the magma essentially in a S-undersaturated condition to avoid loss of PGE through precipitation before its subsequent emplacement at crustal level; Segregation of an immiscible liquid by S-saturation and subsequent partitioning of PGEs to this liquid, to give rise to mineralization of economic importance. Different modes of origin for PGE deposits like magmatic, high temperature late magmatic and low temperature hydrothermal deposits in association with varied lithofacies are evoked by various workers for different deposits from different parts of the Globe.

The overwhelming importance of chromite associated PGE deposits as the major contributor to the world's total PGE production attracted the author's attention to work on PGE mineralization associated with the chromite deposits of ***Sukinda Ultramafic Complex (SUC)*, Orissa, India**. Such an idea has real aided motivation from recent discoveries of few PGE deposits of India, especially that of *Baula-Nausahi complex* which is in close *spatial-temporal* relation with SUC. Although, the major contribution of chromite production is shared by SUC, the area had not been taken up in detail for the PGE mineralization and its pattern, if there is any.

Moreover, the chromite associated PGE deposits are long believed to be formed by the similar *process* as that of the chromites. Chromites are one of the best *petrogenetic indicators* that keep record of the magmatic history. The genetic aspect of SUC has long been a controversial topic amongst the geoscientist and there are broadly two schools of thought: i. stratiform type deposit associated with *layered ultramafic complexes* and ii. Podiform type deposit associated with *ophiolitic complexes*.

With these considerations and in the virtual absence of any other primary phases excepting few relict olivines, the **objective** of the work mainly concentrated around study the primary PGE mineralization pattern in the light of Cr-spinel composition and sulfide phase composition, and their relation to their geotectonic set up of SUC.

The SUC extends from *Tomka* (*85°55'E: 21°7'N*) in the east to *Kathpal* (*85°41'E: 21°1'N*) on the west spreading over an area of 40 sq. km in NE-SW direction in Jajpur and Dhenkanal districts of Orissa. The regional **structure** is broadly a westerly plunging syncline with easterly closure. Field evidences support the idea of a pre-tectonic emplacement of SUC with respect to Iron ore orogeny, and is intrusive into and co-folded with the quartzites of *Iron Ore Group (IOG)*.

The two generations of **ultramafics** of SUC are: i. *older* chromitite hosting altered dunitic-peridotites, and ii. *younger* orthopyroxenites devoid of chromitites. On the basis of physical character, structure and proportion of gangue, the chromite ores of Sukinda Valley may be classified as massive, banded, laminated varieties. Based on the level of alteration two different varieties of **chromitites** are identified: i. *grey* ores (hosted in serpentinites)

and, ii. *brown* ores (hosted in limonites). The grey ores forms the main attraction for the present work as it relies largely on the primary phase relations, and least affected by the alteration, the Cr-spinels from these ores can provide the best possible approximation to the primary magmatic conditions. Grey ores are found mainly in two areas: i. Kathpal chromitites **(Zone-1)** virtually detached from main SUC defines a highly brecciated zone similar in disposition and intensity of deformation to that of the Bangur breccias of Boula complex, and ii. Kalarangitta chromitite **(Zone-2)** of main SUC presenting the *Band-I* of *six* regional bands reported. Systematic sampling of different varieties of grey ores and associated serpentinized host rock along individual sections of the two zones for detail study.

Host rocks show dominance of serpentine psuedomorphs after olivine and/or pyroxene with meshwork, ribbon type and bladed mat textures in the petrographic study. Fibrous serpentines *i.e.* crysotiles indicative of shearing are also found. Qualitative mineralogical study of the host rock using XRD (IIT Roorkee) confirms the major phases observed microscopically. Trace elements concentrations are determined using ICP-MS in combination with acid digest technique (NGRI, Hyderabad). The Primitive Mantle (PM) normalized trace elements spider plots shows almost near mantle values with slight enrichment of LILE which may be attributed to mobilisation of these elements during serpentinization. The PM normalized plot of transition elements reveals that the serpentinites are enriched in Cr indicating anomalously high Cr concentration of the source magma and/or possible role of chromite crystallization consequent upon increase in fO_2. Secondary phases like haematite and goethite are also observed.

Chromite proportion varies from <5% in host rocks to as high as 90% in massive chromitite with a dominant cumulus texture. Cr-spinel composition has been determined by EPMA (IIT Roorkee). The chromites show a general high Cr# and Mg# with low TiO_2-content. The variation in the range of these ratios are dependent on the subsolidus redistribution of Mg^{2+} and Fe^{2+} between olivine and Cr-spinel, and depends upon their relative proportion. Hence the primitive composition of the parent magma can best be commented on the basis of Cr-spinel composition of the chromitite. Cr# and Mg# range of the Cr-spinels of chromitite varies between 0.71-0.79 and 0.62-0.81 respectively indicating a high-Mg parentage formed from high degree of partial melting of the mantle and support the trace element signatures. The the relict olivines are also highly Mg-rich (~ Fo_{95}) is also indicate the same. Such a high degree partial melting may remove high amount of S from the mantle and one of the pre-requisite for the potential PGE mineralization.

Sulfides occur only in trace amounts not exceeding 1% by volume and are relatively higher with higher proportion of the silicates indicating a probably a decrease in a fO_2. The sulfides are analyzed by EPMA (IIT Roorkee) and SEM-EDS (IGEM Muscow) and are found to bedominated by Ni-rich magmatic varieties *e.g.* heazlewoodite and Ni-pentlandite, and altered to millerite *etc.* and mostly crystallized in magmatic crystallization sequence without seggragation.

The whole rock **PGE** analyses are done by NiS FA ICP-MS (NGRI, Hyderabad). The PGE and, Ni and Cu ratios indicate a mantle-like source similar to the trace element data. Although the total PGE concentration is subchondritic (28 to 311ppb) but shows enrichment of IPGE with respect to

the mantle like that of Cr. This is further in confirmation that the total PGE and IPGE values are high in the chromitites of respective to the host rocks of individual section and spotted ores and a possible fractionantion of IPGE during chromite crystallization. The dominance of IPGE is also observed from the rare micro nuggets of IPGE rich mineralogy as determined by SEM EDS (IGEM Muscow).

The low modal proportion of sulfides, high IPGE and IPGE-rich PGM mineralogy indicates that chromite crystallization of SUC has a pronounced bearing on the kind and pattern of PGE mineralization associated with it. As the answer to the S-rich fraction of original melt it is proposed that this is concentrated in residual melt which is probably responsible for the PGE mineralization of Bangur breccia zone of Boula-Nausahi complex on the basis of similar pattern but elevated REE-concentration compared to serpentized chromite bearing host ultramafics, and PPGE rich PGM mineralogy of Bangur gabbro and similarity in the breccia zone reported from SUC to that of Bangur. Accordingly a model based on ***plume concept*** is suggested for the chromite and PGE mineralization of *SUC* and *Boula-Nausahi* complex to best explain the *ophiolitic geochemical* affinity as well as *layered* nature of these intrusive of *Precambrian* age with bulk *peridotitic* composition.

ACKNOWLEDGEMENTS

It is my proud privilege to thank and acknowledge all those who have came forward to help me in so many ways to reach at the final outcome of this thesis.

I feel greatly obliged to **Dr. A. K. Sen**, my mentor and guide, always being supportive and considerate to me. His unfailing encouragement and inputs during the last stages of compilation of the work are deeply appreciated.

I would like to thank the Head of Department, **Prof. R. P. Gupta**, and former Head, **Prof. V. N. Singh,** for not only extending all the support and facilities during the course of this research work, but also for their personal well wishes for me.

I feel immensely grateful to **Dr. A. K. Saraf** and **Dr. V. C. Goyal** for their inspiration which helped me to shape my research carrier.

Council of Scientific and Industrial Research is gratefully acknowledged for the financial support to carry out the work in the form of CSIR-NET fellowship to me.

Present and former members of my *Student Research Council (SRC)* and *Departmental Research Council (DRC)*, **Dr. R. G. S. Shastry**, **Dr. S. Singh**, **Dr. S. Sarkar**, **Prof. Sri Niwas**, **Prof. P. K. Gupta**, **Prof.**

Manickavasagam and **Dr. G. J. Chakrapani** are duly acknowledged for their valuable suggestions during the course of the work.

My thanks are due to **Prof. O. P. Varma** (retd.) and **Dr. B. C. Sarkar** of ISM, Dhanbad; **Prof. S. K. Upadhyay** (retd.), **Prof. B. B. S. Singhal** (retd.), **Prof. D. C. Srivastava**, **Prof. D. K. Mukhopadhaya**, **Dr. (Mrs.) I. Sarkar** (now at MITS) and **Dr. R. Krishnamurthi** of IIT Roorkee; **Mr. Ashim Choudhury** of CIMFR, Dhanbad; and **Dr. Dilip Kanungo** of IBM, Nagpur for their constant encouragement, help and intense academic discussions.

Permissions by **Mr. A. Agarwal**, CMD, FACOR, respective mines Managers of the TISCO, M/S IMFA, M/S Jindal and M/S Misrilal to carry out field work are duly acknowledged. My special thanks to the field personnel, **Mr. K. C. Goswami** and **Mr. Biswajit Jena** of TISCO, **Mr. Pujari**, **Mr. Basu**, **Mr. Pal** and **Mr. Pramanik** of FACOR, Kathpal, Mr. **Reddy** of FACOR, Boula, **Mr. A. K. Singh** of OMC, Sukinda, **Mr. S. Nayak** of OMC, Bangur for providing logistic support to carry out fieldwork in and around the study areas.

The help and co-operation from **Prof. V. V. Distler** and his colleagues of IGEM, Russia for SEM-EDS analysis, **Dr. V. Balaram**, **Dr. (Mrs.) R. Mathur**, **Dr. T. G. Rao** and **Mr. Dasaram** of NGRI, Hyderabad for ICP-MS facility, **Dr. T. K. Ghosh** of IIC, IIT Roorkee for EPMA analysis, and **Mr. Ashish Misra** for remote sensing data processing are sincerely acknowledged.

Insightful discussions with **Dr. Pulok Mukerjee** and **Dr. N. S. Siddaiah** of WIHG, Dehradun on analytical techniques and with **Dr. J. K. Mohanty** of RRL, Bhubaneswar on the local geology helped in planning the work during its early stages.

My loving regards are due to **Dutta da** and **Pramod bhai** for making me dream of becoming a respectable geoscientist of our times.

Special thanks to **Ma'm** (Mrs. Sen) and young **Saswato** (Master Sen) who had spared Dr. Sen from their family hours especially in the final stage of the compilation of this work. They never let me forget the touch of the family and taste of home made delicious food when I use to stay off home for months together during the period of this work.

All the members... **Dr. Rajeev** (IITR), **Dr. Umesh** (USA), **Dr. Dua** (MU), **Gopi** (NHPC), **S. P. Singh** (ONGC), **Dr. Amit** (RITES), **Dr. Ashis** (DU), **Dr. Satvinder**, **Dr. Joshi** (IIP, Dehradun), **Dr. Sharif** (Bangladesh), **Dr. Pokharia** (BITS, Pilani)... of an ill defined group, in terms of batch, age, stream, is acknowledged here for sharing the happiness and sorrows on equal terms during my stay at Roorkee.

I am thankful to my lab-mates...**Dr. (Ms.) Swapnamita** (WIHG), **Partho da** (BHU) and **Aniket** (Switzerland)...they need a special mention for always being supportive and encouraging towards me.

People who always stood by me during the periods of inadvertant deep financial crunch, not only to support financially but also morally, are few of my near and dears...**Satya** (RIL), **Abhijit** (ONGC), **Dibyendu** (RIL), **Subhro** (RIL), **Arif** (AMU), **Saif** (AMU), **Manish** (IITR), **Gaurav** (IITR), **Nandita Ma'm** (CIMFR), **Manish Sir** (CIMFR) and **Babu Bhai** (CIMFR). A big 'Thank You' to all of them.

A special mention of ever inspiring friends like **Nikhilesh** (IFS, Egypt), **Ranjan** (Canada), **Himansu** (USA), **Jayant** (GSI), **Sree** (CGWB), **Devi** (USA), **Amiya** (BHU), **Kalyan** (GAIL), **Unni** (De' beers), **Shouvik** (GAIL),

Kalyan (GIL), **Saumya** (GSI), **Lekhraj** (IITR), **Rajesh** (IOCL), **Saroj** (CIMFR) and **Sanjib** (CIMFR) and many more for their moral support and encouragement during the times of my ebbing self-confidence.

Many of my little stars... **Puru**, **Sarav**, **Suman**, **Ranjan**, **Rakhee**, **Gaurav**, **Silu**, **Sumani**, **Atal**, **Pradeep**, **Mahesh**, **Sunil**, **Praveen**, **Biswa**, **Mahabir**, **Nishchal**, **Tusar**, **Rohit**, **Saraswat**, **Vivesh**, **Abinash**, **Bailochan**, **Krishna**, **Diku**, **Divya**, **Gaju**, **Ishwar, Kunal, Vivek** and **many others**...had always availed themselves to me as and when required. I am very much grateful to them.

The help extended by **Baburam ji, Sarvesh ji, Nair Ji, Ramkaran ji, Rahil ji** and all other technical and non-technical staff-members of Dept. of Earth Sciences, IIT Roorkee; and **Babuli** for field sample collection deserve a large amount of my gratitude for their help in various official and administrative matters.

Late in this sequence, late in life, but certainly at a crucial juncture 'She' (**Ishita**) came into my life *by chance* when I was in a sub-conscious need of someone truly special. Unaware of the scientific intricacies, she brought the most refreshing force and vitality to my strained mind in the moments of monotony, especially during the final stages of this work. I can best acknowledge her as the most beautiful and interesting happening of my life: She is really precious to me.

The words like *grateful* and *thankful* are too short to acknowledge **all my family members** who have promoted me like no other thing through-out my career.

I wish there was a separate page to aptly dedicate this work to the great souls, **My Parents**, rather than merely acknowledging them: *They mean everything to me in my life.*

There can be innumerable excuses for failures but only one ingredient to success – Determination with perseverance. What counted for most part of the work starting from identification of the problem, fieldwork, sample collection, preparation and analysis, data integration and interpretation and, finally compilation of the work is the passion, patience, hardship and intelligence blessed to me by the **Almighty**, for which no amount of thanks can ever suffice.

Thank you so much!

(Debadutta Mohanty)

CONTENTS

Figure No. **LIST OF FIGURES** **Page No.**

Table No. **LIST OF TABLES** **Page No.**

The discovery of the world's most precious metal, platinum in 16th century in Choco District of Columbia (McDonald 1960) was followed by subsequent 19th century discoveries of other *Platinum Group Elements (PGE) i.e.* palladium, rhodium, osmium and iridium with a gap of ~300 years, latest being ruthenium. PGE (Os, Ir, Ru, Pt, Pd & Rh) along with gold (Au) and silver (Ag) are collectively known as *noble/precious* metals. An inherent importance of these transition metals is accredited to the unique combination of their physical and chemical properties *i.e.,* high fusion temperature, high density, chemical inertness, low co-efficient of thermal expansion, efficient catalytic nature, high corrosion resistance, mechanical strength and malleability *etc.* These are further divided into two sub-groups based on their fusion temperature:

i. IPGE (Os, Ir, Ru): 'Refractory PGE' with a very high fusion point

ii. PPGE (Rh, Pt, Pd): 'Fusible PGE' with lower fusion point

In recent years, the evolution of sophisticated techniques to measure these ultra-trace elements and to recover them efficiently from natural matters, blended with growing global concern about the environmental pollution especially due to automotives, lead to many fold increase in consumption of PGE. These are used either in their pure form or as alloys mainly in *four* major sectors namely *jewelry*, *catalyst systems*, *industrial applications* and also as *investment*.

1.1 PGE AND THEIR GLOBAL OCCURRENCES

The PGE occurs in nature in *native state*, as alloys (with other members of the group and/or with base metals) or discrete mineral phases *i.e.*, *Platinum Group Minerals (PGM)* (Crocket 1981) of sulfides, sulfo-arsenides, arsenides, oxides and silicates. PGE concentration varies from *sub-ppb* level (in felsic and intermediate rocks) to 1-100ppb (in mafic and ultramafic rocks), in *terrestrial* conditions. Anomalous concentration of PGE, to designate an occurrence as an *economic* deposit, typically ranges *5-10ppm* with concentration factors in the order of one thousand. Most of the known PGE prospects are mostly confined to mafic/ultramafic rocks and classified on the basis of their association with the type of Ni-Cu sulfide mineralization patterns. Naldrett (1981) divided the whole range of PGE deposits broadly into two main categories:

i. Ultramafic rocks of layered complexes mined mainly for PGE and chromite (BMS as by-product) and, are further divided into two sub-groups as (Naldrett 1989)
   a. 'Reef' type deposits as weak disseminations of sulfides unlike massive BMS deposits, in silicate matrix, associated essentially with the *cyclic*

units of the layered mafic-ultramafic *e.g.* Merensky reef and Plat reef, Bushveld complex, RSA; J-M reef, Stillwater Complex, USA.

b. PGE mineralization associated with chromitites (50% to >95% cumulus chromite, Misra 1998) *e.g.* UG2 chromitite, Bushveld complex.

ii. Base metal sulfide deposits mainly mined for Ni-Cu (PGE as by-product) *e.g.* Noril'sk-Talnak, Russia and Thompson Nickel Belt, Canada.

A comprehensive and detailed classification of PGE mineralization has recently been published by Maier (2005).

Chromitite gained importance as potential targets for PGE exploration from 1908 with the discovery of their occurrence in Mineral range, Bushveld Complex, RSA. Afterwards, subtle attention has been paid to these prospects because of the subsequent discovery of *Merensky reef* (named after *Dr. Hans Merensky*), world's one of the biggest ever bonanza of PGE and limitations to beneficiate these elements from resistance phases like chromites. Reef deposits are thin layers of remarkable lateral persistency in tenor and thickness. Only after the discovery of UG2 chromitite, Bushveld complex as largest PGE resource of the globe and evolved metallurgical techniques (Cawthorn, 1999a) to extrat PGE from chromitites, the interest in chromitites as prospects of PGE has been revived. Layered ultramafic complex contribute 90% of the global PGE resource of which ~75% is locked up in the UG-2 chromitite layer, Merensky Reef and Plat Reef of Bushveld Complex, South Africa (Misra 1998).

Owing to the anomalous concentrations of PGE in chromites and associated mafic/ultramafics, different ophiolitic complexes are also worked out by researchers for their PGE potentialities (Greece: Agiorgitis & Wolf

1978, Augé 1985, Konstantopoulou & Economou 1991, Economous-Eliopoulos & Vacondios 1995; Cyprus: Constantinides *et al.* 1979, Talkington *et al.* 1984, Prichard & Lord 1990; Thetfort ophiolites, Quebec: Oschin & Crocket 1982; New Caledonia: Page *et al.* 1982a; Oman: Page *et al.* 1982b; Turkey: Page *et al.* 1984; Philippines: Bacuta *et al.* 1990). But ophiolitic complexes are found to be discouraging for economic exploitation of PGE because of smaller size (Prichard *et al.* 1981, Gunn 1989) and erratic orientation of the host chromite lenses and, the lower whole rock concentration of total PGE (Augé *et al.* 1995; Ahmed & Arai 2002) with a dominance of IPGE those are relatively more difficult to beneficiate. However, economic concentration of PGE may be expected especially in the lithounits those are associated with chromitites and high sulfide concentrations *e.g.* PGE byproduct from Ni-Cu sulfides associated with Zambles ophiolites (Crocket 1981; Pedersen *et al.* 1993). Economou-Eliopoulos (1996) from a comparative study of available PGE data on different ophilitic complexes have shown that such anomalously high concentration of Pt-Pd±Rh are mostly associated with sulfide rich ultramafics of upper mantle sequence and/or supra-Moho zones. Leblanc (1991) provided an excellent review on PGE potentiality of ophiolite sequences. It is apparent from the above discussion that virtually ultramafic complexes with chromite mineralization form the main/major source of global PGE.

Some other type of PGE deposits (Keays *and* Lightfoot 2000, Misra 1998) can best be exemplified by Munni Munni (Australia), River Valley and East Bull Lake intrusions (Canada) as wider zones of PGE sulfide enrichment

within mafic/ultramafic intrusions; Kambalda (Australia), Cape Smith fold belt (Canada) as stratiform lenses of massive to disseminated Ni-Cu (PGE) sulfides at the base of komatiitic flow units; Sudbury Igneous Complex (Canada) in association with the outer contact phase and the proximal country rocks; Mount Keith (Australia) as strata bound zones of disseminated Ni (Cu-PGE) sulfides within komatiitic rocks; Voisey's Bay (Canada) within feeder zones of magmatic system; within sub-volcanic sills which acted as feeders to continental mafic volcanic sequences.

1.2 CHROMITE ASSOCIATED PGE MINERALIZATIONS

Different modes of origin for PGE deposits like magmatic (Naldrett & Duke 1980, Campbell *et al.* 1983, Barnes & Naldrett 1985, Barnes & Maier 1999) to high temperature late magmatic (Vermaak 1976, Von Gruenewaldt 1979) to those of low temperature hydrothermal deposits in association with varied lithofacies (McCallum *et al.* 1976, Rowell & Edgar 1986, Pasava 1993, McDonald *et al.* 1995, Distler *et al.* 1998, Watkinson *et al.* 2002) are evoked by various workers for different deposits from different parts of the Globe. Genetic aspects of global PGE deposits were dealt in detail by various workers (Barnes *et al.* 1985, Naldrett & von Gruenewaldt 1989, Maier 2005).

PGE behaves as a coherent group of siderophiles but behaves as chalcophiles under upper mantle and crustal conditions of fS_2 (Barnes *et al.* 1985). PGE associated with ophiolitic deposits are dominated by IPGE mineralogy and that with layered ultramafic complexes by PPGE mineralogy. Unlike PGE mineralizations associated with sulfide deposits, those associated with chromite deposits especially with the layered complex are confined to

specific stratigraphic horizons with remarkable persistent in tenor and thickness and are economically attractive. In the context of the present study as well as their overwhelming dominance amongst the PGE deposits, a special emphasis on the later type of deposits is presented here.

The prerequisites for the formation of this kind of deposits are:

i. A melt enriched in terms of PGE compared to the mantle source to give rise to PGE deposits and requires their partitioning to the melt by suitable carrier phases *i.e.*, sulfides (Naldrett 1989, Barnes & Maier 1999). Removal of all the PGE from the mantle source is limited by the S-solubility of the melt and complete removal of these sulfides needs a higher degree of partial melting of the source mantle. Hence is the reason why most of the PGE deposits are associated with Mg-rich magmatic rocks.

ii. Ascend of the magma essentially in a S-undersaturated condition to avoid loss of PGE through precipitation before its subsequent emplacement at crustal level. However, lowering of pressure with the rise of the magma overrides cooling, thereby increasing the S-solubility (Wendlandt 1982, Mavrogenes & O'Neill 1999).

iii. Segregation of an immiscible liquid by S-saturation and subsequent partitioning of PGE to this liquid, to give rise to mineralization of economic importance.

During magmatic differentiation process, the S-bearing capacity (C_S) of basic magma depends on various parameters like temperature, pressure, composition of magma, fO_2, fS_2, *etc.* Immiscible sulfide melt

may evolve when the magma is supersaturated in S-content *i.e.*, S-content exceeds C_S. S-saturation of the melt may be achieved through

- the fractionation of silicates and oxides during differentiation, thereby increasing the S-content of the previously S-undersaturated magma
- the partitioning of Fe^{2+} to the crystallizing Fe-rich phases early in the magmatic history with which sulfur occurs in the form of complexes in the melt, reduces the S-bearing capacity of the co-existing melt, thereby giving rise to an immiscible sulfide liquid (Haughton *et al.* 1974, Shima & Naldrett 1975, Li *et al.* 2001).
- devolatization, partial melting or complete assimilation of S-rich country rock (Irvine 1975, Lesher & Campbell 1993, Li & Naldrett 1993, Ripley 1999) by the rising parent magma producing immiscible sulfide phase.
- increase in fO_2 by crustal contamination and subsequent precipitation of chromite and magnetite, may reduce the S-solubility as a result of partitioning of Fe^{2+} to these phases (Buchanan & Nolan 1979).

PGE get partitioned to immiscible sulfide liquid, which may further cavenge the parent magma or crustal rocks during their percolation towards the floor of the magma chamber to form PGE-rich horizons.

The close association of chromites with the PGE mineralization in ultramafic complexes suggests that the *process* of chromitite formation provides a close insight to *how the* associated *PGE are concentrated* (Kinnaird *et al.* 2002). Different mechanisms proposed by various workers for

the formation of chromite are gravity-induced separation, crystal sorting and settling (Wager & Brown 1968); immiscibility of Cr-rich liquid (Sampson 1932); increase in oxygen fugacity by country rock degassing (Cameron & Desborough 1969); contamination by a siliceous component (Irvine 1975), mixing between resident and new magma (Irvine 1977); lateral growth within a stratified magma column (Irvine *et al.* 1983); injection of a chromite-phyric magma (Eales 2000); and total pressure changes (Cameron 1977). Mainly two different modes of origin proposed for PGE mineralization associated with chromite deposits namely: *magmatic* and/or *hydrothermal*.

Evidences in support of *magmatic* origin for the PGE mineralization are (Naldrett & Duke 1980, Campbell *et al.* 1983, Irvine *et al.* 1983, Barnes & Naldrett 1985, Naldrett 1989) close association of these mineralizations with cyclic units and chromitites of layered complex of magmatic origin, high degrees of correlation of PGE with associated magmatic sulfides, uniformity in PGE values and thickness with considerable lateral extent and the systematic controls of mineralization of the PGE deposits *etc.*

Majority of the workers prefer the magma mixing model over crustal contamination that triggers the S-saturation of the melt after its emplacement at crustal levels. Widely accepted magma mixing model proposed by Naldrett & von Gruenewaldt (1989) envisage that the S-saturated hybrid formed from mixing of extremely fractionated magma with that of a primitive one is potential of giving rise to PGE mineralization of economic concentration. If the liquid is chromite saturated then it gives rise to chromitite layers rich in PGE sulfides like that of UG2 chromitites. Otherwise, this may give rise to PGE rich

sulfide horizons like Merensky reef or J-M reef. However, there is no unanimity amongst the geoscientists regarding the composition and mechanism of mixing of the magmas and interpretations are largely based upon the field evidences and geochemical signatures of different lithounits along the magmatic stratigraphy concern to the complex, in particular (Campbell 1977, Todd *et al.* 1982, Sharpe 1982, Irvine *et al.* 1983, Naldrett & von Gruenewaldt 1989).

However the long accepted magma mixing model proposed by Campbell *et al.* (1983) and, Naldrett and von Gruenewaldt (1989) have been opposed on the following grounds:

- a high R-factor (silicate:sulfide) *i.e.*, large volume of silicate required
- higher Pd:Ir ratio of these sulfides compared to the mantle values (Peach & Mathez 1996)
- uniform mixing of such large volume of magma is seemingly impossible
- Sr-isotopic ratio of the Merensky reef is of the Main zone affinity (Kruger & Marsh 1982) but the PGE concentration is similar to the critical zone magma (Davies & Tredoux 1985)
- abrupt increase in Cu/Pd ratio (Maier & Barnes 1999) and absence of cumulus sulfides (Cawthorn 1999b) just ~1m above the Merensky reef *etc.*
- hybridization of sulfur undersaturated Mg-rich basaltic parent (Bushveld) magma with resident magmas of variable composition can not result in sulfur supersaturation (Cawthorn 2002)

- a sulfide liquid cannot achieve high PGE concentration simultaneously depleting the magma with PGE (Cawthron 2005) as per the principles of chemical partitioning

The higher Pd/Ir values explained by preferential fractionation of Ir to olivine during the formation of parent magma by partial melting or during its fractional crystallization (Ross & Keays 1979, Peck & Keays 1990), or fraction to cumulate chromites compared to residual melt (Oshin & Crocket 1982, Barnes *et al.* 1985, Talkington & Watkinson 1986, Stone *et al.* 1993). Peach *et al.* (1994) suggested such high Pd/Ir ratios may be the manifestation of redistribution of primary PGE by late magmatic/ hydrothermal processes subsequent to their concentration by the sulfides.

Ballhaus (1998) suggested over saturation of the magma with PGE resulting in exsolution of these elements as polymetallic micro-nuggets early in the cooling history followed by their separation by later monosulfide droplets formed on sulfur saturation of the magma to avoid high values of D and R as required in the magma mixing model. Cawthron (2005) suggested a pressure change model for such mineralization for the S-saturation of the magma to form the PGE minarilization of Bushveld complex. His model is independent of the magma mixing and the composition of fresh magma that had been introduced and, purely relies upon physical adherence rather than chemical partitioning of PGE.

The observations in support of a **hydrothermal** mode of origin are

i. the lacunae in the models defending early magmatic formation of PGE mineralization (as discussed above).

ii. occurrence of PGE deposits of obvious hydrothermal origin *e.g.*, New Rambler (McCallum *et al.* 1976), Kupferschiefer of Germany and Poland (Kucha 1982; Hulbert *et al.*, 1992; Pasava, 1993) *etc.*

iii. evidences of the mobility of Pt and Pd as complex form in hydrothermal environments (Fuchs & Rose 1974, Barnes *et al.* 1985, Vlassopoulos and Wood 1990, Wood & Samson 1998)

iv. features of late magmatic/hydrothermal origin associated with specific PGE deposits such as their pegmatoidal nature with volatile rich phases like phlogopite and hornblende (Todd *et al.* 1982), Cl-rich apatite (Boudreau *et al.* 1986), high temperature intercumulus hydrous phases and deuteric alteration of associated cumulates (Volborth *et al.* 1986, Kinloch & Peyerl 1990), extremely patchy nature both in terms of tenor (Bow *et al.* 1982) and varieties of PGM (Kinloch & Peyerl 1990), comparatively REE-enriched pattern with respect to (Mathez 1995) but within the narrow range of D/H ratio (Mathez *et al.* 1994) of other lithounits from the same stratigraphic sequence, Cl-rich fluid inclusions (Ballhaus & Stumpfl 1986) *etc.*

v. The transportation of PGE as chloride complexes (Gammons *et al.* 1992) and as bisulfide complexes (Gammons & Bloom 1993, Pan & Wood 1994) has also been experimental confirmed by different workers.

Hydrothermal models basically relies upon the regeneration of a vapor rich phase (*e.g.*, Cl-rich) capable of scavenging and carrying out base metals, PGE and S from PGE preconcentrated footwall cumulates and, their subsequent precipitation against physico-chemical discontinuities at higher

stratigraphic levels (Boudreau & McCallum 1986, Mogessie *et al.* 1991, Boudreau & Meurer 1999, Willmore *et al.* 2000).

However, the mass balance calculations for S-content and PGE content show inadequacy of such model (Barnes & Campbell 1988, Naldrett & Von Gruenewaldt 1988, Maier & Barnes 1999). Moreover, most of the compositional features envisaged by various workers in support of hydrothermal mode of formation of reefs can equally be explained by magmatic processes as discussed by Barnes & Maier (2002). In many cases, the magmatic PGE mineralizations were masked by the low-temperature hydrothermal overprinting. Only few reported occurrences are there where hydrothermal processes are the major or sole factor controlling the PGE mineralization (Maier 2005). However, it is still a matter of debate that whether such mineralizations are formed primarily by hydrothermal processes or else simply redistribution of original magmatic BMS-PGM by the late magmatic fluids and, still needs appropriate explanations in its support.

1.3 PGE PROSPECTS OF INDIA

The Indian subcontinent was barren of any identified deposits until the discovery of PGE mineralization of *Boula-Nausahi complex*. Although the complex is known for its small but significant contribution to the chromite reserve of the country, only in the late 1980s the Geological Survey of India (GSI) discovered the PGE-rich lithofacies (Thiagarajan *et al.* 1989, Nanda *et al.* 1996, Patra & Mukherjee 1996). Mondal and Baidya (1997) have first reported the occurrence of PGM in this complex and later detailed studies

were carried out by different workers (Augé *et al.* 1999; Baidya *et al.* 1999; Mondal *et al.* 2001; Augé *et al.* 2002a & b). Augé *et al.* (2003) on the basis of zircon dating *(~3.1Ga)* considered this as one of the *oldest* PGE concentrations in the world. Further in early 1990s, the *Hanumalapur complex*, Karnataka has emerged as a new PGE prospect (Devaraju *et al.* 1994, Alapieti *et al.* 1994, Devaraju *et al.* 2005).

Boula-Nausahi PGE prospect is situated in geographical proximity (70 km in the NE direction) and, is in geological harmony with the SUC. It spreads over a small area of 1.5 sq km extending in a general NNW-SSE trend. It consists of four principal lithostructural units *i.e.*, *gabbro–anorthosite* unit (the most extensive unit in the complex), *peridotite* unit (including *three* chromite layers), *pyroxenite* unit and *Bangur gabbro intrusion*.

The peridotite (partially to wholly altered to serpentinite) unit hosts three chromitite layers from hanging wall to footwall are *Durga*, *Laxmi* and *Ganga-Shankar* lodes (Mukherjee & Haldar 1975, Mondal *et al.* 2001) ranging in thickness 2m to 6 m. The contact between peridotite unit and the hanging wall gabbro-anorthosite unit is obscured by the Bangur gabbro (a gabbro norite) intrusion along an N-S shear zone. The Bangur gabbro forms a N- and NW-trending curvilinear apophysis of 2 km length and 1 to 40m wide zone of magmatic breccia. The brecciated zone contains the xenoliths of host peridotite, chromitite and pyroxenite in a gabbroic matrix.

Augé *et al.* 2003 have proposed a two fold classification for this PGE deposits *i.e.*, Type-1 ("contact type") and Type-2 ("hydrothermal type") associated with the Bangur gabbro contact with the ultramafics and the associated breccia zone, respectively. Whereas Mondal *et al.* (2001)

explained that the later type of mineralization is caused by a hybrid magma formed by the assimilation of ultramafic units by the Bangur gabbro and its subsequent emplacement along the pre-existing breccia zone. Augé *et al.* (2002b) on the basis of progressively fine fragmentation and subsequent assimilation of the ultramafic and chromitite blocks in the gabbroic matrix, brecciation pattern and geochemical signatures, evoked about a contemporaneous emplacement of the gabbro with the brecciation. According to Geological Survey of India sources (GSI website http://www.gsi.in), estimated reserves for Type-2 mineralization with a grade of 1.55 g/t Pd+Pt is 7.7 million tonnes.

Type 1 PGE ("contact-type") mineralization (Augé *et al.* 2002b) is platinum-rich (Pt/Pd = 8–9), characteristically lacks BMS. The concentration (in ppm) of different PGE in this type of mineralization is Pt: 1.1–14.2, Pd: 0.1–2.1, Rh: 1.8–3.8, Os: ≤ 0.4, Ir: 0.5–1.3, Ru: 1.2–3.6. Inclusions of PGM in pyroxene and plagioclase point towards an orthmagmatic origin (in relation to gabbroic hosts) for this type of mineralization (Augé *et al.* 2002b). The PGM phases associated with this type of mineralization are typically Pt alloys (isoferroplatinum) and sulfides (braggite, malanite).

Type 2 PGE and associated BMS mineralization are localized in gabbroic matrix through out the brecciated zone. Gabbro matrix suffered a remarkable hydrothermal alteration as indicated by the development of secondary hydrous minerals (Augé *et al.* 2004). The Type 2 PGM and BMS are generally interstitial to or distributed along cleavage surfaces of the secondary silicate phases such as biotite and amphibole (Augé *et al.* 2002b).

Type 2 mineralization is Pd-rich and divided into two subtypes as Type 2A and Type 2B. Type 2A characteristically having Pt/Pd ~ 0.5 and Pd-rich minerals (sudburyite, and metallic alloys like Pd tellurides, bismuthides and antimonides) in association with BMS (generally < 2 modal %). Chalcopyrite, the major sulphide phase (50-80 modal %) with pyrrhotite, pentlandite, violarite, millerite, pyrite, and members of the cobaltite–gersdorffite solid solution series forms the bulk of BMS (Mondal *et al.*, 2001). The PGE concentration ranges for this subtype are typically Pd: 1.8–6.0 ppm, Pt: 0.3–1.6 ppm, Rh: ≤ 50 ppb, Os: ≤ 10 ppb, Ir: ≤ 20 ppb and Ru: ≤ 100 ppb. Type 2B typically shows Pt/Pd ratio in the range 2–3 and the PGM consist of Pt and Pd arsenides and antimonides and virtually devoid of BMS. PGE values for this subtype are Pd: 1.0–5.8 ppm, Pt: 0.4–3.6 ppm, Rh: ≤ 200 ppb , Os: ≤ 10 ppb, Ir: ≤ 70 ppb, Ru: ≤ 200 ppb.

1.4 DEFINING THE PROBLEM

In the present context, the SUC which is the major source of chromite (~95%) in the Indian subcontinent, has got least attention ever since the reported occurrence of platinum by Dasgupta (1959) and the pioneering work produced by Page *et al.* (1985). Though the Sukinda area is much larger compared to Boula-Nausahi complex, the entire complex is covered with lateritic blanket and fresh rock exposures are rare and may be the root cause for getting relatively less attention for detailed PGE investigation. Presently, growing global interest to hit the *'chromite and the associated ultramafic'* targets for these valuables, attracted the author's attention towards the revaluation of PGE potentiality of SUC.

Page *et al.* (1985) in their pioneering work on the Sukinda and the Boula-Nausahi complex reported the maximum values for Pd, Pt, Rh, Ir and Ru as 13ppb, 120ppb, 21ppb, 210ppb and 630ppb respectively. They have suggested that these complexes are Precambrian equivalents of the Palaeozoic and Mesozoic ophiolite complexes based on the close resemblance in their chondrite-normalized PGE patterns which markedly differs from those of the Precambrian stratiform complexes. In Sukinda (Mukherjee 1998), the Pt values range between 2 and 400 ppb and, that of Pd range between 1 and 500ppb. Limonitic capping on ultramafic rocks showed PGE (Pt and Pd) concentrations from 40 to 290ppb. Sulfide content varies from 0.5 to 0.82%. However, any economic concentration of PGE is yet to be identified and the mode of occurrence of PGE is yet to be defined in the Sukinda area.

This work probably presents the first ever direct evidence of the mode of occurrence of PGE in Sukinda ultramafic complex and hence gives better understanding about their paragenesis in relation to the evolution of this complex in the light of compositions of associated Cr-spinels (Sen *et al.* 2005), sulfides (Sen & Mohanty 2005, Sen & Mohanty *under preparation*) and remnants of olivine along with whole rock PGE and trace elements concentrations.

1.5 OBJECTIVES

As mentioned earlier, the author's intention of carrying out this study was concentrated around the re-evaluation of the PGE potentiality of the Sukinda Valley chromites in terms of whole rock PGE concentration of

different lithounits as well as the pristine nature of the PGM. For this, an idea about the evolution (tectono-magmatic as well as post tectonic) of the complex should be known so as to predict the geochemical behavior of these elements under the prevalent physico-chemical conditions and the expected pattern of PGE mineralization. PGE are siderophiles but behave as chalcophiles in the crustal/subcrustal conditions of fS_2. Again there are two subdivisions as mentioned earlier. IPGE are more refractory and less chalcophilic compared to the PPGE. Hence IPGE crystallize early in the magmatic history when the PPGE prefers to stay in the melt. But sulfides are invariably the carrier phase for all the PGE. Crystallisation of these PGE in a sulfide rich horizon depends on the formation of S-rich immiscible liquid phase during fractional crystallization. So the factors controlling the mineralization pattern of PGE are:

- Whether or not the parent magma is fertile in terms of S-content and PGE
- Variation in physico-chemical conditions like total pressure (P), temperature (T), oxygen fugacity (fO_2), sulfur fugacity (fS_2), S-bearing capacity of the melt during different stages from the formation of parent magma by partial melting of mantle till its emplacement at crustal levels
- Role of hydrothermal solutions in the post emplacement modifications

Such an approach requires identification of different litho-facies and confirmation about their mutual relationship. For the purpose, systematic field mapping and sampling were carried out. During field mapping it was found that the different lithounits suffered variable but extensive degrees of auto-metasomatism or serpentinization, followed by low temperature modifications

characteristic of tropical terrains *i.e.* lateritization. Accordingly, two main types of chromite ore and host rock associations are identified: *'brown'* chromites hosted in limonitized/ latiritic rocks dominating over *'grey'* chromites hosted in serpentinites/ 'black dunites' those had escaped the wrath of lateritization. Cr-spinels are most reliable petrogenetic indicators being very sensitive to variations in physico-chemical conditions prevailing during magmatic processes. So 'grey' ores form the centre of attraction of the present study as the only resistance phase *i.e.*, the Cr-spinel from this type of ores has escaped latritization and, with few exception, serpentinization. These Cr-spinels are the true representatives of the primary or unaltered spinel phase. Under the prevailing circumstances, these Cr-spinels can selectively be used to trace back the magmatic evolution of the complex. Very rare remnants of olivine, coexisting with Cr-spinel, are also studied in order to predict the source magma composition as well as the evolution of the melts during the crystallization process. Mineralogical study of the bulk rock and compositional analyses of the ground mass were carried out to detect the post-crystallization and the post-emplacement modifications and, to have a qualitative idea about such processes on PGE mineralization pattern. In this regard, the PGE carrier phases *i.e.*, the BMS are extensively studied to found out:

- The role of BMS as carriers of PGE to give any economic concentrations
- The nature of hydrothermal/low temperature magmatic fluids and its effect on remobilization of the BMS

Finally, the whole rock PGE concentrations of various lithofacies are measured and the modes of occurrence of PGE are confirmed.

To begin with the author would like to attract the attention towards the most debating subject regarding Sukinda Valley chromites, that is, its mode of formation *(whether ophiolitic or layered complex),* which in part forms the objective of the present study. This is dealt in the light of detailed Cr-spinel composition from different zones of the complex those are of geologic significance along with the study of few remnants of olivine grains. The whole rock PGE & trace element data have been used to interpret the nature of source magma as well as the tectono-magmatic evolution of the Complex.

Based on all the aspect studied, a genetic model is proposed to fit the mode of formation of the Sukinda Valley chromites with that of the kind of PGE mineralization style observed. In brief, the objective of the present study concentrates around:

- To understand the genesis of chromite ore and its type: podiform or stratiform
- To find out physicochemical conditions for chromite formation and its bearing on PGE mineralization
- To suggest a possible ore genetic model of PGE mineralization for SUC

1.6 METHODOLOGY

The methodology followed in the work (Fig. 1.1):

- Systematic sampling and detailed petrographic studies of host rock and chromite ore

- Qualitative mineralogical studies of the host rock and chromite using XRD
- Chemical analyses of Cr-spinel, BMS, olivine and serpentines using EPMA
- Determination of whole rock trace element concentration of the host rocks using acid dissolution technique in combination with ICP-MS
- Determination of noble metal concentration of the host rocks and chromite ore using NiS-fire assay technique in combination with ICP-MS
- Analyses of various sulfide phases and PGM using SEM-EDS
- Data synthesis and data interpretation

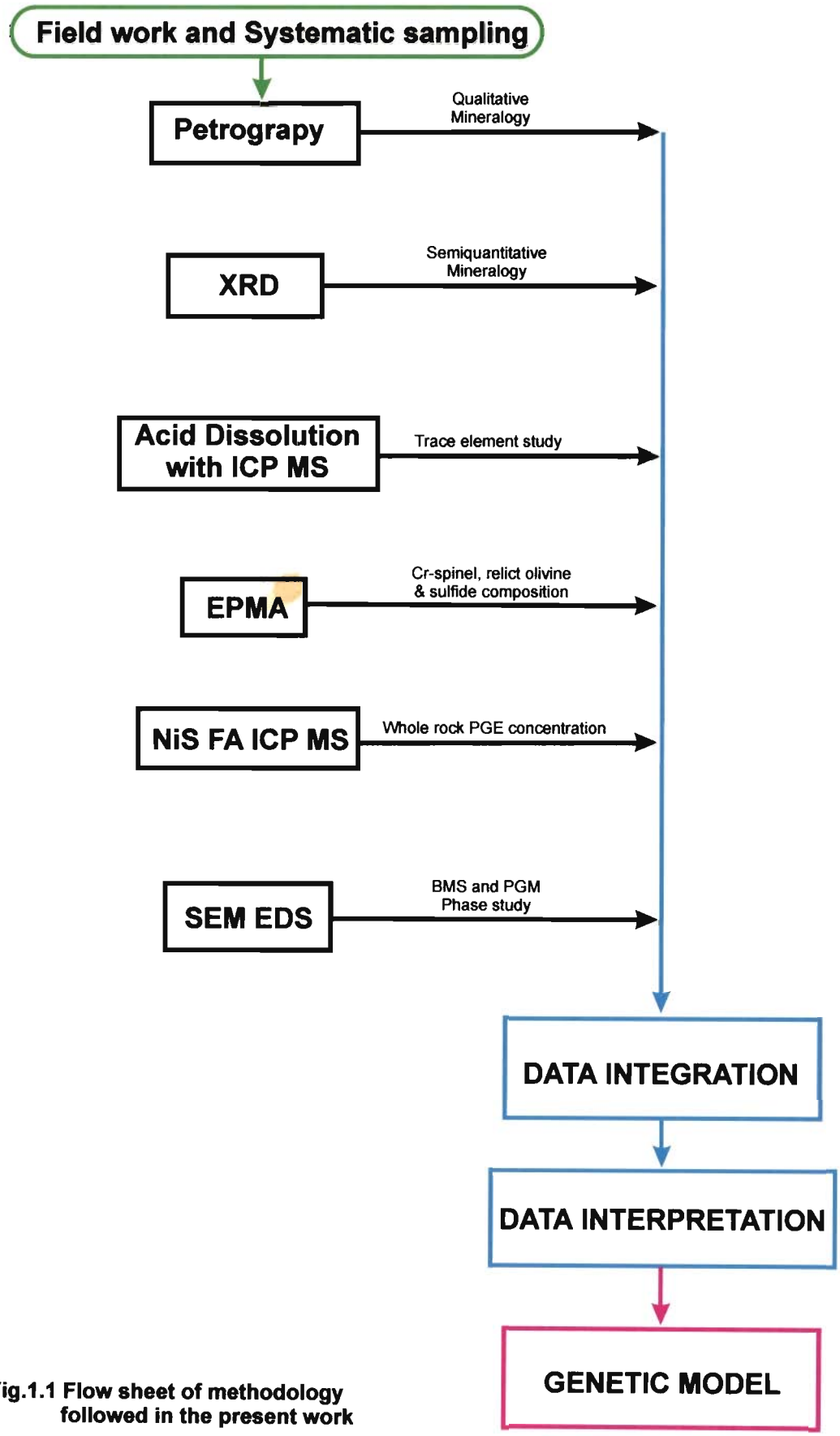

Fig.1.1 Flow sheet of methodology followed in the present work

Chromite hosted ultramafics complexes are broadly found in two types of geological setting: i. layered ultramafic complexes of Precambrian age with bulk gabbroic composition and, ii. Ophiolitic complexes of Cenozoic age with bulk peridotitic composition. As discussed in Chapter-1, the two chromite hosted ultramafic complexes have distinct variety of PGE mineralogy and tenor, former being high in tenor with PPGE dominated mineralogy is more attractive than the later. Again, the PGE mineralizations associated with chromite deposits have a better lithological control than those with base metal deposits. So a better understanding of the complex is essential for evaluation of its PGE potentiality.

2.1 CHROMITE DEPOSITS OF INDIA

Chromite deposits in India are distributed in a broad range of space and time. These are mainly associated with Precambrian-Archaean and Mesozoic-Tertiary rocks. The major component of the chromite inventory is locked-up in the ultrabasic rocks of Precambrian age which are intrusive into

the pre-existing metavolcano-sedimentary sequences, aligned parallel to the major tectonic regimes of peninsular India. In *Sukinda* ultramafic complex (Banerjee 1972, Chakraborty 1972 & 1973, Sahoo & Kadeen 1976) and *Boula-Nausahi* complex (Chakraborty 1958, Deb & Chakraborty 1962, Mukherjee 1962, Haldar 1967, Varma 1964 & 1965, Mohanty & Sahoo 1995) of Orissa and *Jojohatu* complex (Banerjee 1960, Singh 1971) of Jharkhand chromite hosted by serpentinized dunite-peridotite that intrudes the Iron Ore Group (IOG) of rocks. *Kondapalle* chromite deposits in the Eastern Ghats of Andhra Pradesh (Chakraborty & Mukherjee 1971, Leelanandam, 1997) and the *Sittampundi* complex of Salem District, Tamil Nadu (Subramanium 1956) are exceptions to chromite deposits in the serpentinized dunite-peridotite where the hosts of chromitite are interlayered sequence of serpentinite, pyroxenite and anorthosites and cites unequivocal examples of stratiform type of deposits.

2.2 SUKINDA CHROMITE DEPOSIT

The majority of India's Chromite production (~95%) comes from two ultramafic complexes of Orissa namely *Sukinda* ultramafic complex and *Boula-Nausahi* ultramafic complex (~70km in NE of Sukinda Valley and relatively much smaller than SUC), which are geologically related and geographically in close proximity.

2.2.1 Location

The Valley extends from *Tomka* (85°55'E: 21°7'N) in the east to *Kathpal* (85°41'E: 21°1'N) on the west (Banerjee 1972) spreading over an area of 40sq km in NE-SW direction in *Jajpur* and *Dhenkanal* districts of Orissa. It is flanked by the *Tomka* (782.42m amsl)-*Daitari* (847.77m amsl) range to the *north* and *Mahagiri* (707.69m amsl) range to the south. The Valley is largely covered with alluvium and thick mantle of laterite. The main drainage in the Valley is contributed by perennial *Damsal* stream that flows from east to west along the centre of the Valley following the regional synclinal fold axis plunging WSW. Fig 2.1.i-iii shows synoptic views of the Sukinda ultramafic complex depicted in different FCC prepared from LANDSAT images. A detailed image analysis of the image as well as the FCC are carried out to have the first hand information about the study area. A detailed discussion is as follows.

2.2.2 Remote Sensing Image Analysis

Remote sensing images, through synoptic coverage of the whole area, provided a first-hand understanding of the area of interest and allowed identification of distinct geomorphological, structural and lithological features.

The remote sensing image data used in this study include *the Landsat ETM+* multispectral imagery (Path 140, Row, 45) acquired on 2/11/2002, and the panchromatic image data of the same sensor (15m ground resolution). The data is obtained from the GLCF, at the University of Maryland which provide the Landsat data as orthorectified image data with real-world geodetic

positional accuracy of >50m. The salient features of the Landsat ETM+ image data are given in Table 2.1 (after Gupta 2003).

Table 2.1 Salient features of the Landsat ETM+ image data (Gupta 2003)

Band Number	Spectral Range	Name	Ground Resolution	Image size (km)
ETM1	0.45-0.52	Blue	30	185 x 170
ETM2	0.52-0.60	Green	30	
ETM3	0.63-0.69	Red	30	
ETM4	0.76-0.90	Near Infrared	30	
ETM5	1.55-1.75	Shortwave Infrared	30	
ETM6	10.4-12.5	Thermal Infrared	60	
ETM7	2.08-2.35	Shortwave Infrared	30	
ETM8	0.45-0.90	Panchromatic	15	

Lithology: The study area falls in the SW quadrant of the full 185km x 170km ETM+ scene. Fig 2.1.i shows the resolution enhanced modified FCC (bands 7-4-2 coded in R-G-B) displaying the best lithological discrimination. The FCC was generated by fusing the high resolution panchromatic image (15m) with the multispectral data. As much of the study area is dominated by thick vegetation cover which has the highest reflectance in band 4, green hues dominate the image display. The vegetation cover greatly limits the discrimination capability of surface lithology using remote sensing approach as the reflected radiation forming the signal is dominated by the interference due to vegetation.

This effect is best demonstrated by the use of band ratio ETM5/ETM7. Ideally, this ratio generates a clear discrimination of hydoxyl-bearing rocks.

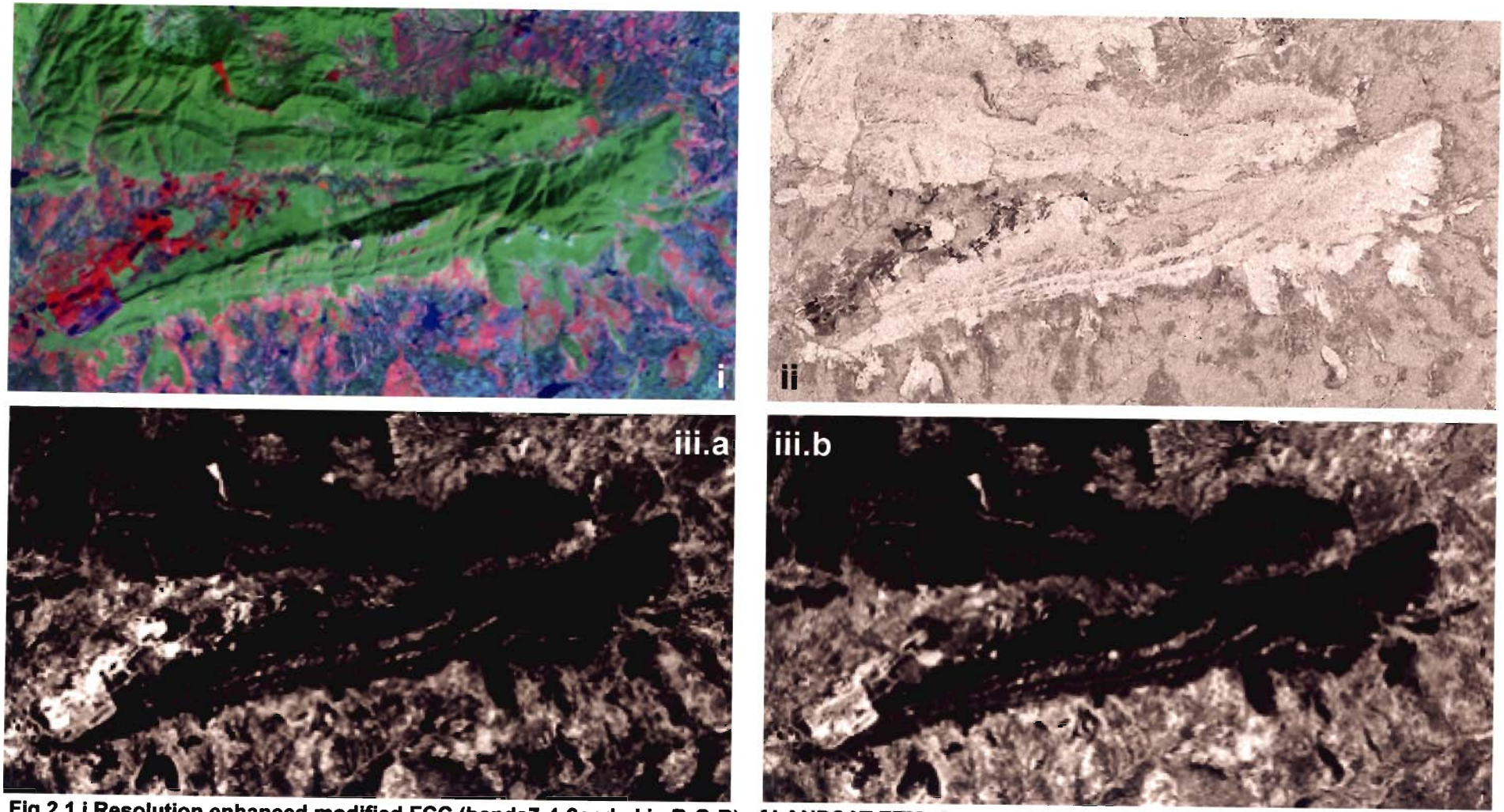

Fig.2.1.i Resolution enhanced modified FCC (bands7-4-2coded in R-G-B) of LANDSAT ETM+ image
Fig.2.1.ii Difference image of ETM5/ETM7 and NDVI of ETM+ data
Fig.2.1.iiia Ratio image of ETM3/ETM1 b. ETM5/ETM4

However, as vegetaion also has higher values for the same band ratio, the discrimination is badly affected. A normalized difference vegetation index (NDVI) image [(ETM4-ETM3)/(ETM4+ETM3)] is used to identify healthy vegetation from the background (Tucker 1979). A difference of the ETM5/ETM7 and NDVI image for sparsely vegetated areas yields good discrimination for hydroxyl-bearing rocks, but for thickly vegetated areas the interference is not fully eliminated. Fig.2.1.ii shows a difference image of ETM5/ETM7 and NDVI of the ETM+ data for the study area. It can be readily observed from the image that the vegetation cover disturbs the discriminability of the ETM5/ETM7 band ratio.

In order to distinguish between the iron oxide and ferrous hydroxides, the image transformations in the form of band ratios (ETM3/ETM1 for FeO, Fig.2.1.iii.a and ETM5/ETM4 for Fe-OH, Fig.2.1.iii.b) were calculated. To avoid erroneous interpretation of band ratios, the atmospheric effects of scattering (path-radiance) were removed using band-minimum subtraction approach. In the band ratio images, the lighter gray tones indicate higher concentration of respective rock chemistry. It is observed that the central part of the area of interest have the greatest variation in the FeO and Fe-OH surface chemistry which is indicative of altered ultramafics of the SUC reported in the literature.

Structure: Interpretation of the resolution-merged multispectral data (Fig.2.1.i) reveals some very striking structural features of the study area. The main structural feature of the study area is SSW plunging regional fold. The axis of the regional fold is traced by the Damsala Nala trending ENE-WSW. The fold closure lies towards the East of the Area of Interest (AOI). Analysis of

the pattern and trend of the small water bodies in the central part of the AOI suggest a close relationship with the regional fold. These water bodies are later confirmed from the field studies to be associated with the mine pits and are located along the strike of the chromite bands. These collectively suggests that the chromite bands and the host ultramafics are co-folded with the quartzites of IOG.

2.2.3 Lithology and Stratigraphy

Sukinda chromite deposit is brought to limelight by the prospecting division of Tata Iron & Steel Company (TISCO) in 1949. Prasad Rao (1950) carried out the first ever systematic mapping of the area. Subsequent geological studies are continued by various workers like Deekshitulu and Perraju (1955), Das Gupta (1959), Sahu and Bagchi (1959), Mitra (1962 & 1973), Acharya (1964), Chakraborty (1972 & 1973), Chakraborty and Majumder (1976) and Sahoo *and* Kadeen (1976) *etc.* However, pioneering work on the regional structure and genetic aspect of the Sukinda Valley chromite deposits are dealt by Prasad Rao *et al.* (1964) and Banerjee (1972). Chakraborty *et al.* (1980) redefined the stratigraphic sequence based on detailed lithological and structural mapping along the Valley.

The *IOG* quartzites (oldest litho-unit exposed in the area) of Mahagiri range and Daitari-Tomka range conformably overlain by banded iron formation of Precambrian age 2700-3200m.a. (Sarkar *et al.* 1969). The quartzites are having dip 60°-85°/N and NNW in Mahagiri range and, 50°-75°/S and SSE in Daitari-Tomka range *i.e.,* towards the centre of the Valley. The BIF capping with few laminations of volcanic tuffs, its alteration products

and quartz-sericite phyllites of the Daitari-Tomka range have similar dip to that of the quartzites of the range, but the extension of the Banded Iron Formation (BIF) is not traceable to *Mahagiri* ranges (Chakraborty *et al.* 1980). Locally developed intraformational conglomerates similar to that found in Iron Ore Series of Jharkhand and Orissa (Dunn 1940), with pebbles and boulders of IOG quartzites in an argillaceous matrix that is devoid of any fragment of BIF and chromites, are found along the eastern margin of Mahagiri ranges. A patch of coarse-grained sandstone conformably overlying a conglomeratic horizon with relicts of BIF but no chromite is found only along the foothills of Daitari, near *Kansa* and *Talangi* villages. Chakraborty *et al.* (1980) have correlated this sandstone along with the basal conglomerate, with the *Kolhans* as this sequence lies in the younging direction of Iron Ore Group without any signature of *stratigraphic inversion*.

In SUC, *two* types of ultramafics are found. One is *older dunite-peridotites* hosting chromitites, altered to serpentine, and at places silicified and talc-serpentine schist due shearing, exposed along the base of the Mahagiri range from Kansa in the east to Kathpal in the west with a sharp contact with the quartzites of IOG. In rest of the Valley the altered ultramafics are concealed underneath the thick proximity of alluvium and laterites. Banerjee (1972) had identified *six* regional bands of chromite ore and are named from I to VI (older being Band-I based on the synclinal structure). The *younger* ultramafic is coarse grained green coloured unaltered *orthopyroxenite*, exposed in the form of a continuous band running NE-SW from *Sukerangi* up to the north of *Kalaringitta* village and then to further south of *Kathpal* village. Orthopyroxenite consisting almost entirely of enstatite is

devoid of any chromitite layers. This orthopyroxenites shows discordant relation with the older ultramafic suite thereby indicates a younger age for these intrusive. Intrusive relation of the ultramafic with the quartzites of IOG is confirmed on the basis of inclusions of quartzite found within the ultramafics around *Kathpal* area and along the course of *Damsala* stream (Fig.2.2). They could not establish any definite age relationship with the *Kolhan* group owing to their scanty exposures. But Srinivasachari (1979) considered the Kolhan group to be older than the ultramafics as they dip away from the Iron ore group rocks exposed in the parallel hills to the north and south of the Valley.

Few patches of granitoids and leucogranite, petrographically are exposed near the Kathpal village. These are having a crosscutting relation with the ultramafics (Fig.2.3.i) and defines a brecciated zone similar to that of Bangur breccias of Boula complex but different in magnitude. The *youngest of all intrusives* are a group of dolerite dykes having discordant relationship with all other rock types exposed in the Valley. Based on their marked coherency with Newer Dolerites of Singhbhum region in terms of petrographic and chemical properties (Saha *et al.* 1973), a Cambrian age has been assigned to these dolerites by Dunn (1940) and Sarkar *et al.* (1969). A generalized stratigraphic sequence had been given by Chakraborty *et al.* (1980) for Sukinda Valley based on the above observations (Table 2.2).

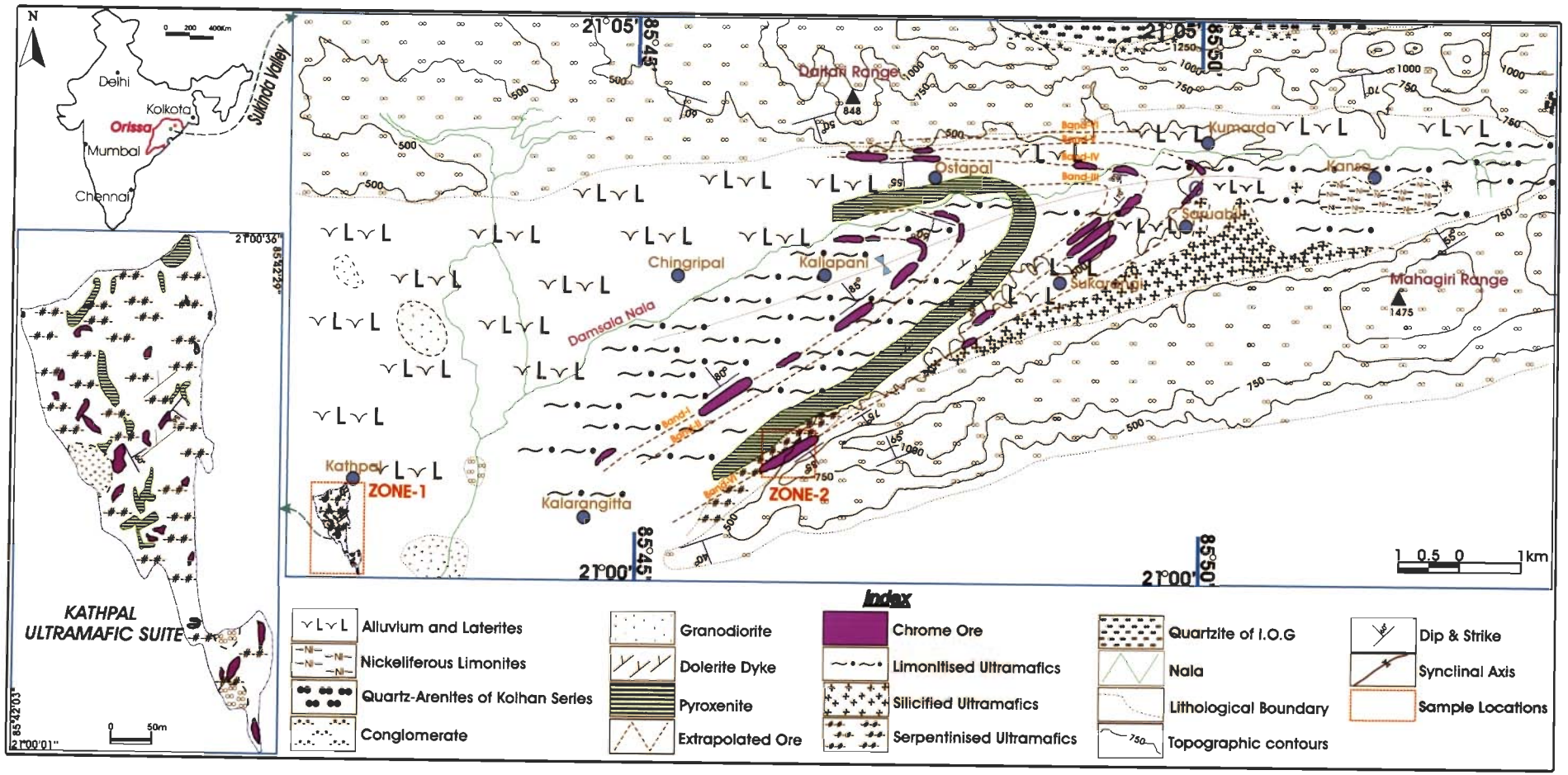

Fig.2.2 Geological map of the Sukinda Ultramafic Complex. Geological map of Kathpal area is in Inset (modified after *Banerjee 1972, Chakraborty & Chakraborty 1984*)

Fig.2.3.i Brecciated chromite, ii minor folds in chromite band, iii serpentinized host ultramafics, iv limonitized host ultramafics

Table 2.2 Stratigraphy of Sukinda Valley, Orissa (after Chakraborty *et al.* 1980)

Alluvium
Laterite (nickeliferous at places)
Dolerite
Granite and granitic gneisses
Orthopyroxenite (Enstatitite)
Ultramafic intrusion with chromitite
Sandstone (quartz-arenite): Kolhan Group
Conglomerate
-------- Unconformity --------
Banded Iron Formation with interbedded volcanic tuff and altered products
Quartzite with intraformational conglomerate
------ Basement not exposed ------

2.2.4 Structure

Banerjee (1972) established the regional structure of the Valley as a syncline that plunges towards WSW and a closure on the eastern side (Fig.2.2). Apart from this, minor plunging synformal and antiformal structures with subparallel axes were recognized in quartzites. However, Chakraborty *et al.* (1980) on the basis of detailed structural analyses of the terrain suggested a *doubly plunging cross-folded synclinal* structure for the Valley with the culmination zone located around *Tungaisuni* and *Champajhar* region (beyond the eastern coverage of the map shown in Fig.2.2). The main fold axis trend ENE-WSW and the axis of the cross fold trends NNW-SSE.

The structural coherency of the minor folds in the chromitite layers (Fig.2.3.ii) with the regional fold pattern suggests pre-tectonic emplacement of

the chromite hosted ultramafic intrusive which were subsequently co-folded with the older rocks of the Iron Ore Group during Singhbhum Orogeny (Chatterjee & Banerjee 1964). There exist a number of small localized faults running nearly east-west on the two limbs and are confined within the rocks of the Iron Ore Group. These are mostly dip-slip faults striking parallel to the regional trend of the host rocks (Chakraborty *et al.* 1980).

On the basis of similarity in fold patterns a overprinting relation of Eastern Ghats Orogeny (~1570-1625Ma, Sarkar *et al.* 1964) on Iron-Formation and Chromite bearing ultramafics of SUC, Narayanswamy (1966) suggested that the IOG and the SUC rocks were pre-existing.

2.2.5 Sukinda Ultramafic Complex: *'Deformed Layered'* or *'Precambrian Ophiolite'*!!!

The unresolved controversy of whether Sukinda Valley chromite deposits represent a deformed layered complex or an ophiolitic complex needs to be discussed here to have better idea about the evolutionary history of the complex and its relation to the PGE mineralization style. A brief account on the geological set up and geochemical signature of the two types of chromite deposits is presented in Chapter-4.

The chromite deposit of Sukinda is earlier known to be of stratified type (Prasad Rao 1950) while Varma (1953) considered them to be of hydrothermal origin. Haldar (1969) considered them *similar to stratiform type* and intrusive in partly solid state. Srinivaschari (1979) considered the Boula-Nausahi ultramafics as the continuation of Sukinda ultramafics, forming a single complex, intervening gap being concealed under the alluvial cover with few exposures of IOG rocks. Mohanty & Sahoo (1995) attributed the variation

in trend of the foliation between the two areas to the post-consolidation rotational tectonic movements. Srinivaschari (1979) designated the Sukinda-Baula complex as stratiform type based on the similarity as regards to the lithology, tectonic setting, mode of occurrence of the chromites, the nature of differentiation trend, lesser amount of alumina in chromites, systematic size and compositional grading across the chromite bands, precambrian age of both. He inferred that these ultramafics are emplaced along the marginal steeply dipping strike faults bordering the geosyncline-craton bounadry formed due to down buckling of immense thickness of Iron ore group volcano-sedimentary sequence formed under geosynclinal condition. According to Srinivasachari (1984) these chromites are formed under primordial crustal condition. From detailed field investigation he suggested that the rhythmic layering of chromite-dunite-peridotite-pyroxenite along with overlying gabbro-anorthosite and granophyre form a composite magmatic sequence that acted as the basement of the iron ore geosyncline. He interpreted the lensoid shapes of the chromite deposits as the result of tight isoclinal folding and associated faults that transect individual bands. Banerjee (1972) based on the average Cr and Ni content of chromite ore correlated the SUC with that of Muskox complex of Canada. Chakraborty (1973) on the basis of unimodal distribution pattern of grain size and percentage increase in fine sized grains suggested a crystallization of these chromites under magmatic condition from a single pulse of magma. Sahoo and Kadeen (1976) on the basis of Cr-spinel composition suggested a stratiform nature of these chromites crystallized essentially from an Mg-rich melt in a stable environment without any injection/mixing with the fresh pulse of magma during the magmatic

history/evolution and correlated this with the chromite deposits of Great Dyke of Zimbawe based on Cr_2O_3 content of chromite. Chakraborty and Chakraborty (1984) designated the Sukinda chromites as 'deformed stratiform' type deposits and a suggested their origin due to fluctuation of fO_2 triggered by the contamination of the magma by the quartzites of IOG.

Ultramafic patches from south to north of the *Singhbhum* Archaean nucleus – Sukinda (chromite), *Baula-Nausahi* (chromite and V-Ti-magnetite deposit) and *Bhalukasuni* (chromite and V-Ti-magnetite deposit), *Kumhardubi-Hatichhar* (V-Ti deposit), show a marked trend in magmatic differentiation along with variation in the ore mineral assemblages. Based on these observations Das *et al.* (1995) suggested that these ultrmafic suites are formed by the differentiation of the tholeiitic basaltic parent magma originated under upper mantle conditions (considering it S-poor in the absence of any sulfide mineralization) and emplaced along the deep seated fracture system encircling the Singhbhum granitic mass.

A closer insight into the regional tectonic set up envisages that the marginal portion of the two major tectonic entity of India *i.e.* Singhbhum Iron Ore Craton in the north and the Eastern Ghats in the south is occupied by a cluster of ultramafics of which the Sukinda ultramafics is the largest and southern most to all. From the close spatial relation and compositional similarity Banerjee (1972) ascertained a broadly contemporaneous emplacement of these ultramafic bodies that can help in tracing the mutual age relationship of the IOG and Eastern Ghats. The ultramafics show greenschist facies of metamorphism compared to the granulitic rocks of Eatsern Ghats with a structural non-coherency; hence he suggested that the

ultramafics are post-tectonic with respect to the later. On the contrary these are co-tectonic in respect to the IOG with which these are co-folded and later intruded by granites followed by the intrusion of the newer dolerites.

Banerjee *et al.* (1987) proposed a model that envisages mantle pluming consequent upon rifting and followed by the emplacement of the ultramafics in response to a major late Proterozoic thrusting event that separates the two cratons. This may be a Proterozoic analogue of Phanerozoic fold belts subjected to the geochronological confirmation that both the emplacement of the ophiolitic sequence and the granitic event, as describe by them, form the part of the same orogenic cycle.

Another feature in favour of ophiolitic origin is dominance of inclusions of silicate in chromite (Johan *et al.* 1982) along with deformation features. The chemical plot for end members shows that Sukinda chromites are rich in magnesio-chromite, also suggesting an Alpine affinity. The plot of Mg# against Cr# of chromite falls within the overlapping region of stratiform and Alpine types. The low TiO_2 content (<0.3 wt %) in chromite and low CaO in orthopyroxene (<1wt.%) is similar to Alpine type deposits (Banerjee 1972, Dickey 1975, Sen *et al.* 2005). A low temperature of intrusion for this intrusive is suggested from the high temperature of crystallization of these refractory Cr-spinels, yet absence of any thermal aureole around the ultramafic body. The emplacement took place either as a crystalline mass or in a solid state by plastic flow. The tectonic evidence (mylonitisation, shear planes, fault breccia, fault gauge and small scale folding) suggests that the mass was affected by shear deformation. Hence the rocks underwent solid/semisolid flowage at an early stage and cataclastic during late stage emplacement (Banerjee 1972).

PGEs also bear the signature of the tectono-magmatic conditions prevalent during the evolution of the complexes with which they are associated, owing to their differing geochemical affinity to oxide and sulfide phases. The strongly fractionated, chondrite normalized PGE distribution of chromitite with enrichment of Ir and Ru compared to Pt and Pd also suggests an ophiolitic affinity (Page *et al.* 1985).

2.3 GEOLOGY OF CHROMITITES

The chromitites of Sukinda Valley is hosted by dunitic peridotites those are thoroughly serpentinized (Fig.2.3.iii) and/or limonitized (Fig.2.3.iv) and, lateratized (by meteoric water alteration), leaving behind rare exposures of hard compact ore called *'gray ores'* and serpentinized *'black dunite'* hosts (those have at least escaped of the lateritization process). Banerjee (1972) suggested a hydrothermal mode of formation for the serpentinites by the co-genetic late magmatic fluids whereas limonitisation likely resulted from the iron metasomatism of the ultramafics by the hydrous phases those derived the extraneous iron from the sediments forming the IOG, part of which is preserved as banded iron ore formations and, silicified utramafics are formed out of siliceous gels expelled during the iron metasomatism. On the contrary, Srinivasachari (1979) suggested a supergene mode of formation for the limonites as these grades to serpentinites and then to fresh dunites at depths observed from the borehole samples. In the virtual absence of unaltered host rock, these gray ores and serpentinized dunitic hosts may give best approximation to the original mineralogical and chemical composition of the

ultramafics compared to the laterites and the associated 'brown ores' and hence chosen for the present study.

The gray ores are mostly confined to the fourth quadrant of SUC (Fig.2.2) *i.e.*, the chromite deposits of Kathpal area (Fig.2.3.v) and Kalarangitta (Fig.2.3.vi) area. Kalarangitta chromite deposit occurs as an integral part of the so-called stratiform type of deposit of the main SUC whereas Kathpal chromites and associated ultramafics occur virtually as a detached patch from the main SUC. Kathpal defines a zone of distinct geological disturbance as indicated by tectonically detached slabs of the chromites where as banded nature of chrome-ore from Kalarangitta, at least in part, explains their formation apparently in a stable environment similar to the stable continental stratiform type of deposit. The chromites of the main Valley are distinctly and conspicuously banded on regional scale, which is inherited from their mode of occurrence and mineralogical as well as size grading. Kathpal ultramafics shows, in contrast, irregular orientation of small lenses, pods of chromite and pyroxenites seemingly embedded in a host of serpentinized "black dunites". Banerjee (1972) elaborated this as a melange type of deposit and suggested the irregular orientation of the blocks of chromite and pyroxenites is due to their emplacement essentially in a solid state associated with some tectonic movement.

Out of the six bands, only Band-I (Fig.2.3.v) (Band-VI according to local nomenclature, Fig.2.2) along with black dunite hosted discordant chromite lenses of Kathpal (Fig.2.3.v) constitutes the junk of hard, lumpy, gray ores of the Complex. Rest of the bands is dominated by friable, brown chromite ores (Fig.2.3.iv). Grey ores are steel grey in colour, hard and compact. On the

contrary, brown ores are dark brown in colour and the grains are loosely packed and friable in nature. The brown colour of these ores is imparted by the oxidation of the chromite grains of grey varaities whereas the friable nature is the result of the grain boundary oxidation and disintegration of the silicate gangue. However, the grain size of the chromite is the expression of the physico-chemical condition prevalent during the crystallization from the parent magma as well as post crystallization tectonic events and alterations and only rarely coarse grained in nature.

On the basis of physical character, structure and proportion of gangue, the chromite ores of Sukinda Valley may be classified as massive (Fig.2.3.vii), banded, laminated (Fig.2.3.viii) and spotted. Massive ores indicate a nearly stable condition of fO_2 whereas laminated ores are indicative of rapidly fluctuating fO_2. The spotted/banded types are the transitional magmatic facies. The friable type is the result of alteration of all other type of ores and is most extensive and predominant type of chromite that supplies the bulk of the metallurgical and chemical grade ore from this area.

As per the objective of the present study, focus has been made on hard, compact and grey variety of chromite ores only, as these could escape the lateritization process, and thereby retaining the primary character of the ore. Grey ores are mostly massive in nature and show prominent gradational contacts with the host rock commonly changing to semi-massive, banded and spotted varieties near the contact zone.

As discussed above, the grey chromite ores, hosted within the serpentinized ultramafics, are concentrated mostly around Kathpal and Kalarangitta areas (Fig.2.2) and differ characteristically in the mode of

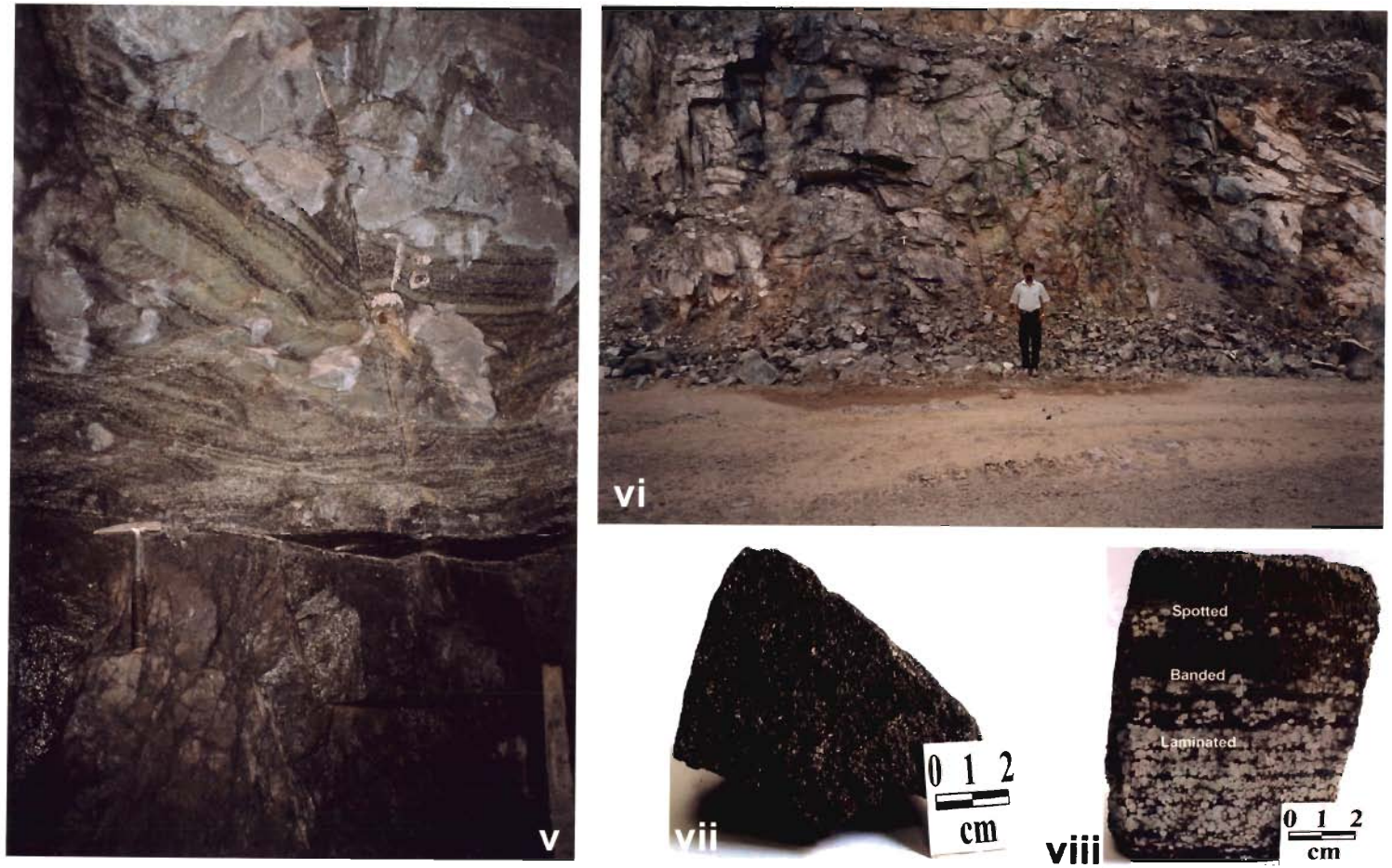

Fig.2.3.v Chromite ore in Kathpal, vi Chromite ore of Kalarangitta (main SUC), vii Massive chromite ore, viii laminated, banded and spotted chromite ore

occurrence. Kalarangitta chromite ore occupies the southern flank of the synclinal valley and occur as a discontinuous layer or seam along a strike length of 3-4km. The ore in *Kathpal* area is present as small, 100-150m long, lensoidal bodies with random orientations. In general, the trend and thickness of the ore bodies at Kathpal show considerable variation whereas the ore body at Kalarangitta is more or less consistent. The mode of occurrence may indicate that the chromites of *Kathpal* area represent a zone of intense geologic disturbance.

Extensive field work had been carried out along the SUC that is especially oriented towards sample collection for geochemical studies of chromites and host ultramafics to study their primary nature and the tectono-magmatic evolution of the Complex with respect it. However, the elementary studies of different lithounits along with their structural relations were also confirmed in the field.

Based on the mode of occurrence of the chromitites, the sampling plan for the present study is formulated for the above mentioned areas (Fig.2.2).

Zone-1 *(Kathpal Area)*: The zone is further divided into sub-zones based on different mines, mining levels and chromite bands.

- Small quarries of Kathpal area ***(Zone-1a)*** expose ores in the surface level. The samples collected from this place are partially affected by the surfacial alteration but still bear compact and banded nature of the chromite.
- The chromite ores from underground mines are more or less fresh and effects of surfacial oxidation are almost negligible. There are two working mines in Kathpal area namely *Jungle* Pit and *Maheswari* Pit.

The samples are collected from two different mining levels of Jungle pit, Kathpal *i.e.*, -40RL ***(Zone-1b)*** and -65RL ***(Zone-1c)***. The ore body of about 5 m thickness strikes NW-SE and dips 40°NE.

Samples are also collected from two chromite ore bodies, *i.e.* minor ***(Zone-1d)*** and major ***(Zone-1e)*** bands, from -65RL mining level of Maheswari pit. The major ore body strikes N-S and dips 76°W with a thickness of 8.5 m. The minor ore body strikes E-W and dips 80°N with a thickness of 3 m.

Zone-2 *(Kalarangitta Area)*

- Here the samples are collected from a section of grey ore (Band-I) exposed in the opencast mine, near Kalarangitta Village of main Sukinda Valley. The ore body with a thickness of 10 m (ranges from 10-25 m) locally strikes NNE-SSW and dips 60°-80°ESE at the sampling section. At places, this ore also shows traces of surfacial alteration.

In all the above mentioned cases, the samples are collected at intervals varying from 1 to 5m after removing 2-3 inches of the top layer. The individual samples along a section represent the all variety of ore, ore-enclosing rock contact zone and the enclosing rocks. While collecting samples, utmost care has been taken to avoid ores as well as host rocks affected by surfacial alteration and weathering. A detail about the analyses carried out for selected samples different sections are listed in Table 2.3.

Table 2.3. Details of Samples used in the present study

Sl. No.	Zone	Sample. No.	Litho unit	Symbol	Petrography	Major Phase (XRD)	Trace Element (ICP-MS)	Cr. Spinel(EPMA)	PGE (ICP-MS)	Sulfides (EPMA)	Sulfides (SEM-EDS)	PGM (SEM-EDS)
1	1a	A3O	SpO	●	–			–				
2		A1O, A3O & B2O	MO	■	–			–				
3	1b	DM-11	HR	▲	–	–	–	–	–	–	–	–
4		DM-12&13	MO	■	–	–		–	–	–	–	–
5		DM-14	SpO	○	–	–		–	–	–	–	–
6		DM-15	HR	△	–	–	–	–	–	–	–	–
7	1c	DM-16	HR	▲	–		–		–			
8		DM-18	MO	■	–				–		–	–
9		DM-19	SpO	○	–				–			
10		DM-20	HR	△	–		–		–		–	–
11	1d	DM-98	HR	▲	–		–		–			
12		DM-99	MO/SmO	■	–				–			
13		DM-100	SpO	○	–				–			
14		DM-101	HR	△	–		–		–			
15	1e	DM-102	HR	▲	–		–		–			
16		DM-103	SpO	●	–				–			
17		DM-104	SpO	○	–		–		–			
18	2	DM-22	HR	▲	–	–	–	–	–			
19		DM-23	SmO	□	–			–		–		
20		DM-24&25	SpO	●	–	–		–	–			
21		DM-26	MO	■	–	–		–	–	–		
22		DM-27	SpO	○	–	–		–				
23		DM-28&29	HR	△	–	–		–	–	–		
24		DM-84	Dolerite	+	–		–	–	–	–		
25		DM-85	Norite	*	–		–		–			
26		DM-86	Dunite	#	–		–		–			

Additionally Sample No.-CF4 has been analyzed in SEM-EDS for PGM and BMS and represent foot wall host rock of Zone-1a, and overall foot wall host rock sample has been study by SEM-EDS after heavy liquid separation for noble metals

HR: Host Rock *(triangle)*, SmO: Semi-massive ore *(square with gray fill)*, SpO: Spotted ore *(circle)*, MO: Massive ore *(square)*; samples are mentioned from foot wall *(solid)* to hanging wall *(hollow)* side of massive ore for individual sections; 1: Kathpal, 2: Kalarangitta, Samples analysed '–'

For better understanding of chromite related PGE mineralization, it is imperative to know about the associated rocks hosting this mineralization. It has been mentioned in the previous chapter that the host ultramafic rocks are almost completely altered by serpentinization. This process of serpentinization not only obliterated the primary mineralogy of the host rocks but also responsible for the possible geochemical changes. The serpentine mineralogy has initially been studied by using simple petrological microscope followed by XRD studies and EPMA analysis. This is necessary to make an idea about the parent mineral: olivine and pyroxene (mainly orthopyroxene). The aim is also to know if there is any difference in the host rock mineralogy of the chromite ore from Kathpal and Kalirangatta areas and also the difference between footwall and hangingwall. Few selected samples were analysed for number of trace elements to discriminate varieties, if any, of serpentinized ultramafic rocks. The trace element signatures are also used for understanding genesis of the host ultramafics.

3.1 PETROGRAPHY
3.2 MINERALOGY
3.3 GEOCHEMISTRY

3.1 PETROGRAPHY

In general, the minerals associated with the ultramafic host may be divided into four major varieties:

i. Silicates: mostly serpentine and other alteration products of primary olivine and pyroxene
ii. Oxide: chromite
iii. Secondary oxides and hydroxides: hematite and goethite
iv. Sulfides/Arsenides: very fine grained and mostly not identifiable under microscope

Silicates are mainly represented by the serpentines formed after the primary olivine and pyroxene. Antigorites are the common serpentine. Cr-chlorite is also present in some sections. Along shear planes development of fibrous chrysotiles are observed. In most of the cases, the original grain boundaries of primary silicates are not preserved due to pervasive serpentinization causing almost complete homogenization of the rock. All gradation of textural varieties of serpentine *i.e.* meshwork (Fig.3.1.i), ribbon type (Fig.3.1.ii) and bladed mat textures (Fig.3.1.iii) are observed. Only very rarely the relict silicates (olivine and/or pyroxene) are visible in the core of the pseudomorphs (Fig.3.1.iv) which are also otherwise filled with serpentine (Fig.3.1.i). The EPMA analysis of relict olivine is given in Table . The olivine is highly Mg-rich and fosterite content is about 95% indicating crystallization at very high temperature and from Mg-rich magma. The serpentine cords, around core, are having definite orientation. Zone-2 host rocks are dominated by a bladed mat texture indicating maturity of serpentinization process. The trails of opaques (Fig.3.1.iii) formed by the release of iron during serpentinization are oriented parallel to the cords.

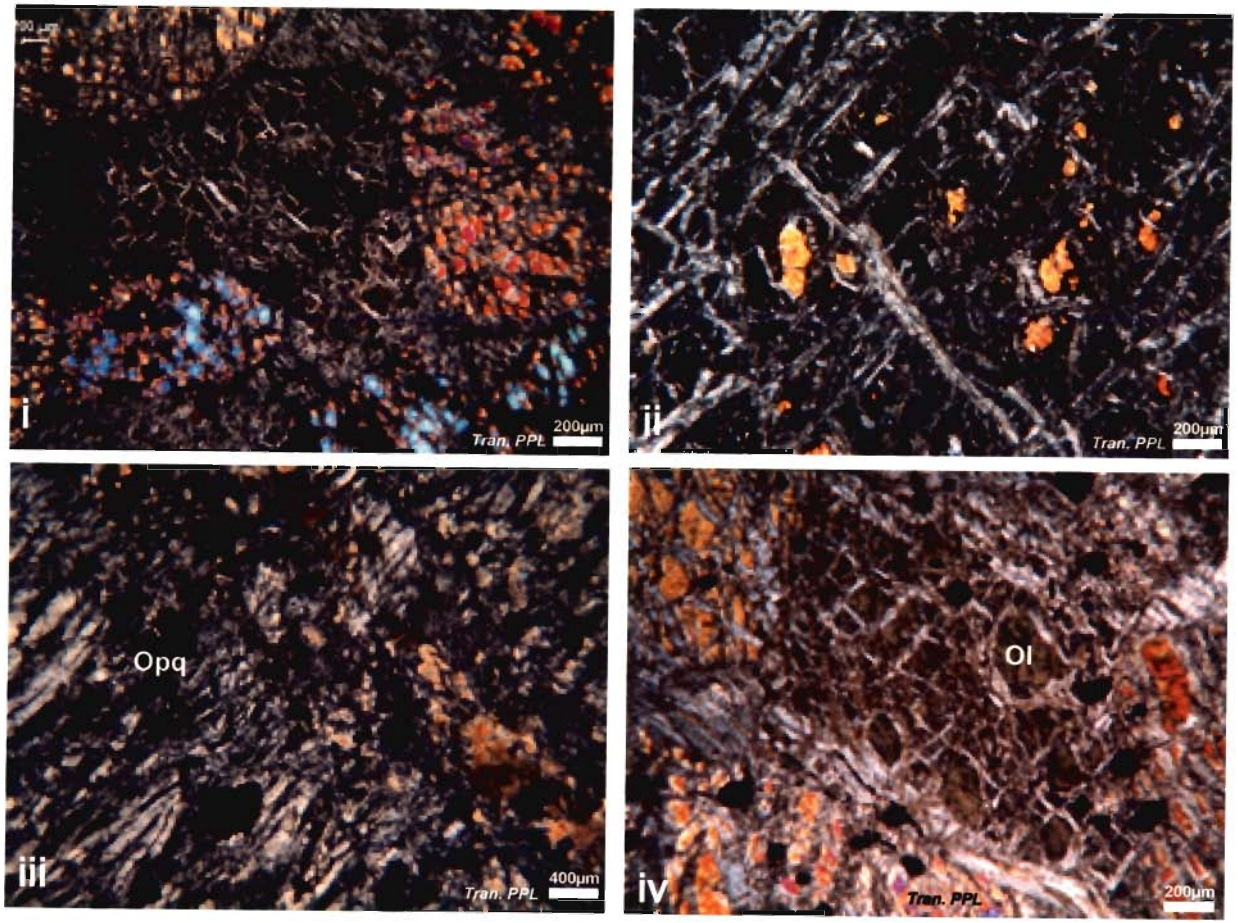

Fig.3.1.i-iii Photomicrographs of different textural varieties of serpentine i. Meshwork, ii ribbon, iii bladed mat iv Photomicrographs of relict olivines in partially serpentinized dinites

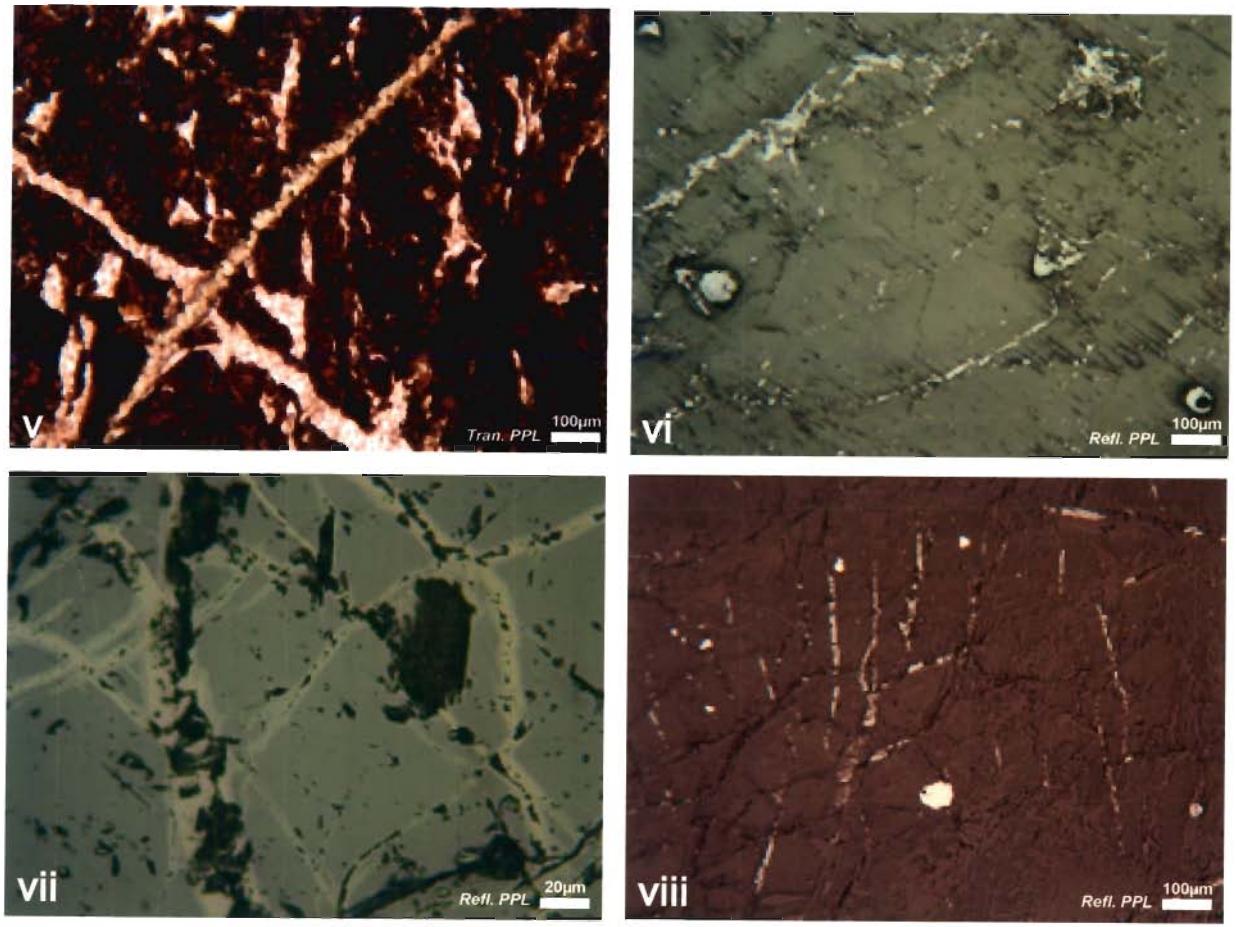

Fig.3.1. v Photomicrographs of sheared chromite ore of Kalarangitta area, vi Photomicrographs of haematite within serpentinized host rock vii Photomicrographs showing different stages of alteration along fractures within chromite grains, viii Photomicrograph showing remobilised stringers of haematite within serpentinized ground mass along with sulfides

3.2 MINERALOGY

Though, it is already mentioned that almost all the litho-units are mono-mineralic or bi-mineralic in composition, it is very difficult to know the exact mineralogical composition of the original ultramafic host due to pervasive serpentinization. Hence, the serpentinized host rocks, excluding limonitized ones, have been investigated for a qualitative idea about the mineralogical composition using XRD method. Samples of host rock along with massive ore, spotted ore, were selected from the representative sections. The samples were crushed to –200 mesh size and analyzed by a *PHILLIPS* make XRD instrument. The target used for the analyses is CuK_{α} and the 2θ ranging between 5° to 60°.

Lithological discrimination of the samples was apparent from the XRD patterns reflecting the approximate proportion of Cr-ore and silicate gangue (Fig.3.2). Altered host ultramafics shows prominent peaks of serpentine around 2Θ values of 12°, 19°, 25°, 36°, 38°, 51° and 59° and, Cr-chlorite 6°, 12°, 19° and 25°. The massive chromites show intense peaks of chromite in the 2Θ range of 18°, 30°, 35°, 43°, 54° and 58°. The spotted varieties show an overlap in the XRD pattern of the host rock and massive ores with moderate peak intensities for serpentine and Cr-chlorite compared to the host rocks, and for chromites compared to that of massive chromite ores. Kathpal ultramafics shows different stages and/or intensities of alteration compared to the main SUC (Kalarangitta) as evident from the number and intensities of the peaks of different mineral species. However, Serpentine and Cr-chlorite peaks of massive ores from Kalarangitta area are more prominent than the massive ores of Kathpal area which may be due to the intense crushing and alteration

Table 3.1 EPMA results of Serpentine

	KATHPAL				KALARANGITTA					
	DM-11	DM-13	DM-14	DM-15		DM-22			DM-24	
	1	2	3	4	5	6	7	8	9	10
SiO_2	35.20	42.10	42.09	42.41	43.31	42.90	42.23	45.23	45.13	44.33
Al_2O_3	0.10	-	-	-	1.02	0.40	0.46	0.43	0.51	0.81
FeO	2.27	1.17	2.24	1.30	1.43	1.94	1.82	0.74	0.76	0.76
MgO	37.17	43.70	42.92	43.96	40.46	40.64	41.26	40.95	41.24	40.48
MnO	0.03	0.05	0.04	-	-	0.02	0.02	0.01	0.00	0.00
CaO	0.44	0.04	0.07	0.04	0.01	-	0.00	0.01	-	0.01
K_2O	0.15	-	-	-	-	0.00	0.00	-	-	-
Na_2O	-	0.03	-	-	-	-	-	-	-	-
TiO_2	0.02	0.03	0.03	0.01	0.02	0.00	0.01	-	-	0.00
NiO	0.28	0.82	0.20	0.10	0.17	0.13	0.18	0.12	0.11	0.11
Total	75.67	87.93	87.58	87.82	86.42	86.03	85.98	87.48	87.75	86.50
Si	3.83	3.90	3.92	3.92	4.04	4.04	3.98	4.14	4.12	4.11
Al	0.01	-	-	-	0.11	0.04	0.05	0.05	0.06	0.09
Fe	0.21	0.09	0.17	0.10	0.11	0.15	0.14	0.06	0.06	0.06
Mg	6.03	6.03	5.96	6.05	5.62	5.70	5.80	5.59	5.61	5.59
Mn	0.00	0.00	0.00	-	-	0.00	0.00	0.00	0.00	0.00
Ca	0.05	0.00	0.01	0.00	0.00	-	0.00	0.00	-	0.00
K	0.02	-	-	-	-	0.00	0.00	-	-	-
Na	-	0.00	-	-	-	-	-	-	-	-
Ti	0.00	0.00	0.00	0.00	0.00	0.00	0.00	-	-	0.00
Ni	0.02	0.06	0.01	0.01	0.01	0.01	0.01	0.01	0.01	0.01
Total	10.17	10.10	10.08	10.08	9.90	9.94	9.99	9.84	9.85	9.85

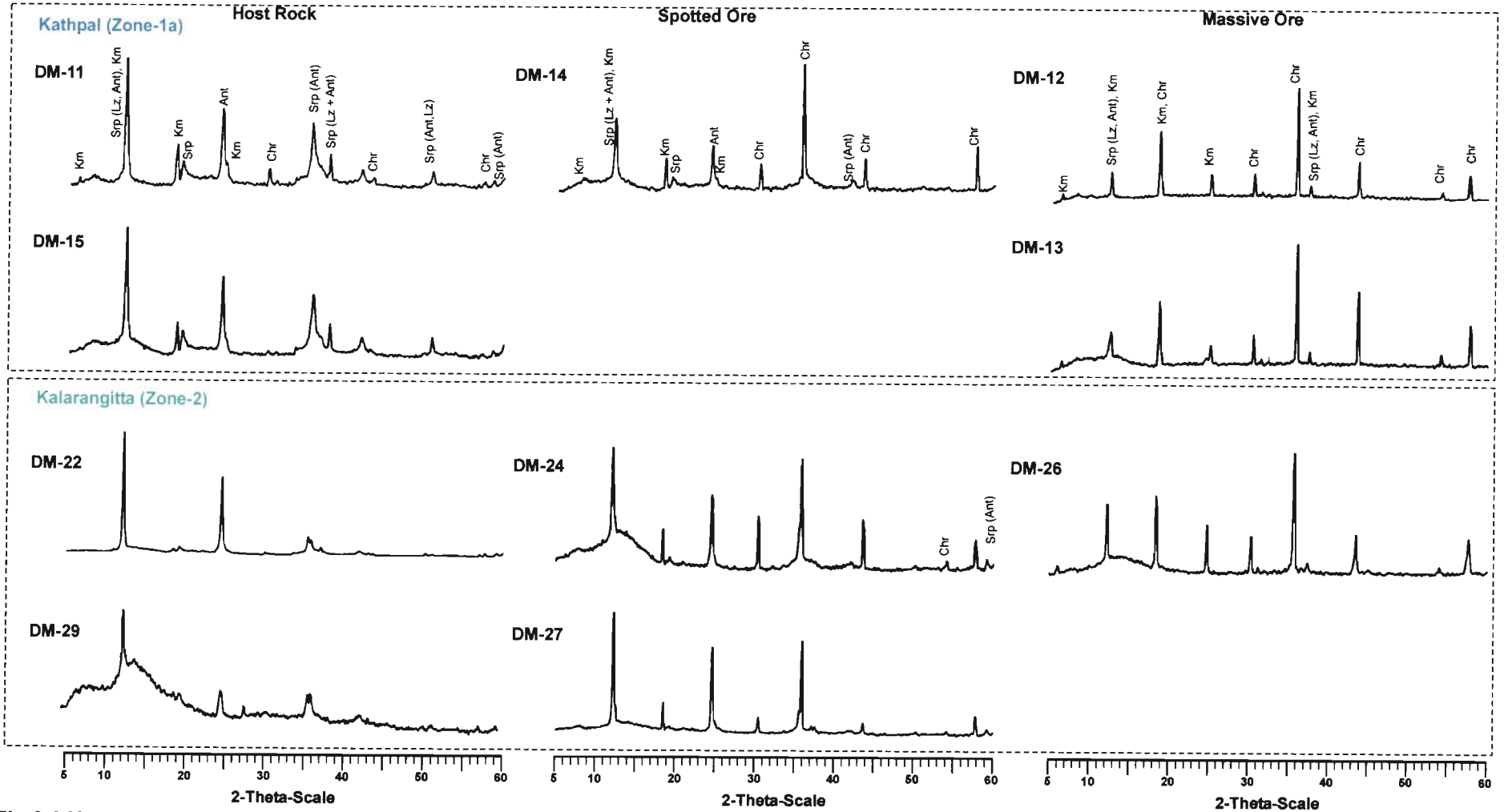

Fig.3.2 XRD results of serpentinized host rocks, spotted ores and massive ores from Kathpal (Zone-1b) and Kalarangitta (Zone-2)

along the shear zone across the central part of the ore body (Fig.3.1.v and Fig.2.3.vii).

Serpentine composition, in some selected points, was determined using *JEOL (Superprobe: model JXA-8600 M)* make Electron Probe Micro Analyzer (EPMA) and are shown in Table 3.1. The values are calculated on the basis of 14 oxygen atoms. The SiO_2 ranges from 45.23 to 42.09, Al_2O_3 from 0.40 to 1.02, MgO from 40.46 to 43.70, FeO_t from 0.74 to 2.24 and NiO from 0.10 to 0.82 wt%. Composition of all the analyzed matches very well with the serpentine minerals and the total oxide percentage varies between 85.98 and 87.93 wt%. This indicates that the effect of serpentinization on the silicate minerals of both host rock and the chromite ores is extensive. Antigorite is the main variety of serpentine. Comparison between the serpentine and the olivine composition (Chapter-4) shows the removal of MgO (and FeO) from the system and followed by formation of magnesite along the cracks and fractures at places.

Chromite is present as a common accessory mineral, both in footwall and hanging wall rocks and is < 5% by volume. The accessory chromite is normally fine (0.5-1.0 mm) in size and irregular to round in shape with corroded boundaries and pitted surfaces. Due to Fe-enrichment, the accessory chromite grains show higher reflectivity compared to ore chromite (detail in Chapter-4). Unlike the ore chromite, the accessory chromites are greatly affected by the alteration process related to serpentinization resulting, partial to complete, conversion of chromite into hematite (Fig.3.1.vi) and/or goethite. Multistage alteration of the original rock can be traced out from the different alteration rims formed along the fractures within the chromite grains

(Fig.3.1.vii). Hematite is also produced from the 'Fe' released from silicates during serpentinization and, is present mainly as fine dots and specks inside the silicate mass. At places, it is remobilized (Fig.3.1.viii) within serpentinized groundmass as stringers.

The sulfides are present in host ultramafic in very small quantity, <1%, by volume. The fine sulfide grains are normally <5μm in size. However, relatively larger sulfide grains, 20-50μm, are also found. Heazlewoodite is the most common sulfide mineral. In general, sulfide minerals are relatively more abundant and also coarser in the hanging wall rock compared the footwall counterpart.

3.3 GEOCHEMISTRY

The analyses of trace elements are mainly constrained by their low absolute abundances and heterogeneous distribution in the geological samples. Now-a-days, ICP-MS is widely used for determination of the trace elements (Jarvis *et al.* 1992, Balaram 1995, Balaram 2001).

In the present study, a total of ***ten*** serpentine samples, five each from footwall and hanging wall representing Zone-1b-e and Zone-2 along with one sample each from partially altered dunitic peridotite, noritic gabbro and dolerite are analyzed for were analysed for trace element composition (Table-1.1, Chapter-1). In total **33** trace elements including REEs and Transition metals are analysed using acid digestion technique (Balaram *et al.* 1995) with *Perkin-Elmer Sciex* make, *Elan DRC II – ICP-MS* at National Geophysical Research Institute (NGRI), India. The details of the instrument and operating parameters and the procedure followed is mentioned in Balaram & Rao 2003.

The standard used for the calibration of the instrument for the serpentine samples is UB-N except for norite and dolerite for which NIM-P is used. The internal standard used to correct for signal drift during analysis is 1ppm Rh solution. Trace element results are shown in Table 3.2.

The Primitive Mantle (PM, Sun & McDonough 1995) normalized trace elements were plotted in spider diagram and shown in Fig.3.3.i. The trace elements are showing concentration level between 1 to 0.1 times with respect to PM. Only few elements, Cs, Rb, Th, U, Ta (partially) & Cr are enriched compared to PM. The level of enrichment of incompatible elements (Cs, Rb, Th, U, Ta) is less than 10 times and is consequence of serpentinization. The trace element concentration of hangingwall and footwall rocks shows more or less similar pattern. The PM normalized plot of transition elements reveals that the serpentinites are enriched in Cr. The Ni and Zn content of serpentine are same as PM and substantially depleted in Sc, Cu, V and Co (Fig.3.3.ii). The high value of Cr is a positive signature of anomalous Cr concentration in the parent magma *i.e.* at the source.

The C1-chondrite normalized REE plot shows the REE values of the serpentine are more or less close to 1 (Fig.3.3.iii). There is no difference in REE trends between the hangingwall and footwall rocks. The $(La/Sm)_{CN}$ is > 1 and varies between 1-3 times (average is close to 2). A small but distinct negative Eu anomaly is noted in the host rock (Fig.3.3.iii). The overall REE pattern and the concentration level of REE of the host rock match very well with that of ultramafic rocks from ophiolite complexes. The REE trend of a rare partially serpentinized dunite shows that the pattern is bowel or saucer

Table 3.2 Trace element concentrations of chromitite hosted serpentinized ultramafic rocks of Sukinda

Sample No.	KATHPAL (Zone-1)								KALARANGITTA (Zone-2)		Dolerite	Norite	Dunite	Primitive Mantle*	C1 Chondrite**
	Zone-1b		Zone-1c		Zone-1d		Zone-1e								
	DM-11	DM-15	DM-16	DM-20	DM-98	DM-101	DM-102	DM-104	DM-22	DM-28	DM-84	DM-85	DM-86		
Cs	0.029	0.04	0.019	0.039	0.24	0.039	0.04	0.094	0.069	0.055	0.171	0.055	0.011	0.0079	0.19
Rb	1.175	0.867	1.081	1.38	2.811	0.787	0.898	1.955	2.195	1.649	1.622	0.448	0.244	0.635	2.3
Ba	12.125	23.578	10.902	20.954	16.328	14.665	15.539	16.584	15.416	18.332	31.583	7.454	5.154	6.99	0.00241
Th	0.115	0.094	0.035	0.184	0.17	0.091	0.126	0.127	0.096	0.195	1.004	0.067	0.009	0.085	0.029
U	0.093	0.073	0.052	0.105	0.125	0.09	0.125	0.132	0.073	0.09	0.039	0.007	0.019	0.021	0.0074
Ta	0.023	0.053	0.038	0.143	0.081	0.034	0.05	0.041	0.042	0.042	0.38	0.024	0.003	0.041	0.0136
Nb	0.178	0.083	0.111	0.09	0.724	0.293	0.289	0.278	0.138	0.183	0.979	0.458	0.022	0.713	0.24
La	0.503	0.629	0.202	0.77	0.695	0.251	0.526	0.403	0.562	0.594	1.012	0.093	0.052	0.687	0.237
Ce	1.09	1.491	0.394	1.963	1.436	0.521	1.183	0.753	1.106	1.133	1.994	0.151	0.098	1.78	0.613
Pr	0.143	0.194	0.056	0.225	0.213	0.08	0.177	0.1	0.154	0.173	0.186	0.015	0.014	0.276	0.0928
Sr	6.478	6.061	4.645	7.739	6.051	6.212	4.244	6.745	5.831	5.508	9.674	2.343	3.292	21.1	7.25
Nd	0.577	0.821	0.241	0.859	0.843	0.369	0.726	0.417	0.632	0.761	0.695	0.091	0.05	1.35	0.457
Zr	3.155	4.562	20.786	11.365	11.634	7.607	6.49	6.399	5.077	5.714	6.012	18.422	4.589	11.2	3.82
Hf	0.055	0.087	0.348	0.212	0.236	0.146	0.163	0.169	0.115	0.115	0.153	0.341	0.075	0.309	0.103
Sm	0.127	0.179	0.06	0.183	0.209	0.13	0.218	0.113	0.153	0.17	0.123	0.019	0.018	0.444	0.148
Eu	0.021	0.045	0.019	0.049	0.072	0.035	0.054	0.033	0.059	0.06	0.058	0.011	0.006	0.168	0.0563
Gd	0.172	0.236	0.074	0.257	0.301	0.189	0.358	0.167	0.246	0.282	0.177	0.042	0.025	0.596	0.199
Tb	0.025	0.032	0.016	0.033	0.064	0.034	0.062	0.029	0.041	0.042	0.014	0.003	0.003	0.108	0.0361
Dy	0.141	0.17	0.079	0.179	0.353	0.207	0.437	0.168	0.252	0.272	0.094	0.032	0.015	0.737	0.246
Y	1.081	1.027	0.56	0.937	2.584	1.541	3.086	1.173	1.612	1.743	0.995	0.362	0.148	4.55	1.57
Ho	0.032	0.038	0.016	0.033	0.089	0.051	0.101	0.036	0.059	0.065	0.017	0.005	0.005	0.164	0.0546
Er	0.101	0.13	0.059	0.106	0.289	0.181	0.324	0.13	0.189	0.195	0.068	0.027	0.018	0.48	0.16
Tm	0.017	0.019	0.008	0.018	0.046	0.033	0.062	0.02	0.028	0.034	0.008	0.005	0.004	0.074	0.0247
Yb	0.125	0.121	0.065	0.096	0.281	0.2	0.365	0.14	0.177	0.197	0.106	0.071	0.023	0.493	0.161
Lu	0.018	0.013	0.012	0.016	0.044	0.03	0.063	0.024	0.026	0.025	0.012	0.008	0.004	0.074	0.0246
Ga	1.329	1.949	1.066	1.632	2.125	2.068	2.285	2.992	1.956	2.155	3.367	2.04	0.498	4	9.2
Sc	6.008	6.383	5.686	6.573	9.073	8.519	10.906	7.293	8.79	8.569	13.765	11.786	5.828	17.1	5.92
Cu	14.252	25.414	30.13	16.348	9.764	10.7	11.784	10.859	20.607	27.583	33.42	7.639	13.208	30	120
V	19.165	17.942	18.34	16.807	30.8	29.585	31.605	38.802	31.125	34.095	84.014	73.014	21.326	82	56
Zn	60.181	39.831	45.137	82.123	38.863	35.941	33.014	33.781	47.142	84.064	97.244	43.647	30.601	56	310
Cr	3544.72	2809.11	6278.94	3170.72	7121.12	4887.25	6777.697	16371.36	5126.95	5063.58	15361.5	16243.2	711.181	2940	2650
Co	46.635	53.089	27.498	50.039	44.442	60.664	21.357	36.072	44.485	73.201	89.261	96.921	115.749	110	500
Ni	2226.76	2029	2123.25	2085.85	1578.6	1765.13	2171.386	1429.526	1631.95	1953.37	641.397	629.295	2263.38	1890	10500

All values are in ppm, *Sun and McDonough (1989), **McDonough & Sun (1995)

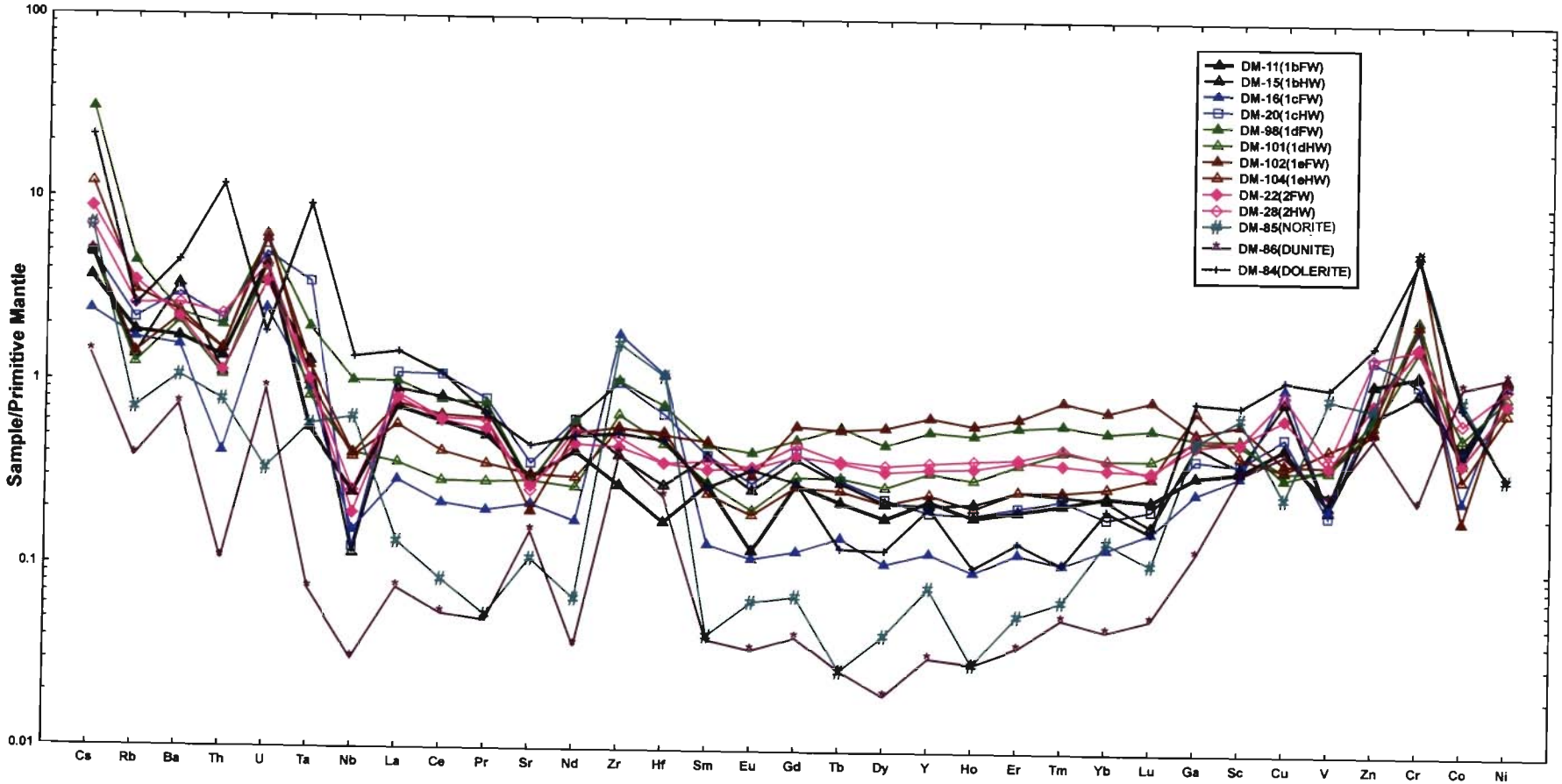

Fig.3.3.i Primitive Mantle normalized *(values after Sun & McDonough 1989)* **trace element plot of serpentinized host ultramafics of chromitites**

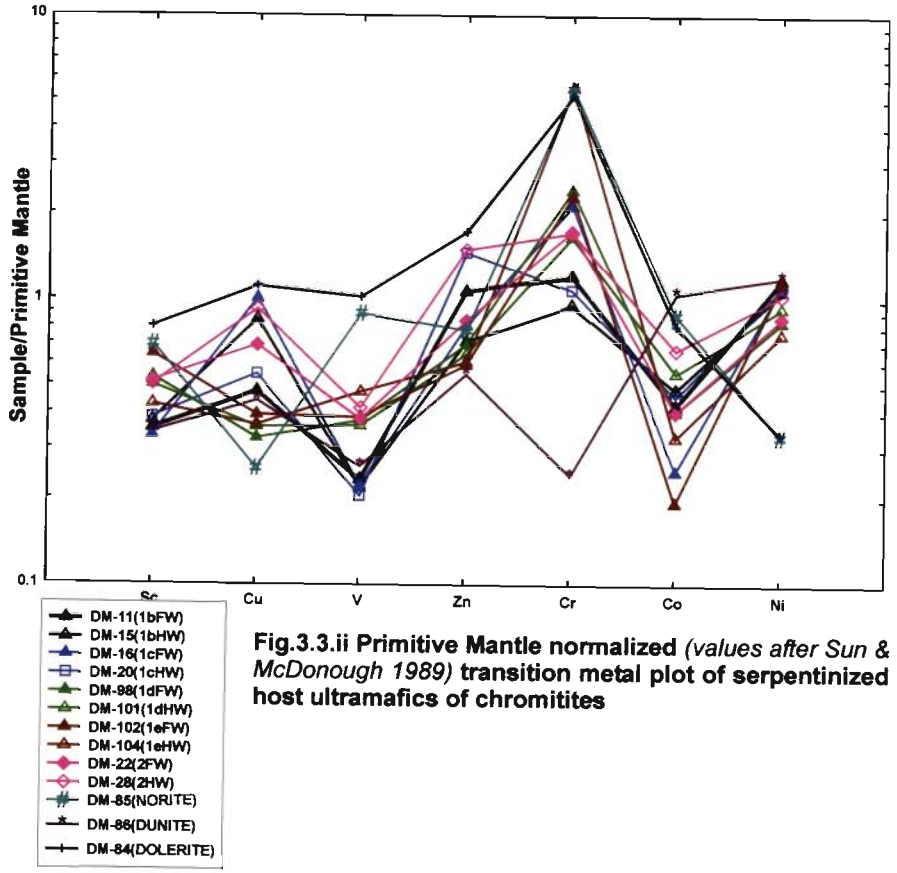

Fig.3.3.ii Primitive Mantle normalized *(values after Sun & McDonough 1989)* **transition metal plot of serpentinized host ultramafics of chromitites**

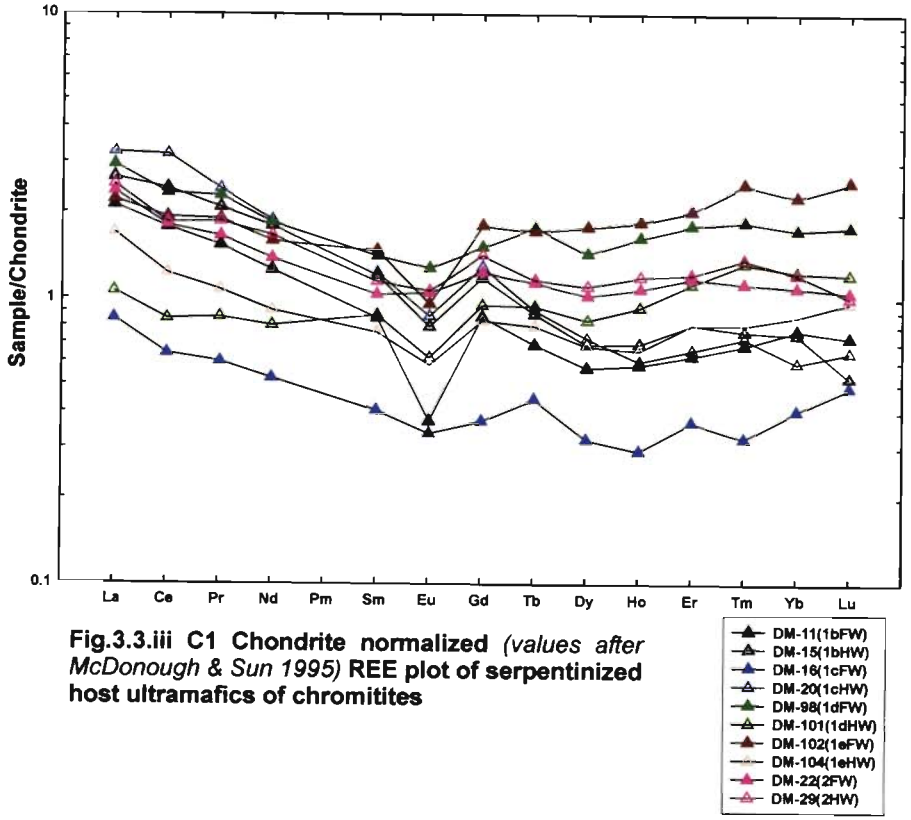

Fig.3.3.iii C1 Chondrite normalized *(values after McDonough & Sun 1995)* **REE plot of serpentinized host ultramafics of chromitites**

shaped and the concentration level is close to 0.1. This type of pattern and concentration level is also observed in dunite/harzburgite from ophiolite complexes (Menzies 1976). The LREE level in this sample is also little higher compared to HREE but this small but distinct LREE enrichment may be again due to the effect of serpentinization (Frey 1969, Suen *et al.* 1979), though opposite view has also been expressed (Henderson 1989). The geochemical distribution of PGE in host rock and its bearing in PGE mineralization is being discussed in Chapter-5.

The serpentinization process has almost completely altered host ultramafic rocks in SUC. The very high forsterite (<95%) content of remnant primary olivine in serpentinized dunite points out to Mg-rich source magma and crystallization at high temperature. The fine-grained (0.5-1.0mm) accessory chromite with corroded boundaries constitutes <5% by volume. The accessory sulfide minerals, mostly Ni-rich, are present both as relatively larger specks of 20-50 microns size and also as very fine dust homogeneously distributed within the silicate groundmass. The earlier group may be of magmatic origin whereas the later variety is certainly product of serpentinization process. The trace elements composition of the host serpentine largely follows the trends of such rocks reported from serpentinized ophiolite complexes around the globe. The host rock is anomalously enriched in Cr and, Cu and Ni-content similar to mantle value. The low-level enrichment of incompatible elements (Cs, Rb, Th, U, Ta) perhaps resulted from serpentinization process. The C1-chondrite normalized REE values of the host rock is bowel or saucer shaped and the concentration level is between 1.0 to 0.1 with a small but distinct negative Eu anomaly characteristics of

ultramafic rocks from ophiolite complexes signifying absence of Ca-rich phases in the rock, e.g. plagioclase. The late serpentinization process might have an overprinting relation on the magmatic differentiation signatures in terms of trace and REE geochemistry of the host ultramafics.

Being one of the most resistant phases at low temperature, Cr-spinels are treated as a suitable petrogenetic indicator for the parent melt of the associated ultramafics. Cr-spinel composition is sensitive to physico-chemical conditions prevalent during its crystallization and indicative of contemporaneous geodynamic conditions. Hence, the variation in Cr-spinel composition keeps record of the tectono-magmatic evolution of any complex. The role of Cr-spinel as a petrogenetic indicator becomes increasingly important in the virtual absence of any other unaltered primary mineral species in thoroughly serpentinized peridotitic complexes like SUC. The petrographic and Cr-spinel composition of different varieties of chromite are studied in detail for the assessment of the parent melt composition and the prevalent physico-chemical condition and their controls on the PGE mineralization patter, if there is any.

4.1 ORE PETROGRAPHY

4.2 CHROME SPINEL COMPOSITION

4.1 ORE PETROGRAPHY

The Cr-spinel content of the ore varies from >90% to about 20-30% by volume. The main chromitite ore is massive (>90%) to semi-massive (90->70%) in nature. Massive/semi-massive ore grades into spotted/banded/laminated ore at the contact zone containing ~50% or less chromite.

4.1.1 Massive/Semi-Massive Chromites

The shape of chromite grains, excepting the ones from Zone-1b, varies from polygonal to round. The massive/semi-massive ore from Zone-1b&c and Zone-2 is medium grained (1-2mm) and from Zone-1d it is finer, about 0.5 mm, in size. In Zone-1e, the chromite crystals are 0.1-1.0 mm in size and affected by fracturing. Chromite crystals show blood red colour under plane polarized transmitted light (Fig.4.1.i). Massive chromites show characteristic *cumulus* texture. Well-developed polygonal chromite grains and formation of triple junctions (Fig.4.1.ii) are characteristics of the massive ore from Kathpal mine (Zone-1b). Here, the postcumulus silicates forming the intercumulates does not exceed 7% of the total volume hence assigning an adcumulate texture to these ores. It is apparent that the tectonic conditions are more stable during the formation of such layers. The chromite ore from Zone-1d&e is semi-massive and poorer in grade compared to Zone-1b, with a chromite concentration varying between 60-80% by volume (Fig.4.1.iii). The texture indicates that the chromite crystals are not completely segregated to form the massive ore. The silicates occupy the intergranular spaces indicating cooling and consolidation before complete gravity settling of the chromite crystals. Consequently the texture varies from *mesocumulate* (*7%-25%* by volume of intercumulus materials) to *orthocumulates* (*25%-50%* by volume of intercumulus materials) and, the grain to grain contact varies from a *'mutual surface of contact'* to a *'point contact'* types respectively rather than development of triple junctions (Philpotts 1994). Grain boundary maturation indicated by formation of triple junction is more pronounced in adcumulates>

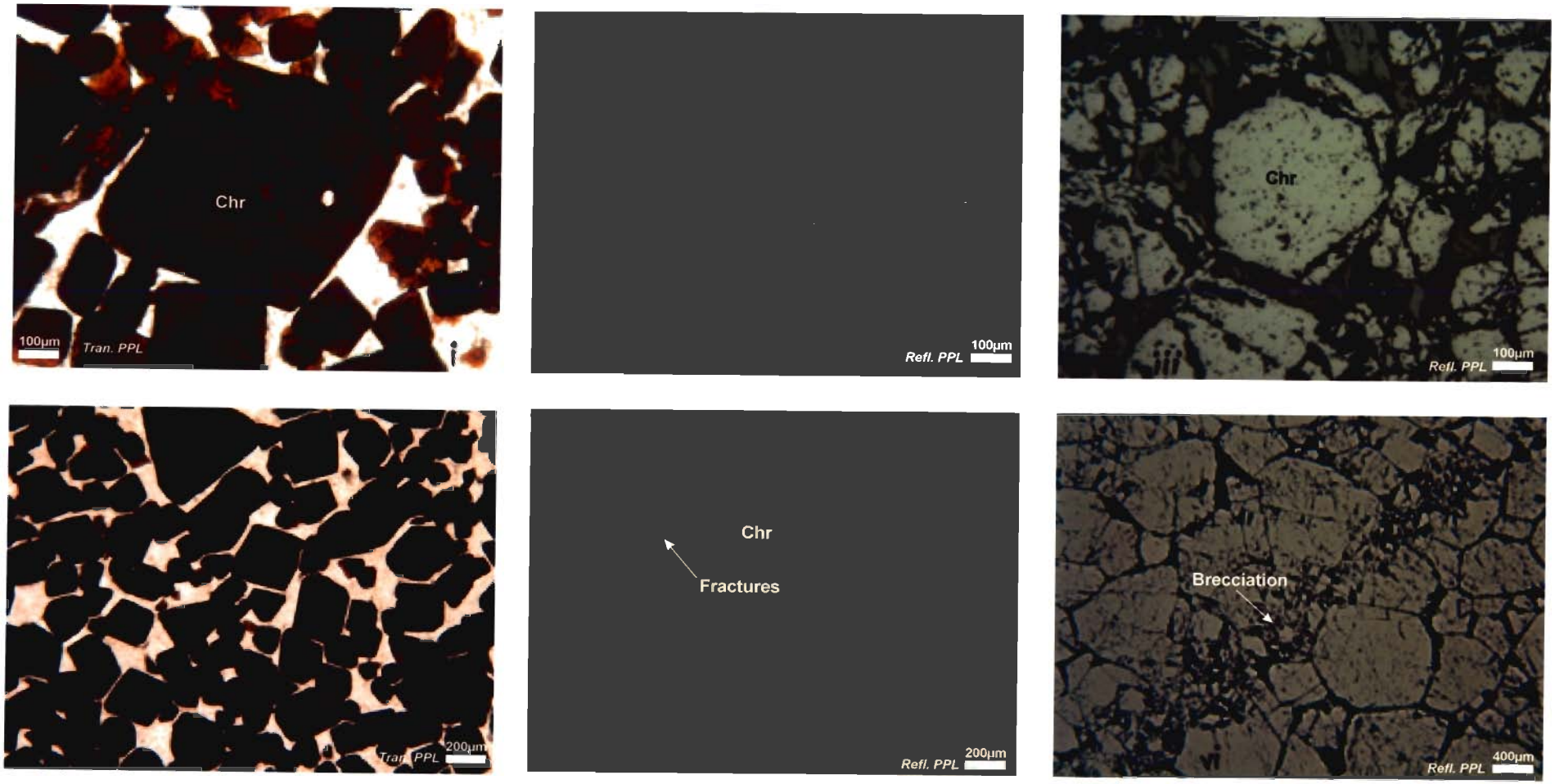

Fig.4.1 Photomicrographs showing i blood red colour of chromite under transmitted light, ii development of triple junction in chromite, iii poor grade chromite ore, iv 'clot' texture in chromite, v fractures confined 'within grain' vi brecciated chromite

mesocumulates> orthocumulates textural varieties. Absence of compositional/optical zoning points out magmatic equilibration and homogenization of these cumulates. The absence of zoning is also supported by more or less uniform chemical composition of individual chromite crystals by EPMA.

The interstitial spaces within the chromite ore are filled with silicates. In certain cases, clusters of subhedral fine grained chromites surrounded by coarser chromite grains to give 'clot' like appearance (Fig.4.1.iv) as described earlier by Mukherjee (1969). The effects of serpentinization on uncrushed massive ores with adcumulate chromite grains are negligible but mesocumulate and orthcumulate chromites sometimes show corroded boundaries, as the only effect of alteration. Hematite is also almost absent in this ore.

The shape of the primary chromite grains mostly varies from cubic to polygonal. Some grains are fractured and the fractures are characteristically confined within the individual grains keeping the outline intact. These fractures might have been developed in a quasi-solid state (Fig.4.1.v) and might have formed in response to the uprise of the melt. These fractures, which are restricted within individual grains, might have aided in post consolidation fracturing thereby intensifying the effects of serpentinization. In many cases, fine fragmentation of coarser chromite crystals (Fig.4.1.vi) and pull-apart textures are manifested due to post consolidation brecciation. These fractures are also filled up with serpentines. The grey chromite ores from Zone-2 is massive, although the primary shape of chromite grains has been obliterated by intense mylonitisation (Fig.3.1.v, Chapter-3), resulting in crushing and

fining of the ore. A well-developed shear zone passes through the central part of this ore body. It can easily be inferred under microscope that the original adcumulate texture of massive and crystalline ore has undergone modification by the invasion of hydrothermal fluids through these fractures. Development of silicate gangue within the fractures is very well preserved indicating that these fractures are the probable channel for movement of fluids for massive post-magmatic serpentinization. Variation in grain shape and size of chromite ore is due to many factors and can be divided mainly into two groups: *syncrystallization conditions* and *postcrystallization modifications* as follows (in chronological order):

Syncrystallization Conditions

- Availability of Cr in the source magma
- fO_2 condition
- Temperature and pressure of crystallization
- Availability of space during simultaneous crystallization of Cr-spinel and silicates

Post-crystallisation Modifications

- Mechanical crushing during shearing
- Serpentinization resulting corrosion and also fracturing due to volume expansion.

Rare occurrence of sulfides in the ore proper (Fig.4.1.vii) may be due to the lower values of initial concentration in the parent magma and higher fO_2 condition, and is resistant to serpentinizing fluids. However, the grey ores of Zone-2 show relatively more concentration of sulfides, which may be

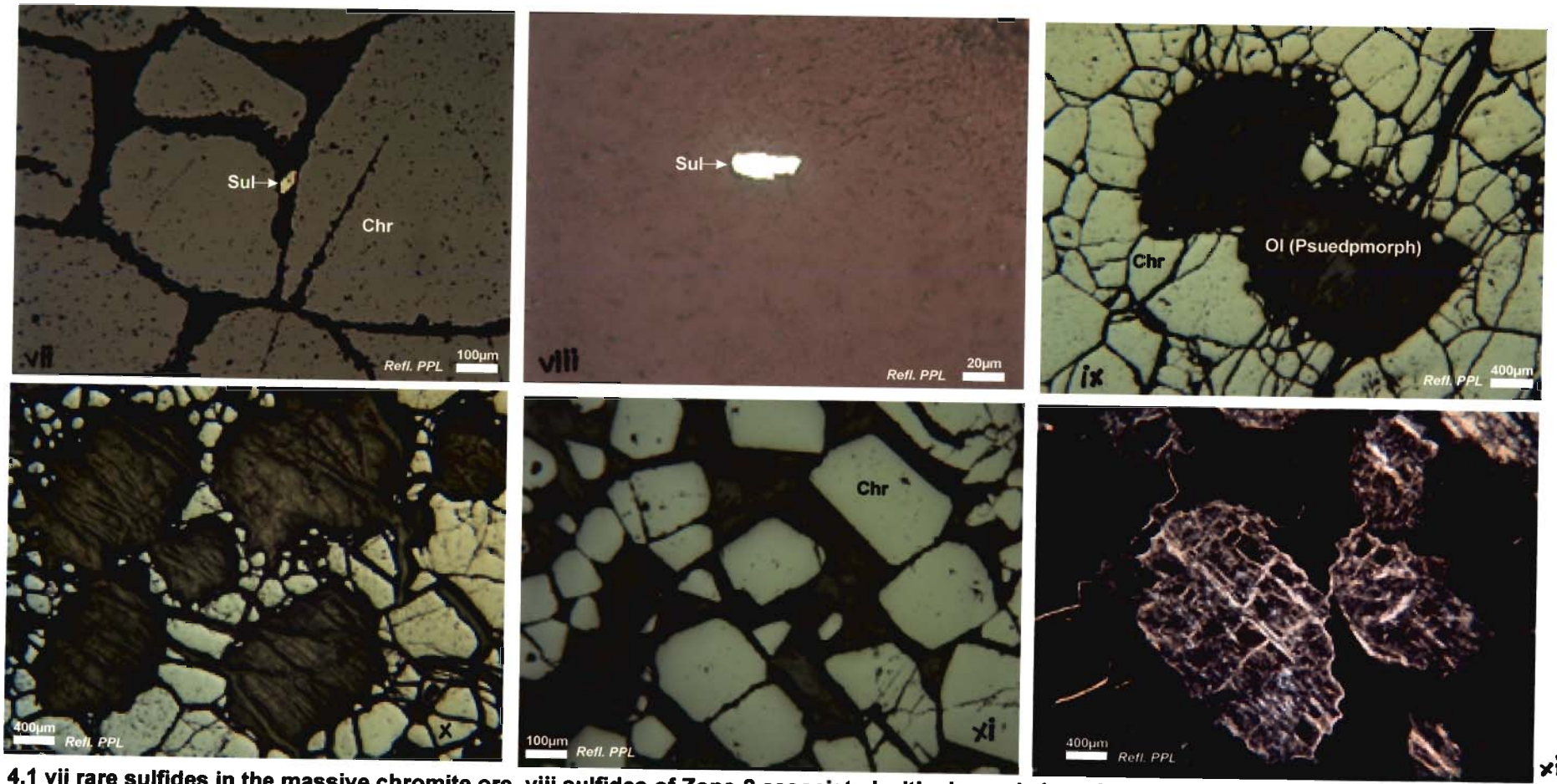

4.1 vii rare sulfides in the massive chromite ore, viii sulfides of Zone-2 associated with sheared chromite, ix 'eye' texture of psuedmorphs after occluded olivine grains, x 'synneus' texture in spotted chromites, xi 'mesocumulate' chromite ores, xii development of serpentine along fractures in olivine

attributed to the late magmatic fluid invasion through the fractures developed in the ore (Fig.4.1.viii).

The silicates (olivine and/or orthopyroxene) occur as occluded grains in the form of *'eyes'* in massive ores of Zone-1b that has originally crystallized as cotectic cumulates are slightly larger in size (2-3 mm) compared to chromite grains (Fig.4.1.ix). This is attributed to the faster growth of the olivine crystals with their *a-axis* normal to the surface of accumulation compared to others during phases of slow accumulation.

Signatures of oscillatory fO_2 conditions can be inferred from the presence of thin silicate (mostly olivine-rich) bands within the ore lens of Jungle pit (Fig. Ch-3). Silicate inclusions within chromite grains are found in some semi-massive chromite ores signifying the presence of early-formed silicates, a dominant feature of chromite deposits of ophiolitic origin (Johan *et al.* 1982).

4.1.2 Gradational Facies: Spotted/Banded Chromite

In spotted ores, the chromites crystallize as intercumulates from the post cumulus liquids. The grain size variation of chromites here are the best examples of variations due to availability of space. The chromites at the triple junction of olivine pseudomorphs are larger than those along the contact of two pseudomorphs. The gradation of massive/semi-massive ore into spotted ore indicates gradual change in P-T-X conditions. Most of the observed contact zones, except that of -40RL of Jungle pit, are marked by the presence of spotted/banded ore. An abrupt change in P-T-X conditions in this particular case compared to others may be postulated as a possible explanation.

Development of chromites around coarser oval silicate psuedomorphs in the form of weakly to well-developed chains, variously known as Synneus Texture (Fig.4.1.x)/Network Texture, are dominant in these ores. Probably with the decrease in fO_2, silicates *i.e.*, olivine appear as the major cumulates phase and the massive chromite ores grades to spotted variety through banded variety at the contact zones. At places thin (1-1.5cm) but persistent laminations are found along the contact zone. In case of spotted varieties, silicates are represented by the oval to rounded psuedomorphs after olivine, megascopically imparting 'clot' like structure to the ore. At places, it shows mesocumulate grains of chromite in silicate groundmass (Fig.4.1.xi). Outline of the original silicates are preserved by the intercumulus chromite grains surrounding it and the fracture patterns within those are marked by the development of serpentine flakes/fibres (Fig.4.1.xii). In few cases, effects of shearing are preserved and manifested by development of fibrous silicates (Fig.4.1.xiii). Finely bladed mat texture is also observed in this ore (Fig.4.1.xiii).

Extensive serpentinization is indicated by complete homogenisation of the groundmass to form a non-psuedomorphic texture and development of fractures due to volume expansion. Subsequent remobilisation of haematites (Fig.4.1.xiv) and sulfides (Fig.4.1.xv) to form trails, are indicative of migration of the fluid phase (Fig.4.1.xvi) through these fractures.

Summarily, the ore body and the enclosing rocks (Chapter-3) do not show any appreciable variations in mineral composition and texture between two mining levels –40RL and –65RL of Jungal Pit, Kathpal. This at least in part confirms that these are not much affected by the surfacial weathering,

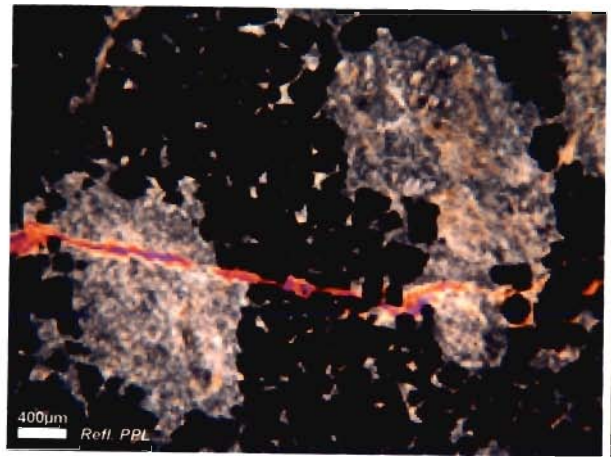

xiii

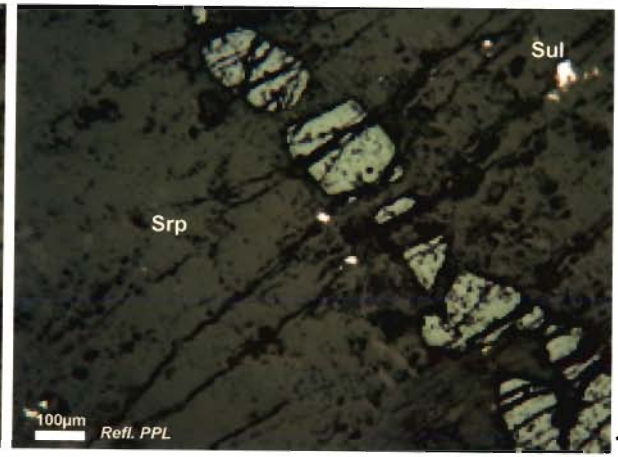

xv

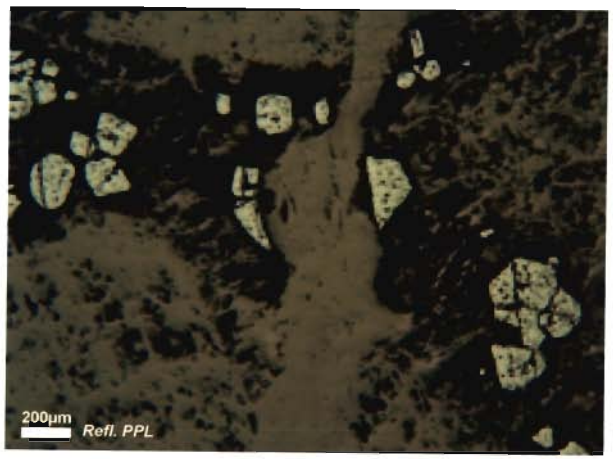

xvi

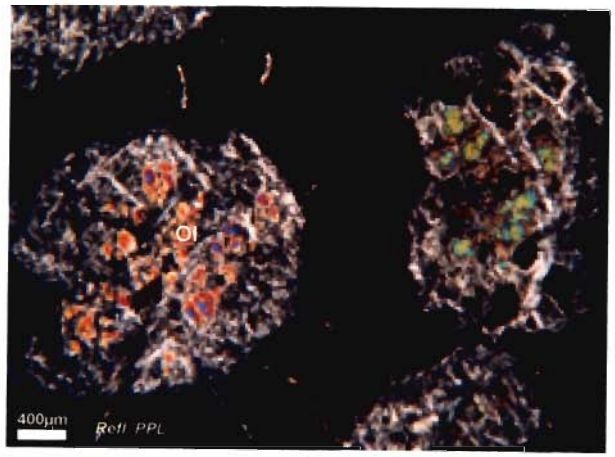

xvii

Fig.4.1.xiii fibrous silicate developed due to shearing, xiv trails of haematite formed by serpentinization, xv remobilised sulfides, xvi fracturing of chromite during late stage serpentinization, xvii relict olivine found in spotted chromite ores

rather suffered massive serpentinization by the deep-seated late magmatic fluids. The silicates are normally alteration product of primary olivine and pyroxenes produced by serpentinization process. Though the pseudomorphs after olivine and pyroxenes are common, rare occurrence of relict islands of these two minerals has also been noticed. The relative proportion of the chromite and the silicates decides the ore body. The massive/semi-massive ores are generally constituted of >70% chromite by volume and spotted/ banded varieties of contact zone constituted of 50-70% chromite by volume. The Cr-spinel content of the host rock is <5% by volume. Though less pronounced and rare, alteration of chromite grains of massive ore along fissures and fractures are noted. However, Cr-spinels, present as accessory mineral phase in the enclosing rocks, are very much affected by alteration process causing partial to complete destruction of the primary Cr-spinel grains to form hematite. Presence of hematite and/or goethite in the silicate is very common. Sulfides are very less in quantity and barely crossing 1% by volume. However, close association of sulfides with silicates is very prominent even in the massive ores. The sulfides are mostly yellowish in colour with high reflectivity under reflected light. Normally, they occur as very tiny (few microns) grains.

Gradational variation in the grain size of primary chromite, relative abundances of chromite grains and sulfide grains, level of alteration of Cr-spinel, nature of Cr-spinel (cumulus/intercumulus/mesocumulus) and psuedomorphs after olivine and/or pyroxene , and gradual change from spotted to banded to massive varieties of ore from wall rocks towards the centre of the ore lens, all indicate simultaneous crystallization of both chromite

and silicate (olivine and orthopyroxene) in a relatively stable magmatic environment. Thus, it can readily be inferred that whatever tectonic disturbance that has resulted in the erratic orientation of the chromite lenses in Kathpal (Zone-1) is mainly post-consolidation in nature. A point to be noted here that the orbicular or nodular chromites those are characteristic of podiform chromites of ophiolitic origin are totally absent, at least in the sections studied.

From the above discussion, it is found that almost all the samples show extensive serpentinization excepting those few massive chromite ore which are composed mainly of the only resistance phase *i.e.*, chromite. The different mineral phases show alteration in the order of olivine> orthopyroxene> chromite> sulfides.

The determination of the exact paragenetic sequence is difficult owing to the pervasive alteration of different lithounits. The sequence of crystallization of chromite and olivine/pyroxene is largely dependent on fO_2. The secondary origin of hematite and goethite during serpentinization is documented beyond doubt. However, it is difficult to say the exact sequence of formation of sulfides which may be either magmatic or hydrothermal (related to serpentinization process?). Remobilisation of late magmatic sulfide at a late stage also can not be ruled out. Correct paragenetic evaluation of the sulfide mineralogy is very important as this may be linked to PGE mineralization. A more detailed account on sulfide minerals is provided in Chapter 5.

4.2 CHROME SPINEL COMPOSITION

On the basis of geochemical and geo-tectonic signatures, global chromite deposits are mainly categorized under two major groups *i.e.* stratiform type associated with layered complexes and podiform type associated with ophiolitic complexes (Thayer 1960). The complexes of undoubtedly layered type intracratonic setting are Bushveld Complex (RSA), Stillwater Complex (USA), Skaergaard Complex (Greenland) *etc.* and ophilitic type subduction zone setting are Troodos Complex (Cyprus), Kempirsai massif (Kazak Republic), Oman ophiolites, Pindos Complex (Greece) *etc.*

Stratiform type deposits are mostly associated with the Precambrian authigenic layered complexes of bulk gabbroic composition formed in stable cratonic environment and post tectonic in nature with respect to the regional tectonics. Chrome-spinels from stratiform deposits are characterized by low Cr/Fe_{total} (<2.5), larger variation in Mg# (~0.2-0.7) than Cr# (~0.6-0.8), high Ti content (≤ 1%), high Fe^{3+}:Fe^{2+} (up to about 1) and a general fractionation trend demarcated by upward decrease in Mg content and Cr content of successive layers along the magmatic stratigraphic column and consequent Fe-enrichment.

On the other hand, podiform deposits are in general forms the part of oceanic ophiolitic sequence re-emplaced as allogenic complex of Phanerozoic age along the plate boundary and are syntectonic in nature. Podiform chromites of mantle tectonites exhibits higher Cr/Fe_{total} (~2.4-4.6), a comparatively higher variation in Cr# (~0.2-0.9) than Mg# (~0.4-0.7), lower Ti content (<0.1%), lower Fe^{3+}:Fe^{2+} (generally <0.5) and, a fractionation trend

indicated by an increase in Cr content and consequent decrease in Al of the Cr-spinels of mantle harzburgite to the overlying tectonites and cumulates.

However, no sharp boundary exist in the natural occurrence of the two categories and at times terms like 'deformed stratiform type' is used for chromite deposits with features similar to stratiform type deposits but intensely deformed like podiform chromite deposits examples of which are Bahia Province (Brazil), Bird River Sill (Canada), Fiskenaesset (Greenland) *etc.*

Present section deals with the overall petrogenetic re-assessment of SUC chromitites and associated ultramafics on the basis of Cr-spinel composition of the samples studied and attempts to detect the micro level physico-chemical variations in ores and host rocks of particular geologic horizon and to correlate with the respective litho-units with other horizons for the tectono-magmatic evolution of the Sukinda ultramafics. It is expected that the physico-chemical parameters estimated by the study of variation in Cr-spinel composition, may give very useful clues on sulfide-PGE ore genesis.

Chromite or Cr-Spinel being a member of the spinel group is represented by the general formula $[R^{2+}][R^{3+}]_2O_4$ where R^{2+}: Mg, Fe^{2+} and R^{3+}: Cr, Al, Fe^{3+}. The principle constituents of spinels behave differently during partial melting, fractional crystallization or subsolidus requilibration processes. Most compatible (Cr, Mg) constituents are partitioned to solid (spinels) phase and incompatible (Al) ones to melt. Therefore, spinel composition keeps a record of the melt composition and petrogenesis of the host rock without having much effect on geochemical evolution of the melt. However, it moderately influences the composition of the associated silicate phases. Mg^{2+} and Fe^{2+} partitioning between spinel and silicates (phase or melt) is sensitive

to temperature and is denoted by magnesia ratio ($Mg:Mg+Fe^{2+}$) or magnesium number (Mg#) of chromite. The partitioning of Cr between the spinel and melt is highly pressure dependent compared to Al. Hence, Cr-rich spinels indicates a low pressures of crystallization. Hence, the chrome ratio (Cr:Cr+Al) or chromium number (Cr#) is indicative of total pressure of crystallization. The $Fe^{3+}:Fe^{2+}$ ratio is the measure of effective activity of oxygen *i.e.* the combined effect of fO_2 and temperature and melt composition.

The Cr-spinel compositional studies are done on carbon coated polished sections using *JEOL (Superprobe: model JXA-8600 M)* make wave length dispersive electron probe micro analyzer (WDS-EPMA) facility available at Indian Institute of Technology Roorkee. The operational conditions were maintained at an acceleration voltage of 15kV with a beam current of 20nA and a counting time of 10s per element and calibrations were performed by SPI multi-standards. Total Fe calculated as FeO and Fe^{3+} value are obtained from stochiometric recalculation as described by Carmichael (1967). The cations are calculated on four oxygen atom basis and values are mentioned in Table 4.1.

Careful selection of chromite grains was done by thorough petrographic studies under the microscope for subsequent EPMA studies. The EPMA analyses were mostly confined to the core of the chromite grains likely to be unaffected by any alteration and weathering. Cr-spinels of host rock (as accessory phase) as well as different varieties of ore (as major phase) are analyzed to study the micro level changes in physico-chemical condition during the magmatic crystallization process. The data points are cross checked on Cr#~Mg# plot which falls in Field – I of Mondal *et al.* (2001)

Table 4.1 Chrome spinel composition of grey ores and serpentinized host rocks of Sukinda Ultramafic Complex

	KATHPAL QUARRY (ZONE-1a)																	
	A3F				A1O			A3O										
	1	*2*	*3*	*4*	*5*	*6*	*7*	*8*	*9*	*10*	*11*	*12*	*13*	*14*	*15*	*16*	*17*	*18*
Oxides	*Recalculated wt%*																	
Cr_2O_3	50.18	51.97	52.07	52.59	55.29	55.77	57.00	57.29	56.08	55.91	57.39	56.20	56.07	56.68	56.01	53.75	54.69	53.77
Al_2O_3	15.66	15.02	14.21	13.73	13.34	12.26	12.38	11.66	12.72	13.25	12.26	12.83	12.50	12.01	13.24	14.12	13.83	14.00
Fe_2O_3	4.66	3.26	4.54	4.12	3.62	3.86	3.10	2.96	3.37	4.41	2.59	3.51	3.78	4.05	3.45	4.20	3.42	4.51
MgO	11.51	10.81	11.77	11.62	12.83	12.79	13.24	13.11	13.07	14.07	13.04	13.40	13.68	13.97	13.68	14.25	13.45	14.44
FeO	16.11	17.51	15.60	15.83	14.06	14.06	13.17	13.33	13.76	12.87	13.78	13.08	12.68	12.13	12.76	12.07	13.26	11.73
TiO_2	0.07	0.30	0.14	0.34	0.05	0.24	0.02	0.20	0.21	0.34	0.18	0.00	0.21	0.14	0.00	0.25	0.20	0.26
MnO	0.35	0.36	0.33	0.46	0.32	0.30	0.33	0.28	0.31	0.41	0.24	0.22	0.32	0.28	0.22	0.21	0.27	0.30
Total	98.53	99.23	98.66	98.68	99.51	99.29	99.24	98.83	99.53	101.26	99.46	99.24	99.24	99.26	99.35	98.84	99.12	99.01
FeO_t	20.78	20.77	20.14	19.95	17.68	17.93	16.27	16.29	17.13	17.28	16.36	16.59	16.46	16.18	16.21	16.27	16.68	16.23
Atoms	*No. of atoms on 4 Oxygen basis*																	
Cr	1.29	1.33	1.34	1.35	1.40	1.43	1.45	1.47	1.43	1.39	1.46	1.43	1.42	1.44	1.42	1.36	1.39	1.35
Al	0.60	0.57	0.54	0.53	0.51	0.47	0.47	0.45	0.48	0.49	0.47	0.49	0.47	0.45	0.50	0.53	0.52	0.53
Fe'''	0.11	0.08	0.11	0.10	0.09	0.09	0.08	0.07	0.08	0.10	0.06	0.08	0.09	0.10	0.08	0.10	0.08	0.11
Mg	0.56	0.52	0.57	0.56	0.61	0.62	0.64	0.64	0.63	0.66	0.63	0.64	0.66	0.67	0.65	0.68	0.64	0.69
Fe''	0.44	0.47	0.42	0.43	0.38	0.38	0.36	0.36	0.37	0.34	0.37	0.35	0.34	0.33	0.34	0.32	0.36	0.31
Ti	0.00	0.01	0.00	0.01	0.00	0.01	0.00	0.00	0.01	0.01	0.00	0.00	0.01	0.00	0.00	0.01	0.00	0.01
Mn	0.01	0.01	0.01	0.01	0.01	0.01	0.01	0.01	0.01	0.01	0.01	0.01	0.01	0.01	0.01	0.01	0.01	0.01
Total	3.00	3.00	3.00	3.00	3.00	3.00	3.00	3.00	3.00	3.00	3.00	3.00	3.00	3.00	3.00	3.00	3.00	3.00
Ionic Ratios[N]																		
Cr#	0.68	0.70	0.71	0.72	0.74	0.75	0.76	0.77	0.75	0.74	0.76	0.75	0.75	0.76	0.74	0.72	0.73	0.72
Mg#	0.56	0.52	0.57	0.57	0.62	0.62	0.64	0.64	0.63	0.66	0.63	0.65	0.66	0.67	0.66	0.68	0.64	0.69
Fe'''#	0.06	0.04	0.06	0.05	0.04	0.05	0.04	0.04	0.04	0.05	0.03	0.04	0.05	0.05	0.04	0.05	0.04	0.05
Cr'''#	0.64	0.67	0.67	0.68	0.70	0.72	0.73	0.74	0.72	0.70	0.73	0.71	0.72	0.72	0.71	0.68	0.70	0.68
Cr/Fe_t	2.34	2.40	2.50	2.55	3.02	3.01	3.38	3.39	3.16	3.14	3.37	3.27	3.30	3.40	3.34	3.21	3.16	3.22
Fe'''/Fe''	0.26	0.17	0.26	0.23	0.23	0.25	0.21	0.20	0.22	0.31	0.17	0.24	0.27	0.30	0.24	0.31	0.23	0.35
Cr/Fe'''	11.30	16.75	12.05	13.41	16.04	15.17	19.32	20.33	17.47	13.33	23.31	16.84	15.58	14.71	17.04	13.46	16.79	12.54
Percentage																		
Cr%	64.37	67.10	67.13	68.31	70.33	71.76	72.69	73.94	71.67	70.02	73.46	71.44	71.61	72.26	70.88	68.22	69.61	68.12
Al%	29.94	28.90	27.30	26.59	25.29	23.51	23.54	22.43	24.23	24.73	23.39	24.32	23.79	22.83	24.96	26.72	26.25	26.44
Fe'''%	5.69	4.01	5.57	5.09	4.38	4.73	3.76	3.64	4.10	5.25	3.15	4.24	4.60	4.91	4.16	5.07	4.15	5.43

[N]Cr# = Cr/ [Cr+Al], Mg# = Mg / [Mg + Fe''], Fe'''# = Fe'''/ [Cr+Al+Fe'''], Cr'''# =Cr/ [Cr+Al+Fe''']

Table 4.1 *Contd.*

	KATHPAL QUARRY (ZONE-1a)												
	A3O										B2O		
	19	*20*	*21*	*22*	*23*	*24*	*25*	*26*	*27*	*28*	*29*	*30*	*31*
Oxides	*Recalculated wt%*												
Cr_2O_3	57.02	53.87	53.92	55.58	54.59	54.02	56.82	54.70	55.43	54.89	55.35	55.26	55.81
Al_2O_3	12.47	14.31	14.64	13.05	12.92	14.48	12.32	14.78	13.41	13.63	14.12	14.47	14.54
Fe_2O_3	3.68	4.23	3.76	3.78	4.51	3.74	3.83	3.91	3.17	3.92	3.95	4.26	3.55
MgO	13.60	14.80	14.55	14.01	14.52	13.92	13.94	14.76	13.24	13.56	16.01	15.79	15.44
FeO	12.92	11.21	11.81	12.22	11.32	12.50	12.28	11.71	13.55	13.12	9.83	10.00	10.29
TiO_2	0.14	0.26	0.32	0.17	0.33	0.11	0.13	0.17	0.20	0.14	0.48	0.12	0.00
MnO	0.48	0.32	0.31	0.26	0.33	0.29	0.36	0.32	0.29	0.28	0.39	0.30	0.41
Total	100.31	98.99	99.32	99.07	98.52	99.06	99.68	100.35	99.29	99.53	100.12	100.19	100.05
FeO_t	16.59	15.43	15.57	16.00	15.83	16.24	16.12	15.62	16.72	17.04	13.78	14.25	13.85
Atoms	*No. of atoms on 4 Oxygen basis*												
Cr	1.44	1.35	1.35	1.41	1.39	1.36	1.44	1.35	1.41	1.39	1.37	1.36	1.38
Al	0.47	0.54	0.55	0.49	0.49	0.54	0.46	0.55	0.51	0.51	0.52	0.53	0.54
Fe'''	0.09	0.10	0.09	0.09	0.11	0.09	0.09	0.09	0.08	0.09	0.09	0.10	0.08
Mg	0.65	0.70	0.69	0.67	0.69	0.66	0.66	0.69	0.63	0.65	0.74	0.73	0.72
Fe''	0.34	0.30	0.31	0.33	0.30	0.33	0.33	0.31	0.36	0.35	0.26	0.26	0.27
Ti	0.00	0.01	0.01	0.00	0.01	0.00	0.00	0.00	0.00	0.00	0.01	0.00	0.00
Mn	0.01	0.01	0.01	0.01	0.01	0.01	0.01	0.01	0.01	0.01	0.01	0.01	0.01
Total	3.00	3.00	3.00	3.00	3.00	3.00	3.00	3.00	3.00	3.00	3.00	3.00	3.00
Ionic Ratios[N]													
Cr#	0.75	0.72	0.71	0.74	0.74	0.71	0.76	0.71	0.73	0.73	0.72	0.72	0.72
Mg#	0.65	0.70	0.69	0.67	0.70	0.66	0.67	0.69	0.64	0.65	0.74	0.74	0.73
Fe'''#	0.04	0.05	0.05	0.05	0.05	0.04	0.05	0.05	0.04	0.05	0.05	0.05	0.04
Cr'''#	0.72	0.68	0.68	0.71	0.70	0.68	0.72	0.68	0.71	0.70	0.69	0.68	0.69
Cr/Fe_t	3.32	3.39	3.36	3.36	3.36	3.22	3.41	3.40	3.20	3.12	3.91	3.78	3.91
Fe'''/Fe''	0.26	0.34	0.29	0.28	0.36	0.27	0.28	0.30	0.21	0.27	0.36	0.38	0.31
Cr/Fe'''	16.30	13.39	15.08	15.46	12.72	15.18	15.57	14.69	18.37	14.71	14.73	13.64	16.51
Percentage													
Cr%	72.07	68.00	67.99	70.69	69.86	68.23	72.07	67.98	70.66	69.53	69.05	68.32	69.02
Al%	23.50	26.92	27.51	24.73	24.65	27.27	23.30	27.39	25.49	25.74	26.27	26.67	26.80
Fe'''%	4.42	5.08	4.51	4.57	5.49	4.50	4.63	4.63	3.85	4.73	4.69	5.01	4.18

[N]Cr# = Cr/ [Cr+Al], Mg# = Mg / [Mg + Fe''], Fe'''# = Fe'''/ [Cr+Al+Fe'''], Cr'''# =Cr/ [Cr+Al+Fe''']

Table 4.1 *Contd.*

	KALARANGITTA (Zone-2)															
	DM-22					DM-23										
	32	*33*	*34*	*35*	*36*	*37*	*38*	*39*	*40*	*41*	*42*	*43*	*44*	*45*	*46*	*47*
Oxides	*Recalculated wt%*															
Cr_2O_3	55.27	55.07	55.05	52.11	51.54	54.56	55.34	54.31	56.25	57.29	54.11	53.43	56.81	55.65	55.93	55.49
Al_2O_3	13.85	13.39	13.35	16.93	16.91	14.14	14.47	14.28	13.15	12.77	15.02	15.02	11.81	13.71	13.48	13.51
Fe_2O_3	0.86	1.37	1.33	1.29	1.85	2.42	2.81	3.06	2.42	1.94	2.73	2.88	2.63	3.21	1.70	2.58
MgO	7.55	7.26	8.46	9.34	9.35	10.33	11.36	11.37	10.40	11.60	11.21	11.22	9.61	11.88	9.76	10.18
FeO	22.48	22.70	20.61	20.50	20.16	18.41	17.01	16.74	18.09	16.07	17.35	17.10	18.91	15.84	19.20	18.64
TiO_2	0.09	0.10	0.05	0.23	0.08	0.20	0.00	0.16	0.03	0.07	0.19	0.20	0.10	0.04	0.19	0.13
MnO	0.49	0.61	0.41	0.39	0.43	0.37	0.36	0.38	0.37	0.32	0.39	0.39	0.49	0.45	0.44	0.36
Total	100.58	100.51	99.26	100.79	100.31	100.42	101.35	100.30	100.71	100.06	101.00	100.24	100.36	100.78	100.70	100.89
FeO_t	23.33	24.07	21.94	21.79	22.01	20.83	19.82	19.80	20.51	18.01	20.08	19.99	21.54	19.05	20.90	21.22
Atoms	*No. of atoms on 4 Oxygen basis*															
Cr	1.44	1.44	1.44	1.32	1.31	1.39	1.39	1.38	1.44	1.46	1.36	1.35	1.47	1.41	1.43	1.42
Al	0.54	0.52	0.52	0.64	0.64	0.54	0.54	0.54	0.50	0.49	0.56	0.57	0.46	0.52	0.52	0.51
Fe'''	0.02	0.03	0.03	0.03	0.04	0.06	0.07	0.07	0.06	0.05	0.07	0.07	0.06	0.08	0.04	0.06
Mg	0.37	0.36	0.42	0.45	0.45	0.50	0.54	0.54	0.50	0.56	0.53	0.54	0.47	0.57	0.47	0.49
Fe''	0.62	0.63	0.57	0.55	0.54	0.50	0.45	0.45	0.49	0.43	0.46	0.46	0.52	0.42	0.52	0.50
Ti	0.00	0.00	0.00	0.01	0.00	0.00	0.00	0.00	0.00	0.00	0.00	0.00	0.00	0.00	0.00	0.00
Mn	0.01	0.02	0.01	0.01	0.01	0.01	0.01	0.01	0.01	0.01	0.01	0.01	0.01	0.01	0.01	0.01
Total	3.00	3.00	3.00	3.00	3.00	3.00	3.00	3.00	3.00	3.00	3.00	3.00	3.00	3.00	3.00	3.00
Ionic Ratios[N]																
Cr#	0.73	0.73	0.73	0.67	0.67	0.72	0.72	0.72	0.74	0.75	0.71	0.70	0.76	0.73	0.74	0.73
Mg#	0.37	0.36	0.42	0.45	0.45	0.50	0.54	0.55	0.51	0.56	0.54	0.54	0.48	0.57	0.48	0.49
Fe'''#	0.01	0.02	0.02	0.02	0.02	0.03	0.03	0.04	0.03	0.02	0.03	0.03	0.03	0.04	0.02	0.03
Cr'''#	0.72	0.72	0.72	0.66	0.66	0.70	0.70	0.69	0.72	0.73	0.68	0.68	0.74	0.70	0.72	0.71
Cr/Fe_t	2.25	2.18	2.39	2.28	2.23	2.51	2.68	2.63	2.62	3.04	2.58	2.56	2.53	2.81	2.55	2.50
Fe'''/Fe''	0.03	0.05	0.06	0.06	0.08	0.12	0.15	0.16	0.12	0.11	0.14	0.15	0.13	0.18	0.08	0.12
Cr/Fe'''	67.73	42.18	43.37	42.59	29.25	23.68	20.67	18.65	24.40	31.02	20.82	19.48	22.71	18.22	34.63	22.60
Percentage																
Cr%	72.04	72.14	72.22	66.33	65.65	69.99	69.54	69.17	71.97	73.29	68.41	68.01	73.86	70.32	72.04	71.07
Al%	26.90	26.15	26.11	32.12	32.11	27.05	27.10	27.12	25.08	24.35	28.30	28.50	22.89	25.82	25.88	25.79
Fe'''%	1.06	1.71	1.67	1.56	2.24	2.96	3.37	3.71	2.95	2.36	3.29	3.49	3.25	3.86	2.08	3.14

[N]Cr# = Cr/ [Cr+Al], Mg# = Mg / [Mg + Fe''], Fe'''# = Fe'''/ [Cr+Al+Fe'''], Cr'''# =Cr/ [Cr+Al+Fe''']

Table 4.1 *Contd.*

	KALARANGITTA (Zone-2)																
	DM-24									DM-25							
	48	*49*	*50*	*51*	*52*	*53*	*54*	*55*	*56*	*57*	*58*	*59*	*60*	*61*	*62*	*63*	*64*
Oxides	*Recalculated wt%*																
Cr_2O_3	55.58	55.86	56.70	55.14	54.62	56.91	55.78	56.13	54.08	57.50	57.46	57.47	56.96	57.59	58.26	57.88	57.14
Al_2O_3	14.40	13.86	13.71	14.23	14.31	13.35	12.59	12.76	13.40	13.13	10.11	12.34	12.76	12.74	12.28	12.29	13.27
Fe_2O_3	3.19	3.99	2.87	3.52	3.48	3.38	3.50	2.23	3.78	2.45	3.88	3.33	3.22	2.93	2.91	2.96	2.45
MgO	14.23	14.82	14.96	13.41	12.64	14.85	11.70	10.76	11.74	12.75	10.28	12.75	12.99	12.82	13.00	12.61	13.09
FeO	12.47	11.65	11.36	13.77	14.85	11.59	15.66	17.26	15.78	14.64	17.33	14.27	14.03	14.37	14.10	14.72	14.21
TiO_2	0.14	0.23	0.32	0.17	0.15	0.25	0.03	0.16	0.23	0.12	0.12	0.00	0.08	0.03	0.08	0.12	0.25
MnO	0.27	0.31	0.31	0.31	0.34	0.22	0.34	0.37	0.41	0.38	0.58	0.35	0.33	0.33	0.37	0.37	0.36
Total	100.29	100.72	100.22	100.55	100.39	100.53	99.59	99.68	99.43	100.97	99.75	100.52	100.37	100.80	101.00	100.94	100.77
FeO_t	15.66	15.64	14.23	17.29	18.33	14.96	19.16	19.49	19.56	17.09	21.21	17.61	17.25	17.30	17.01	17.68	16.66
Atoms	*No. of atoms on 4 Oxygen basis*																
Cr	1.38	1.38	1.41	1.38	1.37	1.41	1.43	1.45	1.38	1.44	1.50	1.45	1.44	1.45	1.47	1.46	1.43
Al	0.53	0.51	0.51	0.53	0.54	0.49	0.48	0.49	0.51	0.49	0.39	0.47	0.48	0.48	0.46	0.46	0.50
Fe'''	0.08	0.09	0.07	0.08	0.08	0.08	0.09	0.05	0.09	0.06	0.10	0.08	0.08	0.07	0.07	0.07	0.06
Mg	0.67	0.69	0.70	0.63	0.60	0.70	0.57	0.52	0.57	0.60	0.51	0.61	0.62	0.61	0.62	0.60	0.62
Fe''	0.33	0.31	0.30	0.36	0.39	0.30	0.43	0.47	0.43	0.39	0.48	0.38	0.37	0.38	0.38	0.39	0.38
Ti	0.00	0.01	0.01	0.00	0.00	0.01	0.00	0.00	0.01	0.00	0.00	0.00	0.00	0.00	0.00	0.00	0.01
Mn	0.01	0.01	0.01	0.01	0.01	0.01	0.01	0.01	0.01	0.01	0.02	0.01	0.01	0.01	0.01	0.01	0.01
Total	3.00	3.00	3.00	3.00	3.00	3.00	3.00	3.00	3.00	3.00	3.00	3.00	3.00	3.00	3.00	3.00	3.00
Ionic Ratios[N]																	
Cr#	0.72	0.73	0.74	0.72	0.72	0.74	0.75	0.75	0.73	0.75	0.79	0.76	0.75	0.75	0.76	0.76	0.74
Mg#	0.67	0.69	0.70	0.63	0.60	0.70	0.57	0.53	0.57	0.61	0.51	0.61	0.62	0.61	0.62	0.60	0.62
Fe'''#	0.04	0.05	0.03	0.04	0.04	0.04	0.04	0.03	0.05	0.03	0.05	0.04	0.04	0.04	0.03	0.04	0.03
Cr'''#	0.69	0.70	0.71	0.69	0.69	0.71	0.72	0.73	0.70	0.72	0.75	0.73	0.72	0.73	0.73	0.73	0.72
Cr/Fe_t	3.42	3.47	3.85	3.08	2.87	3.68	2.80	2.75	2.67	3.23	2.61	3.15	3.18	3.20	3.30	3.15	3.29
Fe'''/Fe''	0.23	0.31	0.23	0.23	0.21	0.26	0.20	0.12	0.22	0.15	0.20	0.21	0.21	0.18	0.19	0.18	0.16
Cr/Fe'''	18.28	14.71	20.76	16.45	16.51	17.70	16.76	26.42	15.01	24.67	15.55	18.11	18.61	20.64	21.06	20.55	24.47
Percentage																	
Cr%	69.40	69.55	71.00	69.18	68.92	71.11	71.63	72.64	69.64	72.41	75.38	72.71	72.06	72.56	73.44	73.26	72.09
Al%	26.80	25.72	25.58	26.62	26.91	24.87	24.09	24.62	25.73	24.66	19.77	23.27	24.07	23.92	23.07	23.18	24.96
Fe'''%	3.80	4.73	3.42	4.20	4.18	4.02	4.27	2.75	4.64	2.94	4.85	4.01	3.87	3.52	3.49	3.56	2.95

[N]Cr# = Cr/ [Cr+Al], Mg# = Mg / [Mg + Fe''], Fe'''# = Fe'''/ [Cr+Al+Fe'''], Cr'''# =Cr/ [Cr+Al+Fe''']

Table 4.1 *Contd.*

	KALARANGITTA (Zone-2)															
	DM-26					DM-27										
	65	*66*	*67*	*68*	*69*	*70*	*71*	*72*	*73*	*74*	*75*	*76*	*77*	*78*	*79*	*80*
Oxides	*Recalculated wt%*															
Cr_2O_3	57.30	58.48	60.17	58.88	58.70	53.73	54.46	54.20	55.25	55.65	56.24	54.52	53.15	53.89	53.60	53.55
Al_2O_3	14.68	13.94	10.76	12.63	12.73	14.81	14.36	15.90	13.73	13.56	13.72	13.58	14.23	14.00	14.52	14.94
Fe_2O_3	1.91	1.90	1.36	2.45	1.80	1.27	1.84	2.46	3.42	3.07	3.66	2.46	2.58	2.10	1.76	3.20
MgO	15.30	15.18	13.60	14.72	14.72	8.21	9.97	12.74	12.26	12.22	13.84	9.76	8.16	8.20	8.48	11.01
FeO	10.70	11.19	12.24	11.38	11.50	21.57	18.62	15.42	15.42	15.54	13.15	18.84	21.54	21.58	21.41	17.57
TiO_2	0.00	0.11	0.13	0.04	0.25	0.13	0.10	0.29	0.14	0.20	0.13	0.12	0.15	0.17	0.36	0.17
MnO	0.30	0.27	0.38	0.29	0.24	0.43	0.47	0.32	0.31	0.26	0.30	0.42	0.49	0.39	0.47	0.38
Total	100.19	101.07	98.65	100.39	99.93	100.15	99.83	101.32	100.53	100.51	101.04	99.71	100.30	100.32	100.59	100.82
FeO_t	12.61	13.09	13.61	13.83	13.29	22.84	20.46	17.88	18.84	18.62	16.81	21.31	24.12	23.68	23.17	20.77
Atoms	*No. of atoms on 4 Oxygen basis*															
Cr	1.41	1.44	1.55	1.47	1.47	1.39	1.40	1.34	1.39	1.41	1.40	1.41	1.38	1.40	1.38	1.35
Al	0.54	0.51	0.41	0.47	0.48	0.57	0.55	0.59	0.52	0.51	0.51	0.52	0.55	0.54	0.56	0.56
Fe'''	0.04	0.04	0.03	0.06	0.04	0.03	0.04	0.06	0.08	0.07	0.09	0.06	0.06	0.05	0.04	0.08
Mg	0.71	0.70	0.66	0.69	0.69	0.40	0.48	0.59	0.58	0.58	0.65	0.48	0.40	0.40	0.41	0.52
Fe''	0.28	0.29	0.33	0.30	0.30	0.59	0.51	0.40	0.41	0.42	0.35	0.52	0.59	0.59	0.58	0.47
Ti	0.00	0.00	0.00	0.00	0.01	0.00	0.00	0.01	0.00	0.00	0.00	0.00	0.00	0.00	0.01	0.00
Mn	0.01	0.01	0.01	0.01	0.01	0.01	0.01	0.01	0.01	0.01	0.01	0.01	0.01	0.01	0.01	0.01
Total	3.00	3.00	3.00	3.00	3.00	3.00	3.00	3.00	3.00	3.00	3.00	3.00	3.00	3.00	3.00	3.00
Ionic Ratios[N]																
Cr#	0.72	0.74	0.79	0.76	0.76	0.71	0.72	0.70	0.73	0.73	0.73	0.73	0.71	0.72	0.71	0.71
Mg#	0.72	0.71	0.66	0.70	0.70	0.40	0.49	0.60	0.59	0.58	0.65	0.48	0.40	0.40	0.41	0.53
Fe'''#	0.02	0.02	0.02	0.03	0.02	0.02	0.02	0.03	0.04	0.04	0.04	0.03	0.03	0.03	0.02	0.04
Cr'''#	0.71	0.72	0.78	0.74	0.74	0.70	0.70	0.68	0.70	0.71	0.70	0.71	0.69	0.70	0.70	0.68
Cr/Fe_t	4.36	4.28	4.22	4.10	4.23	2.24	2.54	2.91	2.82	2.87	3.23	2.45	2.11	2.17	2.20	2.48
Fe'''/Fe''	0.16	0.15	0.10	0.19	0.14	0.05	0.09	0.14	0.20	0.18	0.25	0.12	0.11	0.09	0.07	0.16
Cr/Fe'''	31.50	32.32	46.41	25.20	34.35	44.35	31.17	23.12	16.97	19.02	16.13	23.26	21.62	26.98	32.02	17.57
Percentage																
Cr%	70.74	72.13	77.63	73.56	73.94	69.76	70.16	67.54	69.96	70.63	70.15	70.70	69.19	70.20	69.69	67.89
Al%	27.01	25.64	20.70	23.52	23.91	28.67	27.59	29.54	25.92	25.66	25.51	26.26	27.61	27.19	28.13	28.24
Fe'''%	2.25	2.23	1.67	2.92	2.15	1.57	2.25	2.92	4.12	3.71	4.35	3.04	3.20	2.60	2.18	3.86

[N]Cr# = Cr/ [Cr+Al], Mg# = Mg / [Mg + Fe''], Fe'''# = Fe'''/ [Cr+Al+Fe'''], Cr'''# =Cr/ [Cr+Al+Fe''']

Table 4.1 *Contd.*

	KALARANGITTA (Zone-2)															
	DM-28							DM-29								
	81	*82*	*83*	*84*	*85*	*86*	*87*	*88*	*89*	*90*	*91*	*92*	*93*	*94*	*95*	*96*
Oxides	*Recalculated wt%*															
Cr_2O_3	47.44	48.42	48.82	48.98	48.89	46.81	48.85	46.78	46.55	46.54	46.54	46.58	46.04	46.25	48.83	49.03
Al_2O_3	17.70	16.65	16.05	15.28	15.86	17.18	15.06	18.21	17.34	17.15	17.15	16.59	16.97	16.46	16.35	16.64
Fe_2O_3	3.36	2.85	2.89	3.92	3.43	4.12	3.66	4.37	4.01	3.97	3.97	4.62	4.60	4.04	3.35	3.22
MgO	7.83	7.77	7.71	8.46	8.86	7.46	7.32	7.89	7.64	7.67	7.67	7.22	7.17	7.04	9.47	9.45
FeO	23.29	22.73	22.71	21.02	20.61	23.29	22.67	23.03	22.89	22.88	22.88	23.25	23.15	23.49	19.83	19.82
TiO_2	0.70	0.59	0.66	0.47	0.54	0.54	0.48	0.43	0.54	0.62	0.62	0.50	0.44	0.75	0.53	0.39
MnO	0.41	0.39	0.42	0.42	0.39	0.45	0.47	0.58	0.49	0.42	0.42	0.58	0.64	0.57	0.34	0.38
Total	100.72	99.38	99.26	98.55	98.58	99.85	98.50	101.30	99.46	99.25	99.25	99.34	99.00	98.60	98.70	98.94
FeO_t	26.65	25.57	25.60	24.94	24.05	27.42	26.33	27.40	26.90	26.86	26.86	27.87	27.74	27.53	23.18	23.05
Atoms	*No. of atoms on 4 Oxygen basis*															
Cr	1.21	1.26	1.27	1.28	1.27	1.21	1.29	1.19	1.21	1.21	1.21	1.22	1.20	1.22	1.26	1.26
Al	0.67	0.64	0.62	0.60	0.62	0.66	0.59	0.69	0.67	0.66	0.66	0.65	0.66	0.65	0.63	0.64
Fe'''	0.08	0.07	0.07	0.10	0.09	0.10	0.09	0.11	0.10	0.10	0.10	0.11	0.11	0.10	0.08	0.08
Mg	0.38	0.38	0.38	0.42	0.43	0.36	0.36	0.38	0.37	0.38	0.38	0.35	0.35	0.35	0.46	0.46
Fe''	0.63	0.62	0.63	0.58	0.57	0.64	0.63	0.62	0.63	0.63	0.63	0.64	0.64	0.65	0.54	0.54
Ti	0.02	0.01	0.02	0.01	0.01	0.01	0.01	0.01	0.01	0.02	0.02	0.01	0.01	0.02	0.01	0.01
Mn	0.01	0.01	0.01	0.01	0.01	0.01	0.01	0.02	0.01	0.01	0.01	0.02	0.02	0.02	0.01	0.01
Total	3.00	3.00	3.00	3.00	3.00	3.00	3.00	3.00	3.00	3.00	3.00	3.00	3.00	3.00	3.00	3.00
Ionic Ratios[N]																
Cr#	0.64	0.66	0.67	0.68	0.67	0.65	0.69	0.63	0.64	0.65	0.65	0.65	0.65	0.65	0.67	0.66
Mg#	0.37	0.38	0.38	0.42	0.43	0.36	0.37	0.38	0.37	0.37	0.37	0.36	0.36	0.35	0.46	0.46
Fe'''#	0.04	0.04	0.04	0.05	0.04	0.05	0.05	0.05	0.05	0.05	0.05	0.06	0.06	0.05	0.04	0.04
Cr'''#	0.62	0.64	0.65	0.65	0.65	0.61	0.65	0.60	0.61	0.61	0.61	0.62	0.61	0.62	0.64	0.64
Cr/Fe_t	1.70	1.81	1.82	1.89	1.95	1.64	1.78	1.64	1.66	1.66	1.66	1.61	1.60	1.61	2.02	2.04
Fe'''/Fe''	0.13	0.11	0.11	0.17	0.15	0.16	0.15	0.17	0.16	0.16	0.16	0.18	0.18	0.15	0.15	0.15
Cr/Fe'''	14.83	17.87	17.72	13.12	14.96	11.93	14.03	11.24	12.18	12.31	12.31	10.59	10.53	12.03	15.31	15.99
Percentage																
Cr%	61.59	63.75	64.66	64.88	64.50	61.32	65.33	59.91	61.07	61.32	61.32	61.52	60.82	61.97	63.92	63.76
Al%	34.25	32.68	31.69	30.17	31.19	33.54	30.01	34.76	33.91	33.69	33.69	32.67	33.41	32.88	31.91	32.25
Fe'''%	4.15	3.57	3.65	4.94	4.31	5.14	4.66	5.33	5.01	4.98	4.98	5.81	5.78	5.15	4.17	3.99

[N]Cr# = Cr/ [Cr+Al], Mg# = Mg / [Mg + Fe''], Fe'''# = Fe'''/ [Cr+Al+Fe'''], Cr'''# =Cr/ [Cr+Al+Fe''']

Table 4.1 *Contd.*

	KATHPAL UNDERGROUND MINES (Zone-1a)														
	DM-11					DM-13				DM-14				DM-15		
	97	*98*	*99*	*100*	*101*	*102*	*103*	*104*	*105*	*106*	*107*	*108*	*109*	*110*	*111*	*112*
Oxides	*Recalculated wt%*															
Cr_2O_3	55.58	55.99	55.69	55.98	55.83	58.56	60.71	60.23	59.24	61.40	60.55	61.29	61.04	54.75	55.22	55.14
Al_2O_3	12.16	12.04	12.52	11.92	11.67	12.73	11.47	11.94	12.02	9.38	10.77	10.61	10.22	12.61	12.57	12.99
Fe_2O_3	2.80	2.68	2.77	3.09	4.22	4.71	2.88	3.64	3.01	3.98	2.51	2.47	2.94	3.07	3.84	3.31
MgO	10.44	10.72	10.97	10.55	11.27	17.45	16.65	17.61	16.90	14.41	14.34	14.58	14.42	9.84	10.52	9.79
FeO	17.32	16.83	16.77	17.34	16.34	7.57	8.32	7.40	7.52	11.66	11.54	11.40	11.61	18.58	17.91	19.01
TiO_2	0.11	0.09	0.14	0.13	0.14	0.09	0.10	0.28	0.05	0.13	0.04	0.10	0.16	0.13	0.17	0.07
MnO	0.38	0.36	0.33	0.35	0.32	0.25	0.23	0.23	0.26	0.31	0.32	0.34	0.36	0.25	0.33	0.37
Total	98.78	98.71	99.19	99.36	99.79	101.35	100.36	101.34	99.00	101.26	100.06	100.79	100.76	99.24	100.56	100.68
FeO_t	20.12	19.51	19.54	20.44	20.56	12.28	11.20	11.04	10.53	15.64	14.05	13.87	14.55	21.65	21.75	22.32
Atoms	*No. of atoms on 4 Oxygen basis*															
Cr	1.45	1.46	1.44	1.46	1.44	1.43	1.50	1.47	1.48	1.55	1.53	1.54	1.54	1.43	1.42	1.42
Al	0.47	0.47	0.48	0.46	0.45	0.46	0.42	0.43	0.45	0.35	0.41	0.40	0.38	0.49	0.48	0.50
Fe'''	0.07	0.07	0.07	0.08	0.10	0.11	0.07	0.08	0.07	0.10	0.06	0.06	0.07	0.08	0.09	0.08
Mg	0.51	0.53	0.54	0.52	0.55	0.80	0.78	0.81	0.80	0.68	0.68	0.69	0.68	0.48	0.51	0.47
Fe''	0.48	0.46	0.46	0.48	0.45	0.19	0.22	0.19	0.20	0.31	0.31	0.30	0.31	0.51	0.49	0.52
Ti	0.00	0.00	0.00	0.00	0.00	0.00	0.00	0.01	0.00	0.00	0.00	0.00	0.00	0.00	0.00	0.00
Mn	0.01	0.01	0.01	0.01	0.01	0.01	0.01	0.01	0.01	0.01	0.01	0.01	0.01	0.01	0.01	0.01
Total	3.00	3.00	3.00	3.00	3.00	3.00	3.00	3.00	3.00	3.00	3.00	3.00	3.00	3.00	3.00	3.00
Ionic Ratios[N]																
Cr#	0.75	0.76	0.75	0.76	0.76	0.76	0.78	0.77	0.77	0.81	0.79	0.79	0.80	0.74	0.75	0.74
Mg#	0.52	0.53	0.54	0.52	0.55	0.80	0.78	0.81	0.80	0.69	0.69	0.70	0.69	0.49	0.51	0.48
Fe'''#	0.03	0.03	0.03	0.04	0.05	0.05	0.03	0.04	0.04	0.05	0.03	0.03	0.04	0.04	0.05	0.04
Cr'''#	0.73	0.73	0.72	0.73	0.72	0.71	0.75	0.74	0.74	0.78	0.77	0.77	0.77	0.72	0.71	0.71
Cr/Fe_t	2.65	2.75	2.73	2.63	2.62	4.69	5.26	5.33	5.48	3.81	4.15	4.25	4.05	2.43	2.44	2.37
Fe'''/Fe''	0.15	0.14	0.15	0.16	0.23	0.56	0.31	0.44	0.36	0.31	0.20	0.19	0.23	0.15	0.19	0.16
Cr/Fe'''	20.87	21.94	21.14	19.02	13.91	13.07	22.11	17.36	20.67	16.21	25.33	26.12	21.79	18.72	15.11	17.52
Percentage																
Cr%	72.77	73.20	72.33	73.00	72.28	71.41	75.37	73.90	74.03	77.56	76.65	77.14	77.19	71.59	71.15	71.01
Al%	23.74	23.47	24.25	23.17	22.52	23.13	21.22	21.84	22.39	17.65	20.32	19.91	19.27	24.59	24.15	24.94
Fe'''%	3.49	3.34	3.42	3.84	5.20	5.46	3.41	4.26	3.58	4.78	3.03	2.95	3.54	3.82	4.71	4.05

[N]Cr# = Cr/ [Cr+Al], Mg# = Mg / [Mg + Fe''], Fe'''# = Fe'''/ [Cr+Al+Fe'''], Cr'''# =Cr/ [Cr+Al+Fe''']

indicating there relevance to select the grains for the study of primitive magmatic composition (Fig.4.2.i).

The three principal faces of the spinel compositional prism represent the 98% of the terrestrial varieties (Stevens 1944) and are used here for geodynamic appraisal of the Sukinda chromites.

For the assessment of parent magma composition, Cr-spinel composition of the massive chromites are only considered so as to give the best approximation of the initial melt composition in the near absences of co-existing olivines with which it could have equilibrated at lower temperatures during the crystallization (Augé 1987).

4.2.1 Geotectonic Set Up: Cr-Spinels from Massive Chromites

The values of Cr# mostly lie between 0.71 to 0.79 and that of Mg# between 0.62 to .81 for the massive ores suggesting about a high-magnesia parentage resulted from the higher degree of partial melting of the mantle. The values of Cr# and Mg# preclude the possibility of abyssal origin of the complex but matches well with the Type-III alpine spinel peridotites of Dick and Bullen (1984). These may be *tectonically* similar to that of chromites found in Archaean greenstone belts (Fig.4.2.i) and the podiform chromites (Fig.4.2.ii) of ophilitic complexes, and *genetically* (Fig.4.2.iii) related to the boninitic and komatiitic magmas as it plots close to the corresponding fields as defined by Barnes and Roeder (2001). The Ti-content of the cr-spinels are significantly low for all the varieties of ores and host rocks, not exceeding 0.02%. In the TiO_2 ~ Cr# plot of Arai (1992), the Cr-spinels of the chromitites are plotted in the boninite field (Fig.4.2.iv.a). When plotted for the octahedral

cations, the Cr-spinels plot (Fig.4.2.v.a) in the overlapping zone of the ophiolitic, boninitic and komatiitic fields (Barnes & Roeder 2001) in the Cr^{3+}~Al^{3+}~Fe^{3+} triangular plot. The plot of Fe^{3+}#~Mg# from the chromitites mostly fall in the overlapping zone of Alpine type peridotite and Stratiform complexes of Irvine (1974) (Fig.4.2.vi.a). The close resemblance of the parent magma with the komatiitic melts is also evident from Cr_2O_3~Al_2O_3 (Fig.4.2.vii.a) and Cr_2O_3~FeO_t (Fig.4.2.viii.a) plots of Mitra and Bidyananda (2003) (modified after Bai & Zhou 1988) for the chromitites and host rocks. Fo% of few relict olivine grains (Fig.4.1.xvii, Table 4.2) when plotted against the Cr# of associated Cr-spinel exhibit high-Cr and high Fo trend (Fig.4.2.ix) in the *olivine-spinel mantle array (OSMA)* of Arai (1994). Such high Fo-content of olivines are reported from sub-cratonic spinel harzburgites especially from African craton (Boyd & Nixon 1975, Hervig *et al.* 1980) and are related to Mg-rich magmas such as komatiites or picrites (Takahshi 1990). The Cr# ranges from 0.63 to 0.81 corresponding to the values for on-land alpine peridotites and fore arc peridotites on the plot of Cr# (Fig.4.2.x) reproduced by Lee (1999).

4.2.2 Physico-Chemical Condition & Melt Composition: Cr-Spinels from Ores and Host Rocks

The Cr-spinels of host rock and different varieties of ores were studied to observe the variation in the physico-chemical conditions and melt composition during crystallization and, subsolidus re-diffusion processes. Relatively smaller variation in Cr# (0.63-0.81) compared to the higher degree

Table 4.2 Composition of olivine-spinel pair from chromitites of Sukinda Ultramafic Complex

Olivine Composition													
Oxides	*1*	*2*	*3*	*4*	*5*	*6*	*Atoms*	*1*	*2*	*3*	*4*	*5*	*6*
SiO_2	43.36	43.38	43.14	42.55	42.11	43.21	Si	1.01	1.02	1.01	1.01	1.01	1.01
Al_2O_3	-	-	0.03	-	-	-	Al	-	-	0.00	-	-	-
FeO	3.52	3.78	3.37	3.71	3.06	3.43	Fe	0.07	0.07	0.07	0.07	0.06	0.07
MgO	54.68	54.07	54.35	53.37	53.38	54.86	Mg	1.90	1.89	1.90	1.90	1.91	1.91
MnO	0.07	0.08	0.05	0.08	0.04	0.07	Mn	0.00	0.00	0.00	0.00	0.00	0.00
CaO	-	0.01	0.00	0.01	0.02	0.01	Ca	-	0.00	0.00	0.00	0.00	0.00
K_2O	-	-	-	-	-	-	K	-	-	-	-	-	-
Na_2O	-	0.01	0.01	-	0.00	-	Na	-	0.00	0.00	-	0.00	-
TiO_2	-	-	-	0.01	0.00	0.00	Ti	-	-	-	0.00	0.00	0.00
Total	101.63	101.32	100.95	99.73	98.61	101.58	Total	2.99	2.98	2.99	2.99	2.99	2.99
							Fo%	93.95	93.47	94.16	93.50	94.58	94.12
Spinel Composition													
Oxides	*1*	*2*	*3*	*4*	*5*	*6*	*Atoms*	*1*	*2*	*3*	*4*	*5*	*6*
Cr_2O_3	60.71	60.23	61.40	60.55	61.29	61.04	Cr	1.50	1.47	1.55	1.53	1.54	1.54
Al_2O_3	11.47	11.94	9.38	10.77	10.61	10.22	Al	0.42	0.43	0.35	0.41	0.40	0.38
Fe_2O_3	2.88	3.64	3.98	2.51	2.47	2.94	Fe'''	0.07	0.08	0.10	0.06	0.06	0.07
MgO	16.65	17.61	14.41	14.34	14.58	14.42	Mg	0.78	0.81	0.68	0.68	0.69	0.68
FeO	8.32	7.40	11.66	11.54	11.40	11.61	Fe''	0.22	0.19	0.31	0.31	0.30	0.31
TiO_2	0.10	0.28	0.13	0.04	0.10	0.16	Ti	0.00	0.01	0.00	0.00	0.00	0.00
MnO	0.23	0.23	0.31	0.32	0.34	0.36	Mn	0.01	0.01	0.01	0.01	0.01	0.01
Total	100.36	101.34	101.26	100.06	100.79	100.76							
							Ionic Ratios[N]						
							Cr#	0.78	0.77	0.81	0.79	0.79	0.80
							Fe'''#	0.03	0.04	0.05	0.03	0.03	0.04
							Cr'''#	0.75	0.74	0.78	0.77	0.77	0.77
[N]Cr# = Cr/ [Cr+Al], Mg# = Mg / [Mg + Fe''], Fe'''# = Fe'''/ [Cr+Al+Fe'''], Cr'''# =Cr/ [Cr+Al+Fe''']							T (°C)	905	993	791	798	760	779

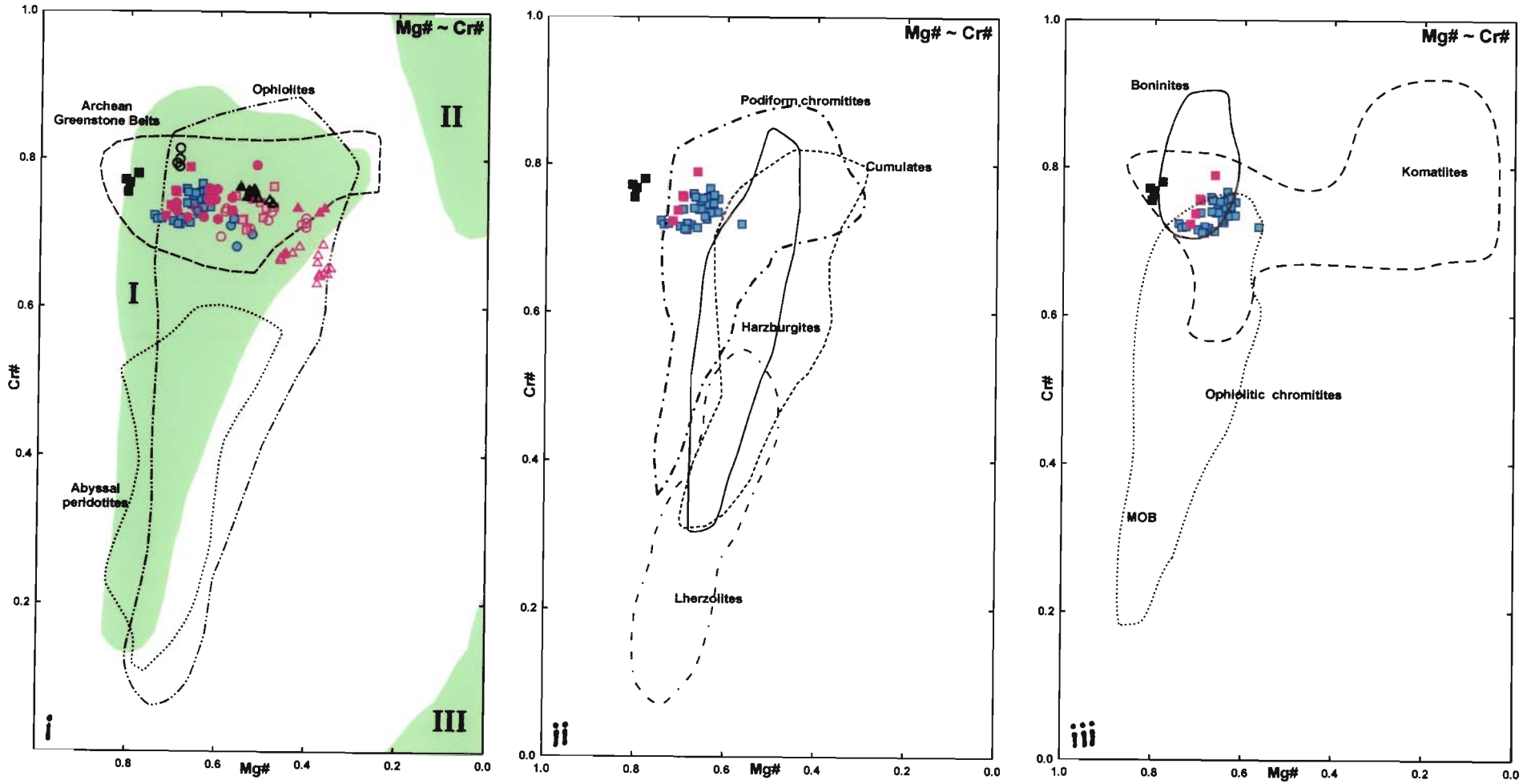

Fig.4.2 Cr#~Mg# plots of Cr-spinels from i all the varieties of ore compared to different tectonic set up and spinel varieties, ii massive ores compared to different units of ophiolitic complex, iii massive ores compared to different magmatic varieties *(fields are from Pober & Faupl 1988, Barnes & Roerder 2001, Mondal et al. 2001)*

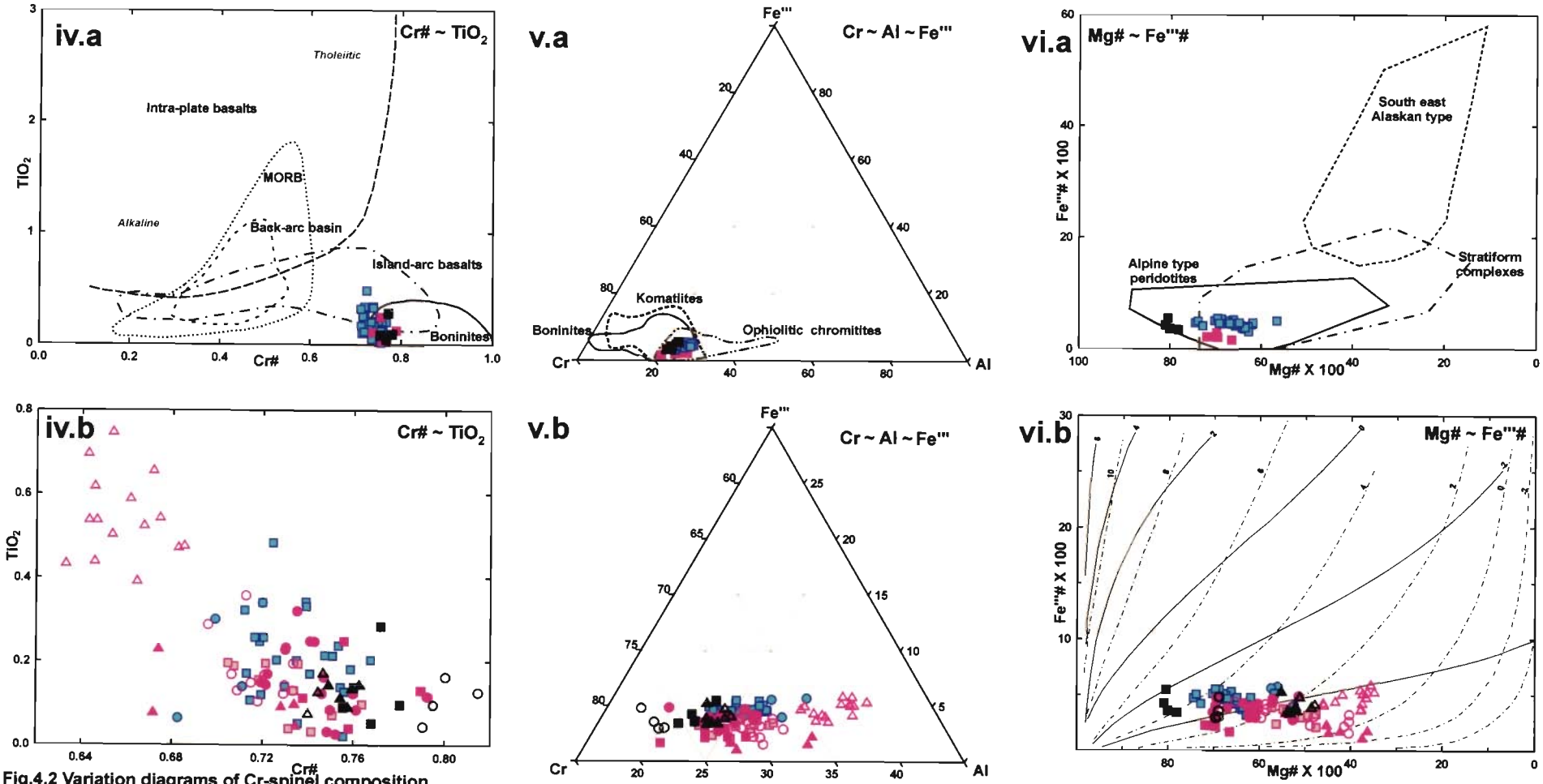

Fig.4.2 Variation diagrams of Cr-spinel composition
iv Cr#~TiO_2 a. chromitite *(fields from Arai 1992)* **b. different varieties of ores,**
v Tringular plot of Cr~Al~Fe''' a. Chromitites *(fields from Barnes & Roeder 2001)*
b. different varieties of ores
vi Mg#~Fe'''# a. Chromitites *(fields are from Dick & Bullen 1984)*
b. different varieties of ores*(contours of constant oxygen fugacity isobars in Al-free [dashed lines] and Cr-free [solid lines] are from Irvine 1965)*

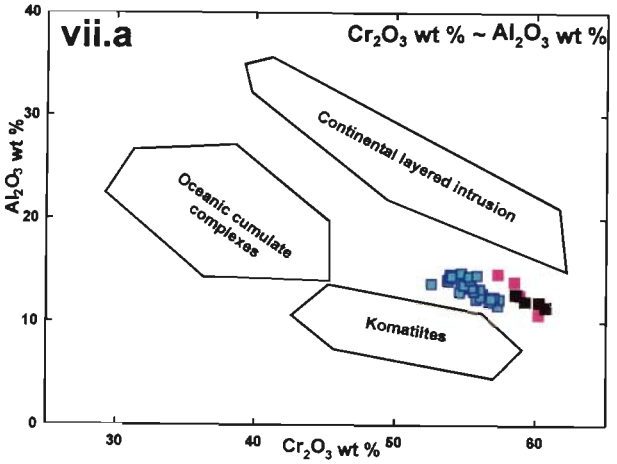

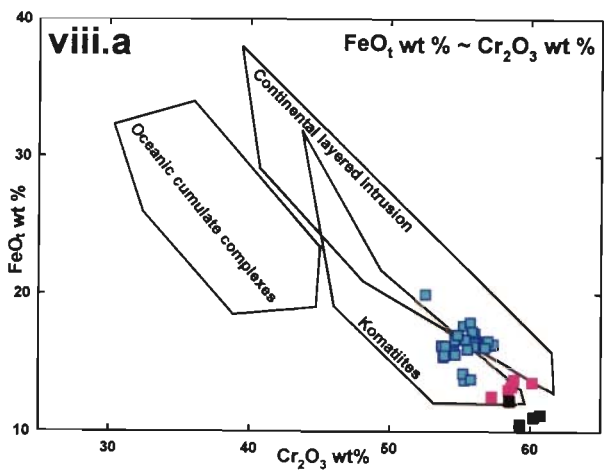

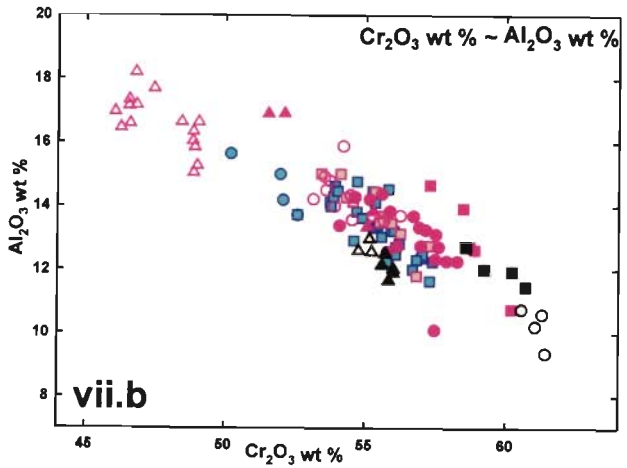

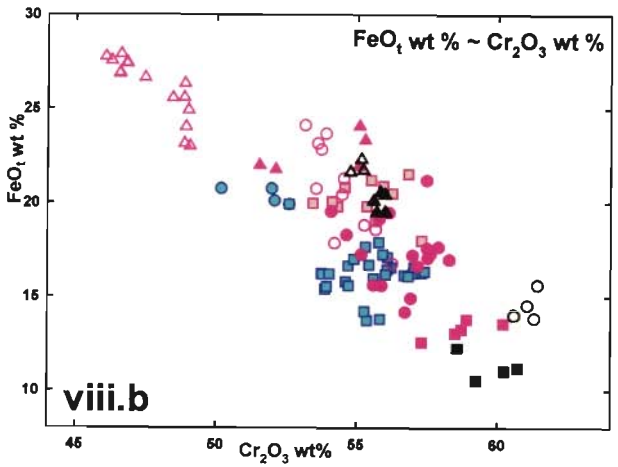

Fig.4.2 Variation diagrams of Cr-spinel composition
vii Cr_2O_3~Al_2O_3
a. chromitite
b. different varieties of ores,
viii Cr_2O_3~FeO_t
a. Chromitites
b. different varieties of ores
(fields from Mitra & Bidyananda 2003)

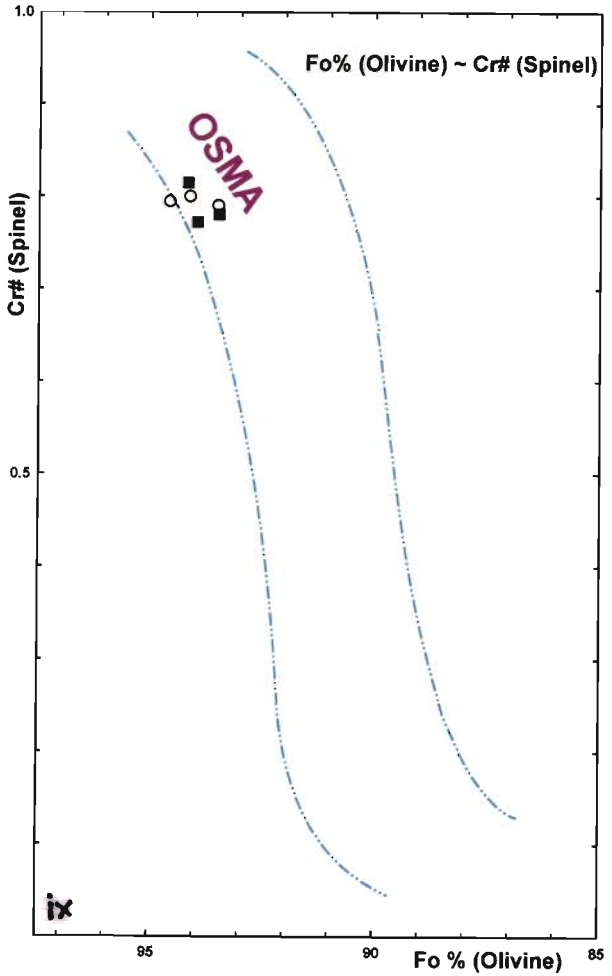

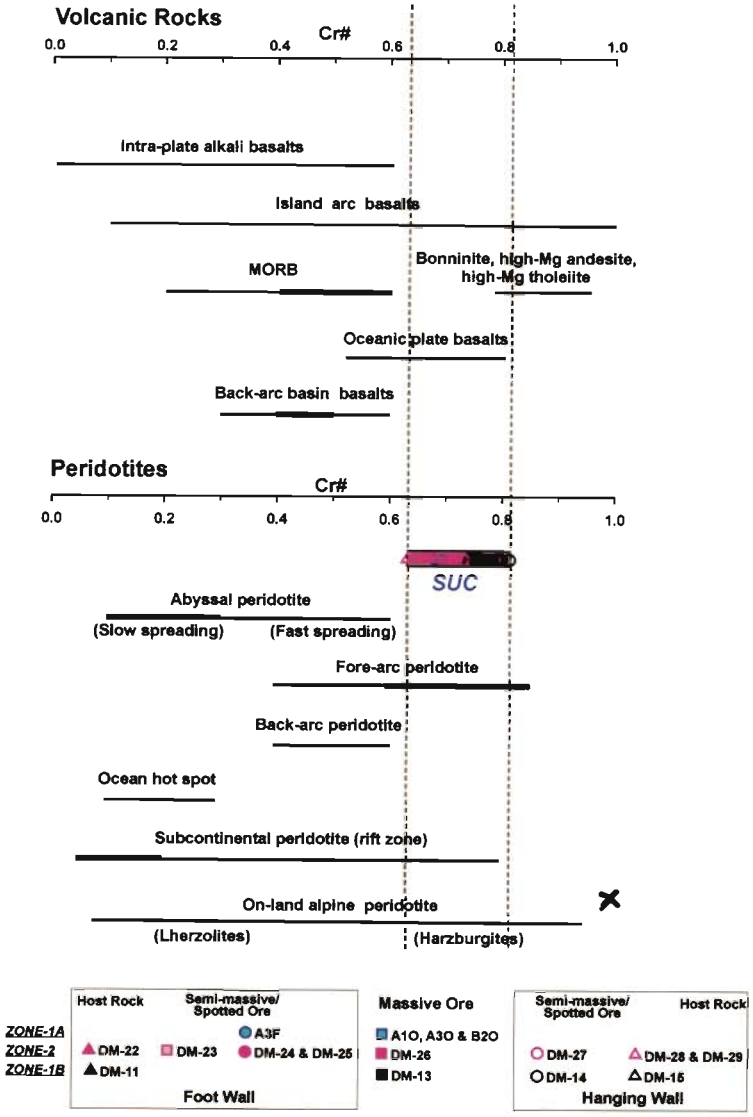

Fig.4.2.ix Plot of Fo (Olivine)~Cr# (Spinel) for chromite ores (Olivine Spinel Mantle Array-OSMA, *from Arai 1994***) x Cr# of Cr-spinel of SUC and, Peridotites and volcanic rocks from different tectonic settings** *(Lee 1999)*

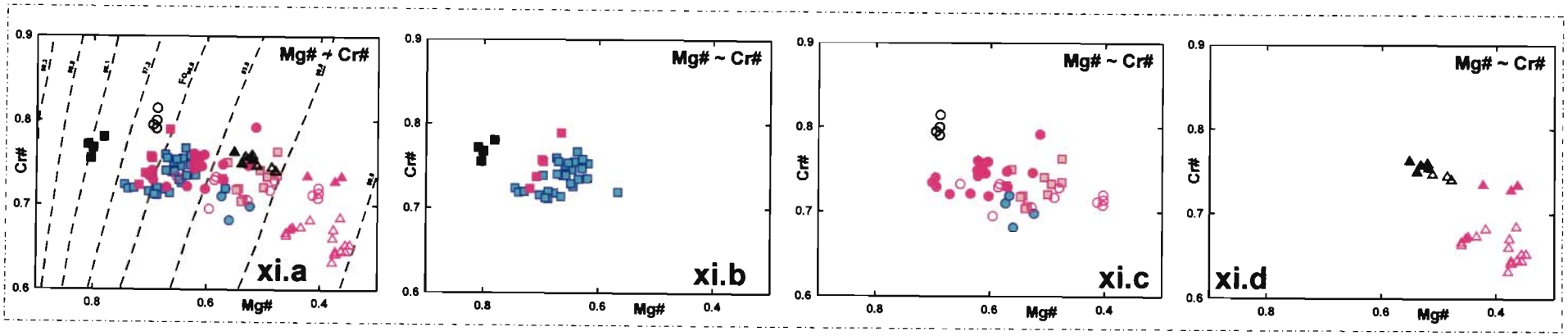

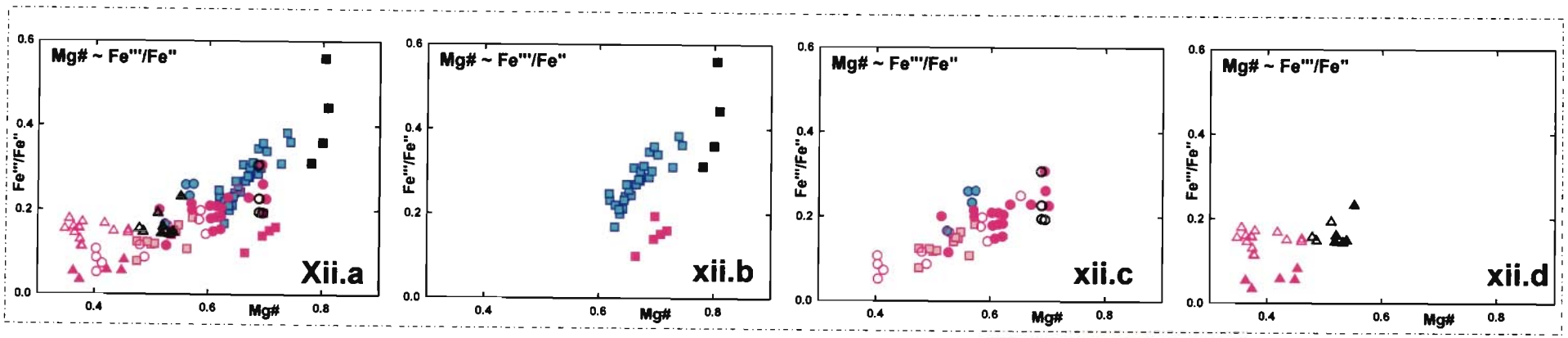

Fig.4.2.xi.a Mg#~Cr# plot of Sukinda chromites with the isopleths *(Dick & Bullen 1984)*, **Mg#~Cr# plots of b massive ore, c Semi-massive/Spotted ores, d host rocks from different sections**

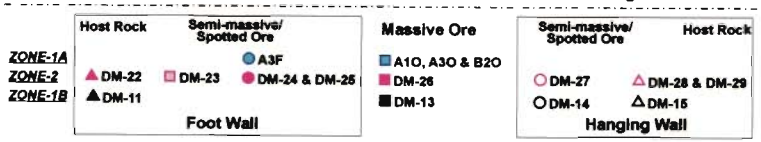

Fig.4.2.xii.a Mg#~Fe'''/Fe" plot of Sukinda chromites Mg#~Fe'''/Fe" plots of b massive ore, c Semi-massive/Spotted ores, d host rocks from different sections

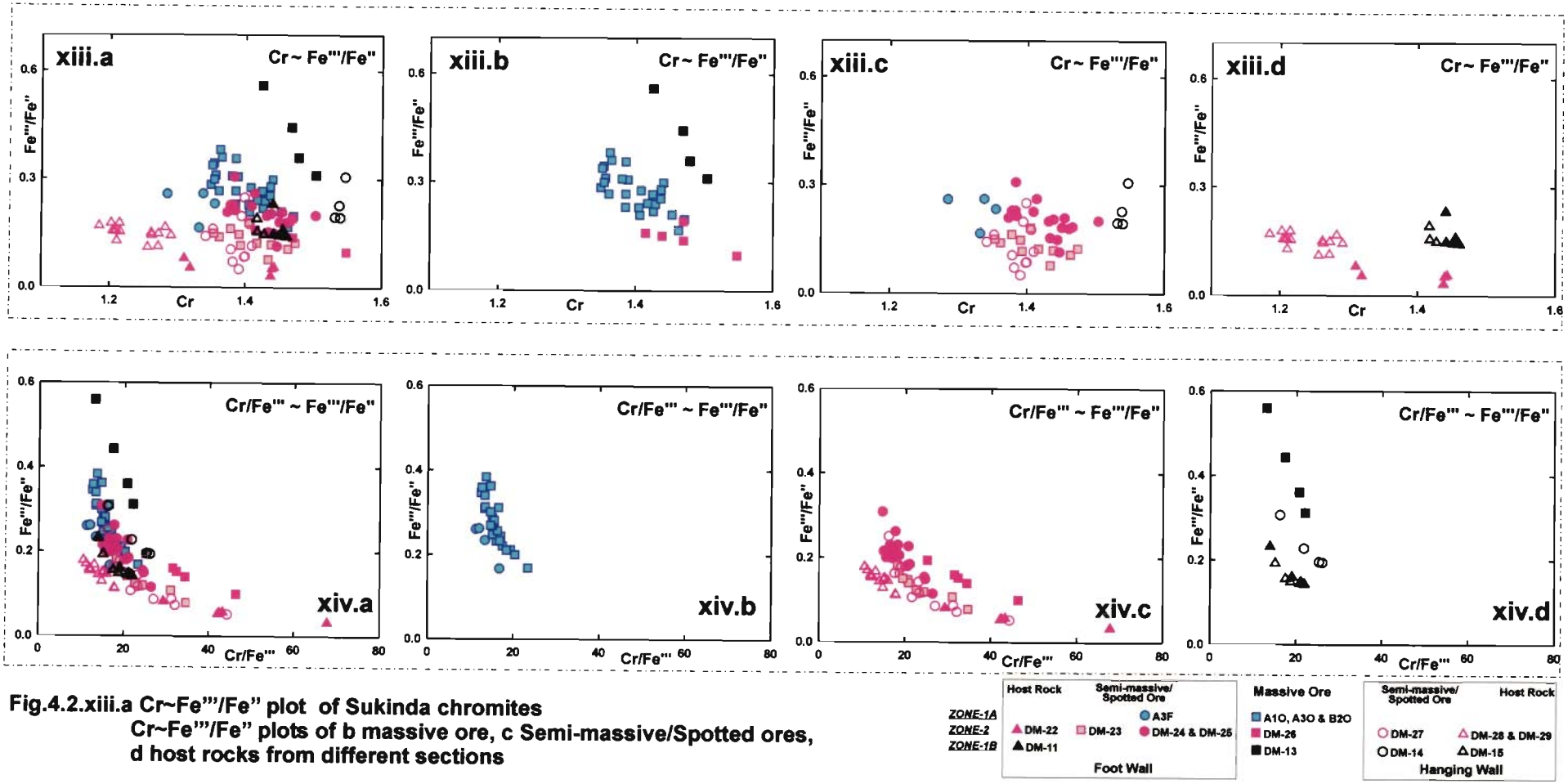

Fig.4.2.xiii.a Cr~Fe'''/Fe" plot of Sukinda chromites
Cr~Fe'''/Fe" plots of b massive ore, c Semi-massive/Spotted ores, d host rocks from different sections

Fig.4.2.xiv.a Cr/F'''~Fe'''/Fe" plot of Sukinda chromites
Cr/F'''~Fe'''/Fe" plots of b massive ore, c Semi-massive/Spotted ores, d host rocks from different sections

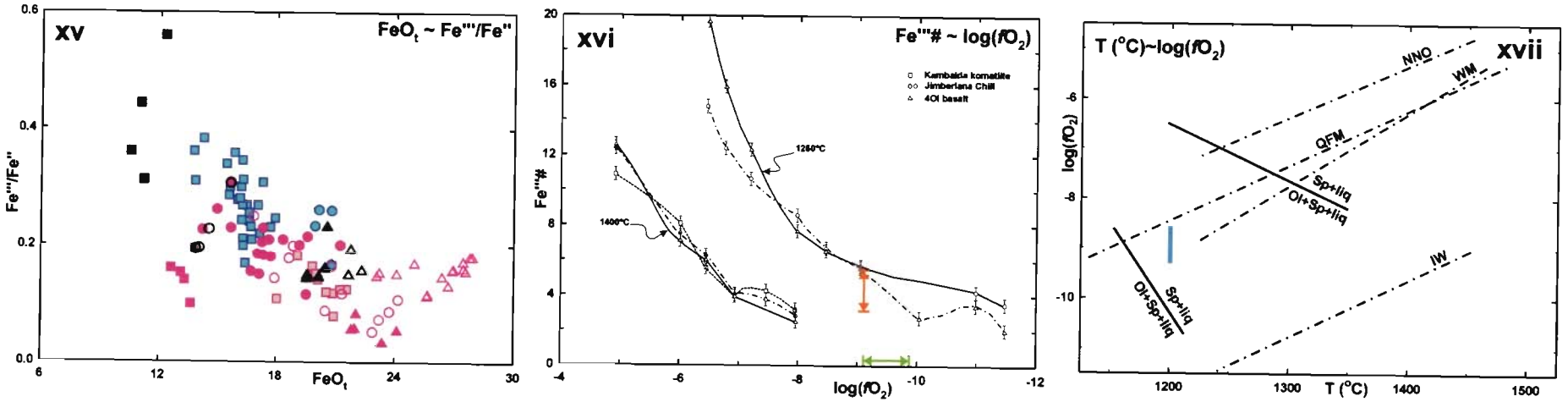

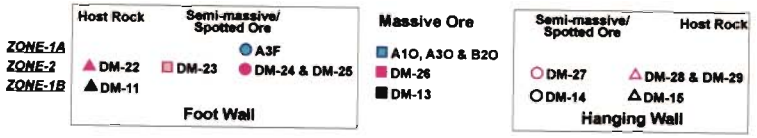

Fig.4.2.xv FeO_t~Fe'''/Fe'' plot of Sukinda chromites

Fig.4.2.xvi $log(fO_2)$~Fe'''# plot *(after Murck & Campbell 1986).* **Green line shows the range of $log(fO_2)$ for the formation of Sukinda chromites**

Fig.4.2.xvii T(°C)~$log(fO_2)$ plot *after Murck & Campbell 1986* **showing the experimental arrangement. Blue block shows range of $log(fO_2)$ for the formation of Sukinda chromites**

of variation in Mg# (Fig.4.2.xi) of the Cr-spinels indicates crystallization almost under relatively uniform pressure condition unlike higher degree of pressure variations (as evident from the higher degree of reciprocal variation of Cr and Al, Dick & Bullen 1984) as recorded in the literatures for alpine type complexes. Very high Cr# indicates crystallization at relatively low pressure (Cr# >0.63) condition *i.e.* at shallower crustal level and through a slow cooling process as indicated by the broader range of Mg# (0.35 to 0.81). The scatter and trend of Cr#~Mg# plot and higher values of Cr# precludes the possibility of abyssal origin of the complex and the Cr# of the Type-III alpine spinel peridotites and herzburgites (Fig.4.2.i). The higher degree of variation in the Mg# indicates partitioning of Mg and Fe" amongst the spinel and silicate phases during equilibrium crystallization reflecting change in melt composition (progressively Fe-rich) with fall in temperature and, is proportional to their relative proportion in the rock. However the possibility of sub-solidus re-equilibration (Lehmann 1983) of the spinel with the silicates can not be ruled out for a slow cooling process as indicated by a broader range of Mg# (Fabriès 1989). Using the isopleth of Dick and Bullen (1984), the composition of the co-existing olivine found to lie between $F_{O98.1}$ and F_{O80} (Fig.4.2.xi.a). Few relict olivine grains found within massive chromites as 'eye' and spotted ores as 'nodules' are analyzed for F_O content (94.6 to 93.5%) and found to be well within the limits defined by the isopleths.

A decrease in Cr# is accompanied by corresponding decrease in Mg# reflects a change in melt composition with the fall in temperature. It is also apparent from the plots of Cr_2O_3~Al_2O_3 and Cr_2O_3~FeO_t. Reciprocal trends are shown both by Al_2O_3 (Fig.4.2.vii.b) and FeO_t (Fig.4.2.viii.b) with that of

Cr_2O_3. The FeO_t content vary from 10.53 to 27.87 wt% and Al_2O_3 vary from 9.37 to 18.21 wt%.

A small but distinctly higher Fe^{3+}/Fe^{2+} value indicates existence of a higher oxygen activity (Fig.4.2.xii, Mg#~Fe"'/Fe") even at higher temperatures (high Mg#) during the crystallization of Cr-rich chromites (Fig.4.2.xiii, Cr~ Fe^{3+}/Fe^{2+}) of chromitites from a relatively Fe-poor (Fig.4.2.viii) melt compared to the host rock. It suggests an obvious higher fO_2 condition during the formation of the ore compared to its host rock. Plot of Cr/ Fe^{3+}~ Fe^{3+}/Fe^{2+} (Fig.4.2.xiv) shows a general increase in Cr/ Fe^{3+} with decrease in Fe^{3+}/Fe^{2+} indicating the preference of Cr for octahedral site compared to Fe^{3+} at low oxygen activity. Accordingly the massive ores shows comparatively low Cr/ Fe^{3+} with respect to the corresponding host rocks and spotted ores though the Cr-content is high in these ores. The Cr/ Fe^{3+} ratio drastically increases below certain oxygen activity level demarcated by the Fe^{3+}/Fe^{2+} value ~ 0.15. However, the variation in the Cr/Fe^{3+} ratio may also be attributed to the change in temperature and melt composition. An inverse variation in Fe^{3+}/Fe^{2+} ratio (0.03-0.56) with respect to the Fe-enrichment of the melt is found (Fig.4.2.xv, FeO_t~Fe^{3+}/Fe^{2+}).

4.2.3 Physico-Chemical Condition & Melt Composition

Few relict grains of olivine are recognized in some of semi-massive/spotted ores those survived the effect of extensive serpentinization. The olivines found to be forsteritic (F_O ~95%). The geothermometric calibration postulated Fabriès (1979) is used for the calculation of respective spinel-olivine (compositions shown in Table 4.2) temperature as the rock is highly Mg-rich.

$$T°\mathrm{K} = \frac{4250Y_{Cr}^{Sp} + 1343}{\ln K_D^0 + 1.825Y_{Cr}^{Sp} + 0.571}$$

Where, $\ln K_D^0 = \ln K_D - 4.0Y_{Fe'''}^{Sp}$

$$K_D = \frac{X_{Mg}^{Ol} X_{Fe''}^{Sp}}{X_{Fe''}^{Ol} X_{Mg}^{Sp}}$$

and $$Y_{Cr}^{Sp} = \left(\frac{Cr}{Cr + Fe''' + Al}\right)^{Sp}$$

The estimated temperatures varies between *993°C* and *760°C* and are less than the experimental values (1250°C±100°C) of Murck and Campbell (1986) for the formation of chromitite layers. These temperatures indicate the blocking in the exchange reactions between spinel-olivine pairs rather than the temperature of formation of chromites. The relict olivines from the massive chromites with accurate measurement of Fe-cations may provide better estimates of temperature of formation of chromitites of SUC. However, a better estimate of temperature of crystallization of chromites (1200°C) is given by Pal and Mitra (2004) from this deposit.

Fe^{3+}#~Mg# plot (Fig.4.2.vi.b) contoured with theoretical constant fO_2 isobars from Irvine (1965) (depicted from Dick & Bullen 1984) for Cr-free

systems and Al-free system. Natural assemblages with variable Cr:Al ratios at constant fO_2 should lie parallel and between these two types of isobars. The data shows existence of variable fO_2 during the formation of different ore grades, highest being for the chromitites and lowest for the host rocks. The $\log fO_2$ is extrapolated from $Fe^{3+}\#$~$\log fO_2$ plot using the curve for 1250°C of Murck and Campbell (1986) and, found to vary between *-9.1* to *-9.8* for the chromites both from Kathpal and Kalarangitta area (Fig.4.2.xvi). According to Murck and Campbell (1986), an error of 200°C yields a difference of ~0.5 log unit in fO_2 value. Considering this error and assuming the temperature of formation of chromites to be 1200°C the actual range of fO_2 should be between *-8.6* to *-9.3* and is *-0.1* to *-0.8* log units with respect to QFM buffer (Fig.4.2.xvii).

The refractory nature of the parent melt is much clear from the high forsteritic content of the olivine and, Mg# and Cr# values of spinel. The Al_2O_3 content of the melt is determined using the equation postulated by Maurel and Maurel (1982) in Augé 1987 *i.e.*,

$$(Al_2O_3)_{Sp} = 0.035(Al_2O_3)_{liq}^{2.42} \qquad (Al_2O_3 \text{ in wt\%})$$

The range of values found to be 10.08 to 13.26% with a standard deviation of 0.6 and average value as 11.79% from host rock to massive chromitites.

The FeO/MgO ratio of the parent melt can be determined from the monominerallic rocks. Following the formula (Maurel 1984 in Augé 1987) used for the FeO/MgO ratio of the parent melt from spinel composition of chromitites with the reservation that the spinels are sensitive to sub-solidus re-diffusion processes and most massive ore contains 5 to 10% of silicates.

$$\ln\left(\frac{FeO}{MgO}\right)_{Sp} = 0.47 - 1.07Y_{Sp}^{Al} + 0.64Y_{Sp}^{Fe'''} + \ln\left(\frac{FeO}{MgO}\right)_{liq} \qquad \text{(FeO and MgO in wt\%)}$$

The whole range of $(FeO/MgO)_{liq}$ found to be 0.32 to .87 (Avg 0.66, σ 0.15).

The range of $(FeO/MgO)_{liq}$ ratio for individual zones varies small but distinctly being 0.49 to 0.87 (Avg. 0.71, σ 0.10) for Kathpal Quarry chromitites (Zone-1A), 0.57 to 0.69 (Avg. 0.62, σ 0.05) for Kalarangitta chromitites (Zone-2), 0.32 to 0.38 (Avg. 0.35, σ 0.03) for Kathpal under ground chromitites (Zone-1B). Cr-spinels from these zones indicate a distinct range with some overlap in terms of their Mg# (Fig.4.2.xi.b), Cr-content (Fig.4.2.xiii.b), TiO_2 (Fig.4.2.iv.a), Al_2O_3 (Fig.4.2.vii.a) and FeO_t (Fig.4.2.viii.a). This indicates that these chromitites are formed at different crustal level from progressively evolved melt fraction in the cooling history of the parent magma most primitive being for Zone-1B followed by Zone-2 and Zone-1A respectively. However, the microlevel variation in the individual zones from ore to host rock is attributed to the equilibrium crystallization and the relative proportion of chromite and silicates (Fig.4.2.xi-xiii & xv).

In brief, the high Cr# (>0.71), high Mg# (>0.62), higher Cr/Fe_t (>3.01), lower Ti-content (<0.01) and low Fe^{3+}/Fe^{2+} (<0.56) of the chromitites, all indicate a high magnesia parentage geochemically very much similar to that of podiform chromites of ophiolitic complexes or komatiitic magmas of Achaean greenstone belts. A note may be made of the trend of Mg#~Cr# plot for SUC shows a decrease in Cr# is accompanied with decrease in Mg# and cross-cuts the F_O-isopleths of Dick and Bullen (1984) indicating varied compositions for the olivines, unlike those of Alpine type peridotites. The age of SUC may be as high as 3.1 Ga, age of Bangur gabbro of Boula-Nausahi

complex (Augé et al. 2003), if the SUC and Baula-Nausahi complex are considered to have resulted from a single, protracted magmatic event and the SUC emplaced early in the sequence. Mondal et al. (2006) had also given a similar age from a correlation study of different stratigraphic units and related to SUC chromitites to supra-subduction set-up. Precluding the possibility of an ophiiolitic origin, equilibrium crystallization from a komatiitic parent magma may be thought of for SUC in a relatively stable tectonic environment making due considerations to the Archaean mantle composition and earth movement process and, nature of compositional variations exhibited by the Cr-spinels of SUC. The oxygen fugacity is found to be the major controlling factor for the formation of the chromitites and may have triggered by the silica contamination during the rise of the magma.

The main SUC may be considered to have formed from a later more evolved magmatic fraction compared to Kathpal chromites. This along with the geological set up indicates that the Kathpal chromites are formed in the 'mini magma chambers' at deeper crustal levels from early melt fractions and structurally affected in a quasi-solid state by the later the intrusion of later melt fraction. The Kathpal chromites are brecciated by granodiorite(?) and gabbroic intrusions similar to that of Bangur gabbro of Baula-Nausahi complex, representing the extreme fractionated product of the parent magma and may be a possible locus of PGE mineralization.

Platinum Group Elements (PGE) form a coherent group of siderophile elements and hence major portion of these elements are probably concentrated in the core during early stage of differentiation of the silicate earth significantly reducing the mantle concentration of these elements (White, 2000). The geochemical behavior is not well understood subjected to the limitations for determining the trace quantity and their association with varied lithologies formed in different physico-chemical condition. However, development of sophisticated instrumental techniques and available natural as well as the experimental data made it clear that these elements behave as chalcophiles under upper mantle and crustal condition of fS_2 and sulfides act as the carrier for PGE. It is further well established that the fractionation of these elements depends on the initial melt composition, temperature, fS_2 and fO_2 and, are grouped as IPGE (Ir, Os, Ru) and PPGE (Pt, Pd, Rh). Genetically, the IPGE bearing phases are dominated in mantle sequence of the ophiolitic complexes whereas the PPGE bearing phases dominate the cumulate crustal sequence of the layered ultramafic complexes. Present section deals with the PGE mineralization in Sukinda ultramafic complex in the light of whole rock PGE abundances, sulfide mineralogy and PGE-bearing phases, if there is any.

5.1 PGE GEOCHEMISTRY

5.2 SULFIDE MINERALOGY

5.3 PLATINUM GROUP OF MINERALS (PGM)

5.4 OTHER NOBEL METAL MINERALOGY

5.1 PGE GEOCHEMISTRY

The analyses of precious metals are mainly constrained by their low absolute abundances and heterogeneous distribution in the geological samples. The precise determination of PGE those are in trace amount needs sophisticated instrumental techniques. Excellent reviews on analysis of precious metal concentration are provided by various workers (Potts 1987, Barefoot and Loon 1999). On the hand, fire assay method of preconcentration remains the commonest sample preparation procedure due to its capability to treat relatively large sample size, typically one *assay ton* (29.167 g), which to some extend compensate for *"nugget effects"* during sub sampling (Enzweiler *et al.* 1995, Gros *et al.* 2002). Their high masses make them particularly well suited to determination by ICP-MS (Jarvis *et al.* 1992, Balaram 1995, Balaram 2001).

In the present study, the *fire assay* technique along with *tellurium co-precipitation* is used for the pre-concentration of the nobel metals and their absolute concentrations are determined with the help of *Perkin-Elmer Sciex, Elan DRC II – ICP-MS* at *National Geophysical Research Institute (NGRI), Hyderabad India*. A total of 23 samples including host rock serpentinites , spotted/semi-massive ores and massive ores from Zone-1b-e and Zone-2 along with one sample each from partially altered dunitic peridotite, noritic gabbro and dolerite are analyzed for precious metal concentrations (for sample details see Table 2.1, Chapter-1). The details of the instrument and operating parameters are mentioned in Balaram and Rao (2003) and the procedure followed is mentioned in Mathur *et al.* (2003) and Balaram *et al.*

(2006). The standard used for the calibration of the instrument for the samples is SARM-7. The internal standard used is 0.2ppm Cd+Tl solution to correct for signal drift during analysis. The results of PGE along with Re, Au and Ag are shown in Table 5.1. This is to mention that the data has been used with the reservation that the values for Os and Ru are *semi-quantitative* owing to their loss as volatile oxides during the *fire assaying*. However, in all likelihood the actual values must be higher than the values determined.

The total of PGE concentration varies between 311.20ppb to 28.2ppb dominated by IPGE. The range of variation in Os, Ir, Ru, Rh, Pt and Pd is 2.20-121.40ppb, 1.80-38.20ppb, 8.40-116.20ppb, 1.2-11.20ppb, 2.20-50.00ppb and 0.80-8.40ppb respectively in different varieties of ore and host serpentinites, indicating their sub-chondritic abundances (Table 5.1). The relative concentrations in the samples are shown in bubble plot (Fig.5.1).To observe the variation in PGE concentration along the particular section, profile are drawn from hanging wall to footwall host rock for IPGE, PPGE, IPGE/PPGE and total PGE values. It is noteworthy that with rare exceptions, the profiles invariably shows prominent peaks for IPGE, total PGE and IPGE/PPGE (Fig.5.2) in the massive chromitites and decreases with decrease in Cr-spinel proportion in the samples. Such enrichment of refractory PGE *i.e.* IPGE is attributed to their fractionation with chromite crystallization (Barnes 1990).

Again, the level of sulfide saturation across any stratigraphic section can be checked by Ni and Cu to PGE ratios as described by Barnes (1990). As crystallization of chromite and olivine has pronounced effect on these ratios, he suggested for considering the ratios of Pd/Ir or Pd/Rh or Pd/Pt

versus Ni/Cu to eliminate the effect of removal of IPGE and Ni by chromite and olivine. Accordingly, the ratio plots host ultramafics are prepared (Fig.5.3.i-vi). These plots indiscriminately show values close to that of mantle. Three important points has been found out *i.e.*, the source is mantle or any high degree partial melt (Fig.5.3.i-vi; see also Cr-spinel composition in Chapter-4), no sulfide saturation has been achieved (Fig.5.3.iv-vi; see also Fig.3.3.ii for transition metal plot in Chapter-3) and the PGE fractionation is mainly triggered by the chromite crystallization (*insets* in Fig.5.3.i-vi).

The triangular plots of combination of different IPGE and PPGE shows the close resemblance of the data with that of the Kempirsai ophiolitic complex, Kazak Republic (data on the global PGE deposits are from *Distler* unpublished, Fig.5.4.i). However, the fractionation trend shows a general increase in Os+Ru with respect to Pt+Pd with the increase in Cr-spinel proportion *i.e.* from host serpentinite to chromitites (Fig.5.4.ii). Similar trend is shown between Ru and Os (Fig.5.4.iii). Ir and Rh show little fraction as evident from Fig.5.4.ii-iii. There is absolutely no definite fractionation pattern amongst the PPGE (Fig.5.4.iv) indicating Cr-crystallization has no bearing on their fractionation and the concentration is typical of S-poor fraction.

Like REE, normalized plots PGE are also used for interpretation of fractionation pattern of different elements and level of enrichment/depletion compared to the probable source materials. But the PGE are arranged with decreasing melting point (*i.e.* decreasing compatibility) in contrast to REE where it is ordered by their increase in atomic number (Barnes *et al.* 1987). The concentration of Ir (representing IPGE) is about 0.1 to 0.007 times of

Table 5.1 *Contd.*

	KALARANGITTA												
	Zone-2												
Sample No.	DM-22	DM-25	DM-26	DM-27	DM-29	Avg.HR	Avg.SM	Avg. MO	DM-84	DM-85	DM-86	Mantle*	CI Chondrite**
Ni	1631.95				1953.37	1930.25			641.40	629.30	2263.38	1890.00	10500.00
Os	2.20	3.60	19.40	10.60	2.80	8.45	21.55	78.55	1.00	1.20	3.20	4.20	490.00
Ir	3.40	7.40	37.80	13.60	2.40	8.65	18.85	36.80	0.40	0.60	1.80	4.40	455.00
Ru	14.60	20.60	86.80	24.80	8.40	23.90	51.75	103.65	3.20	3.00	7.20	6.00	710.00
Rh	1.40	2.00	5.40	2.20	1.20	2.25	4.55	8.10	0.80	0.80	1.20	2.00	130.00
Pt	3.00	2.60	7.00	3.20	3.80	4.45	12.58	6.75	3.60	3.20	4.00	9.20	1010.00
Pd	4.20	0.80	2.60	3.00	3.40	3.98	3.85	4.95	1.20	3.40	6.20	4.40	550.00
Au	11.60	4.20	8.60	25.40	6.20	8.78	14.75	16.50	7.60	7.40	7.20	1.40	140.00
Cu	20.61				27.58	17.06			33.42	7.64	13.21	30.00	120.00
Re	7.60	4.20	3.80	6.20	14.40	7.35	4.30	19.40	9.20	9.40	7.60		40.00
Ag	55.60	20.60	55.80	101.00	75.40	49.98	48.33	60.60	28.20	38.00	71.60		200.00
IPGE	20.20	31.60	144.00	49.00	13.60	41.00	92.15	219.00	4.60	4.80	12.20	14.60	1655.00
PPGE	8.60	5.40	15.00	8.40	8.40	10.68	20.98	19.80	5.60	7.40	11.40	15.60	1690.00
PGE Total	40.40	41.20	167.60	82.80	28.20	60.45	127.88	255.30	17.80	19.60	30.80	31.60	3485.00
IPGE/PPGE	2.35	5.85	9.60	5.83	1.62	3.84	4.39	11.06	0.82	0.65	1.07	0.94	0.98
Pd/Ir	1.24	0.11	0.07	0.22	1.42	0.46	0.20	0.13	3.00	5.67	3.44	1.00	1.21
Ni/Cu	79.19				70.82				19.19	82.38	171.36	63.00	87.50
Ni/Pd	388560.48				574519.71				534497.50	185086.76	365060.81	429545.45	19.09
Cu/Ir	6060.88				11492.92				83550.00	12731.67	7337.78	6818.18	0.26
Pd/Rh	3.00	0.40	0.48	1.36	2.83	1.77	0.85	0.61	1.50	4.25	5.17	2.20	4.23
Cu/Rh	14719.29				22985.83				41775.00	9548.75	11006.67	15000.00	0.92
Pd/Pt	1.40	0.31	0.37	0.94	0.89	0.89	0.31	0.73	0.33	1.06	1.55	0.48	0.54
Cu/Pt	6869.00				7258.68				9283.33	2387.19	3302.00	3260.87	0.12
(Ru/Pt)	7.46	12.15	19.01	11.88	3.39				1.36	1.44	2.76		

All the values are in ppb except Ni and Cu which are in ppm, *Mantle values *after Barnes et al. 87 & references therin, **McDonough & Sun (1995)*

Table 5.1 PGE concentrations of the chromitites and serpentinized host rocks of Sukinda

	KATHPAL (Zone-1)														
	Zone-1b				Zone-1c				Zone-1d				Zone-1e		
Sample No.	DM-11	DM-13	DM-14	DM-15	DM-16	DM-18	DM-19	DM-20	DM-98	DM-99	DM-100	DM-101	DM-102	DM-103	DM-104
Ni	2226.76			2029.00	2123.25			2085.85	1578.60			1765.13	2171.39		1429.53
Os	23.60	109.00	40.40	3.40	7.40	121.40	21.60	11.60	4.60	64.40	28.40	4.40	15.00	36.00	24.40
Ir	35.60	35.80	29.00	9.20	16.00	38.20	22.40	7.80	2.40	35.40	18.60	1.80	6.60	30.20	13.60
Ru	70.80	116.20	56.40	29.00	43.80	102.80	47.80	25.60	10.00	108.80	100.40	11.00	21.80	73.20	47.00
Rh	6.20	10.00	5.60	2.40	3.20	11.20	5.00	2.00	1.60	5.80	8.40	1.40	1.80	6.00	4.00
Pt	9.00	5.80	9.40	3.80	5.40	6.00	50.00	2.80	5.00	8.20	18.00	2.20	6.00	6.40	5.60
Pd	6.00	8.00	3.80	1.20	1.60	3.00	1.00	1.60	6.80	6.20	8.40	4.40	4.20	7.00	5.20
Au	5.40	26.40	14.20	12.40	27.40	24.00	7.60	3.60	10.60	7.00	13.20	10.60	9.80	14.00	12.00
Cu	14.25			25.41	30.13			16.35	9.76			10.70	11.78		10.86
Re	1.00	38.00	1.80	2.80	1.40	33.60	2.80	1.00	6.60	2.20	9.00	13.40	12.00	5.20	3.80
Ag	30.60	49.00	52.00	39.60	33.60	94.20	26.40	50.00	33.80	43.40	56.60	51.00	63.80	54.40	42.00
IPGE	130.00	261.00	125.80	41.60	67.20	262.40	91.80	45.00	17.00	208.60	147.40	17.20	43.40	139.40	85.00
PPGE	21.20	23.80	18.80	7.40	10.20	20.20	56.00	6.40	13.40	20.20	34.80	8.00	12.00	19.40	14.80
IPGE/PPGE	6.13	10.97	6.69	5.62	6.59	12.99	1.64	7.03	1.27	10.33	4.24	2.15	3.62	7.19	5.74
PGE Total	156.60	311.20	158.80	61.40	104.80	306.60	155.40	55.00	41.00	235.80	195.40	35.80	65.20	172.80	111.80
Pd/Ir	0.17	0.22	0.13	0.13	0.10	0.08	0.04	0.21	2.83	0.18	0.45	2.44	0.64	0.23	0.38
Ni/Cu	156.24			79.84	70.47			127.59	161.68			164.96	184.27		131.64
Ni/Pd	371125.83			1690829.17	1327031.88			1303654.38	232146.76			401164.77	516996.67		274908.85
Cu/Ir	400.34			2762.39	1883.13			2095.90	4068.33			5944.44	1785.45		798.46
Pd/Rh	0.97	0.80	0.68	0.50	0.50	0.27	0.20	0.80	4.25	1.07	1.00	3.14	2.33	1.17	1.30
Cu/Rh	2298.71			10589.17	9415.63			8174.00	6102.50			7642.86	6546.67		2714.75
Pd/Pt	0.67	1.38	0.40	0.32	0.30	0.50	0.02	0.57	1.36	0.76	0.47	2.00	0.70	1.09	0.93
Cu/Pt	1583.56			6687.89	5579.63			5838.57	1952.80			4863.64	1964.00		1939.11
(Ru/Pt)	12.06	30.72	9.20	11.70	12.44	26.27	1.47	14.02	3.07	20.34	8.55	7.67	5.57	17.54	12.87

All the values are in ppb except Ni and Cu which are in ppm, *Mantle values *after Barnes et al. 87 & references therin, **McDonough & Sun (1995)*

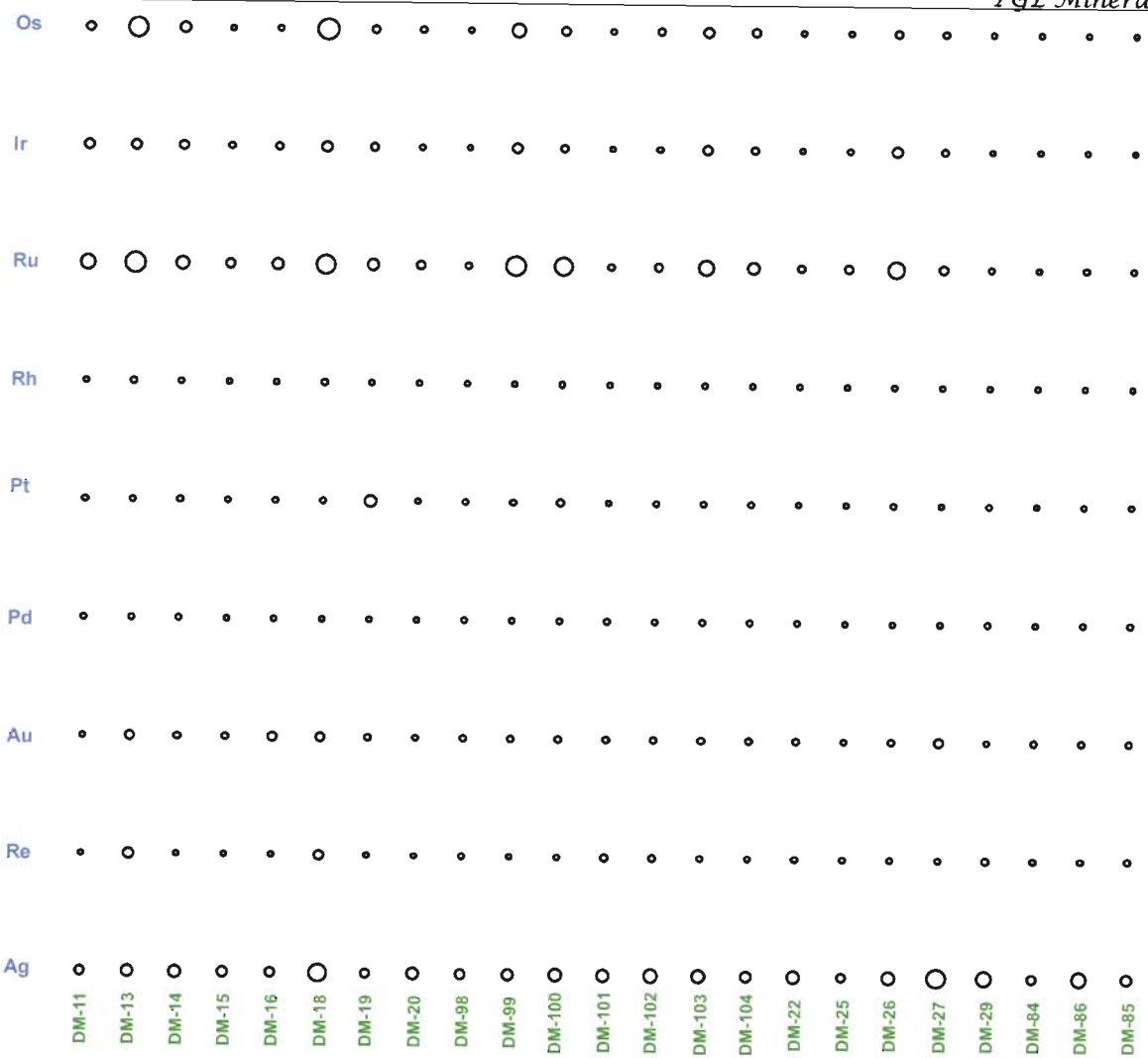

Fig.5.1 Relative concentration of noble metals in the samples

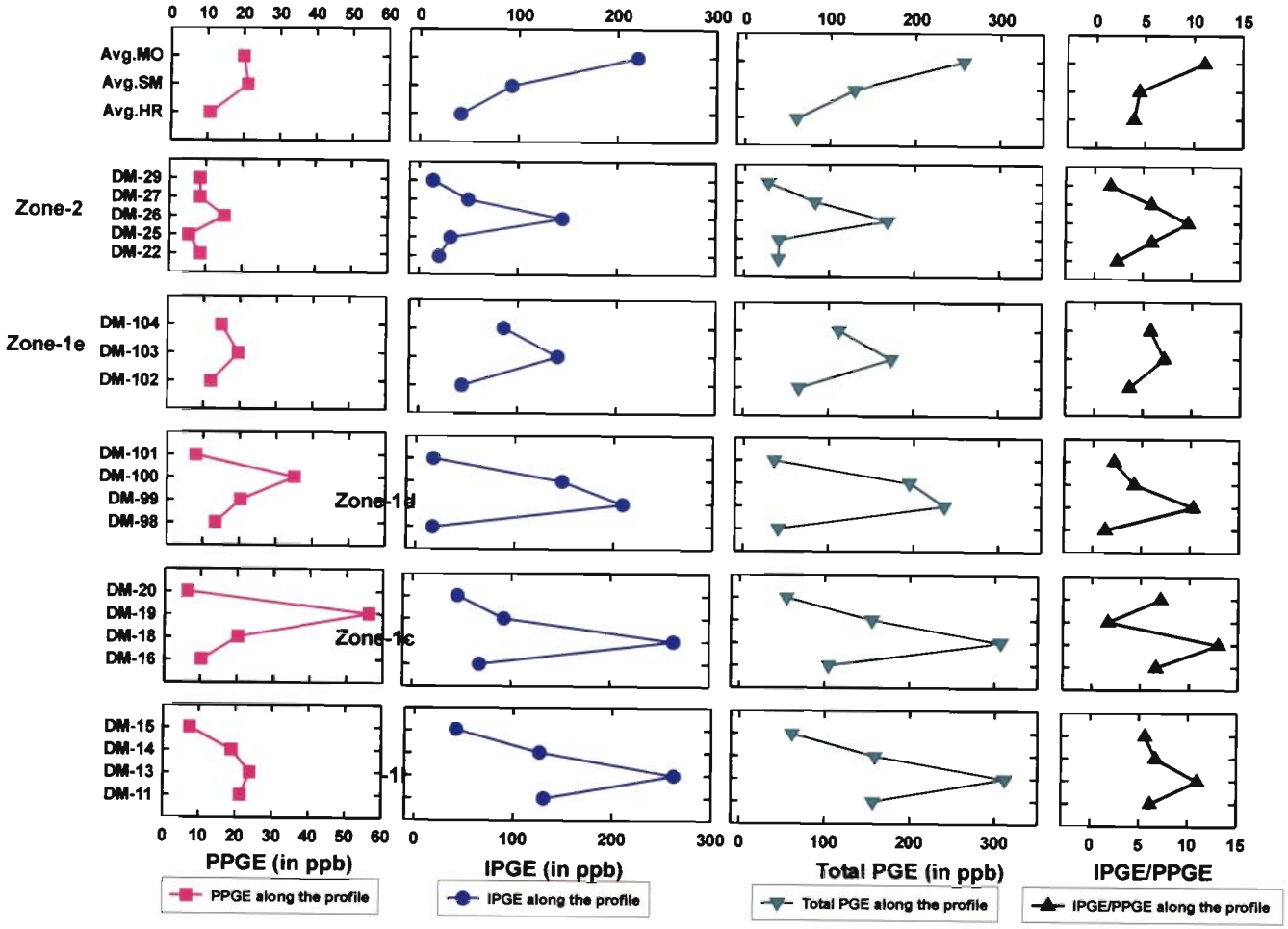

Fig.5.2 Profiles of PPGE, IPGE, total PGE and IPGE/PPGE ratio along different sections

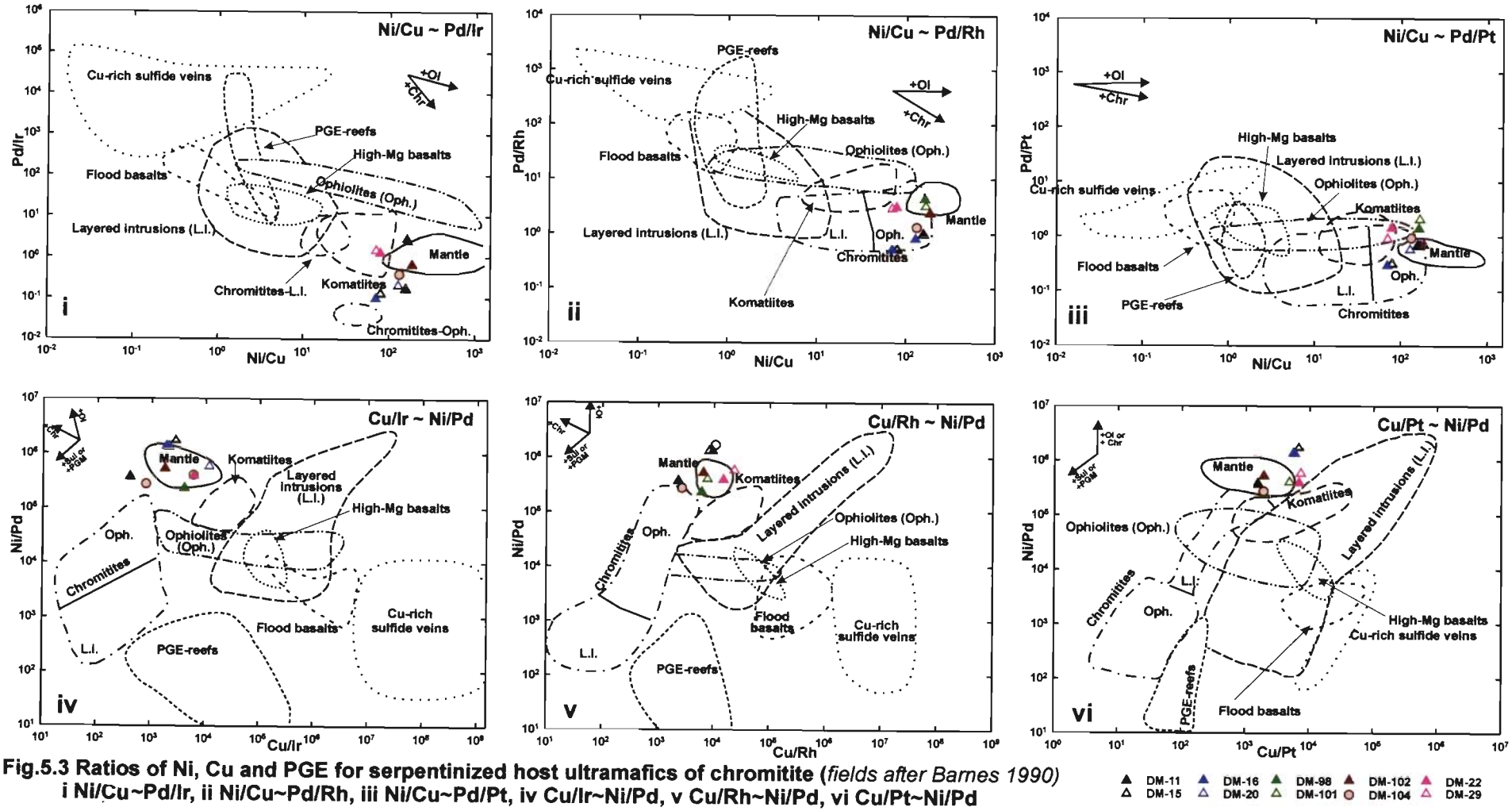

Fig.5.3 Ratios of Ni, Cu and PGE for serpentinized host ultramafics of chromitite (*fields after Barnes 1990*)
i Ni/Cu~Pd/Ir, ii Ni/Cu~Pd/Rh, iii Ni/Cu~Pd/Pt, iv Cu/Ir~Ni/Pd, v Cu/Rh~Ni/Pd, vi Cu/Pt~Ni/Pd

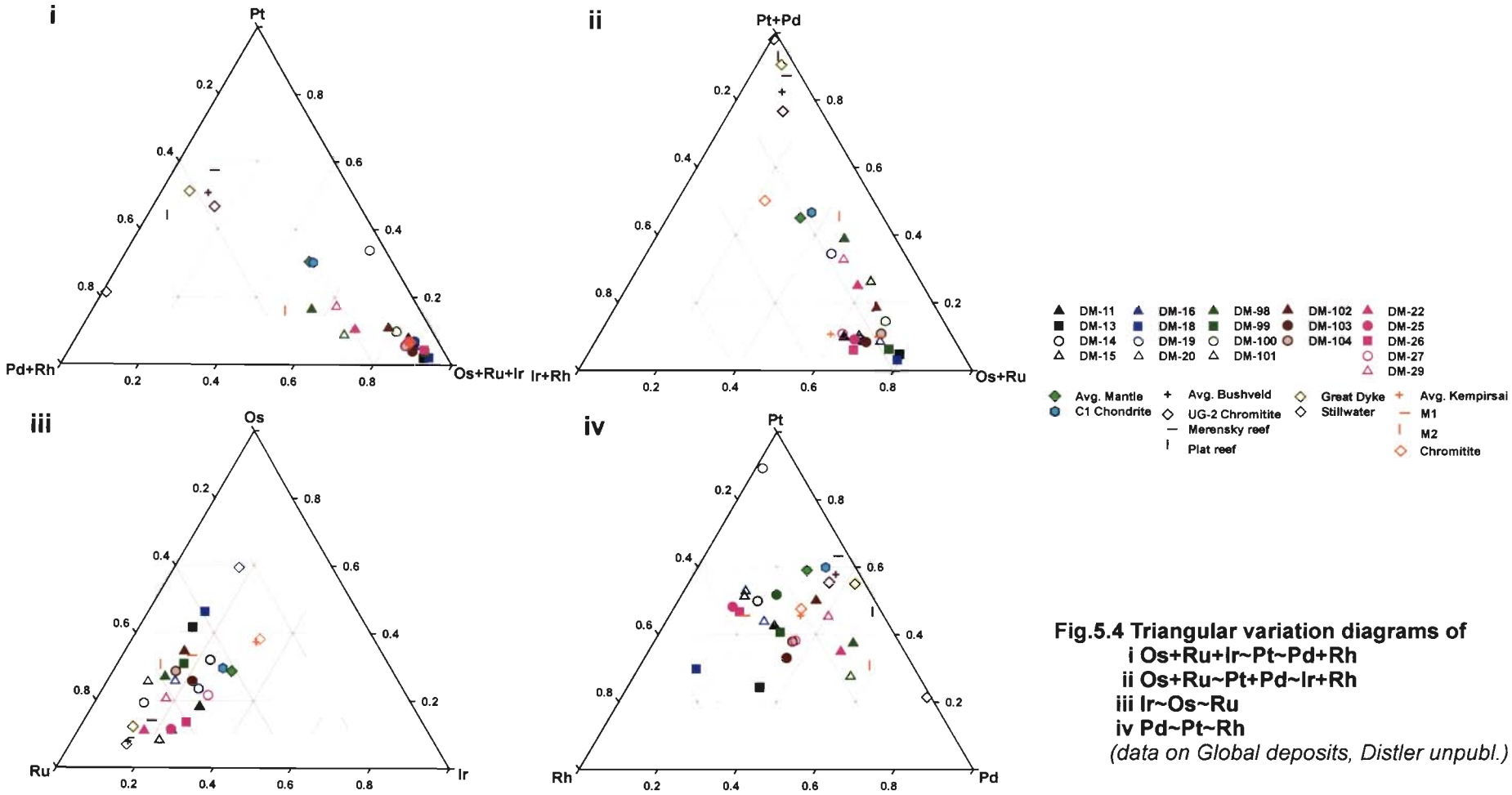

Fig.5.4 Triangular variation diagrams of
i Os+Ru+Ir~Pt~Pd+Rh
ii Os+Ru~Pt+Pd~Ir+Rh
iii Ir~Os~Ru
iv Pd~Pt~Rh
(data on Global deposits, Distler unpubl.)

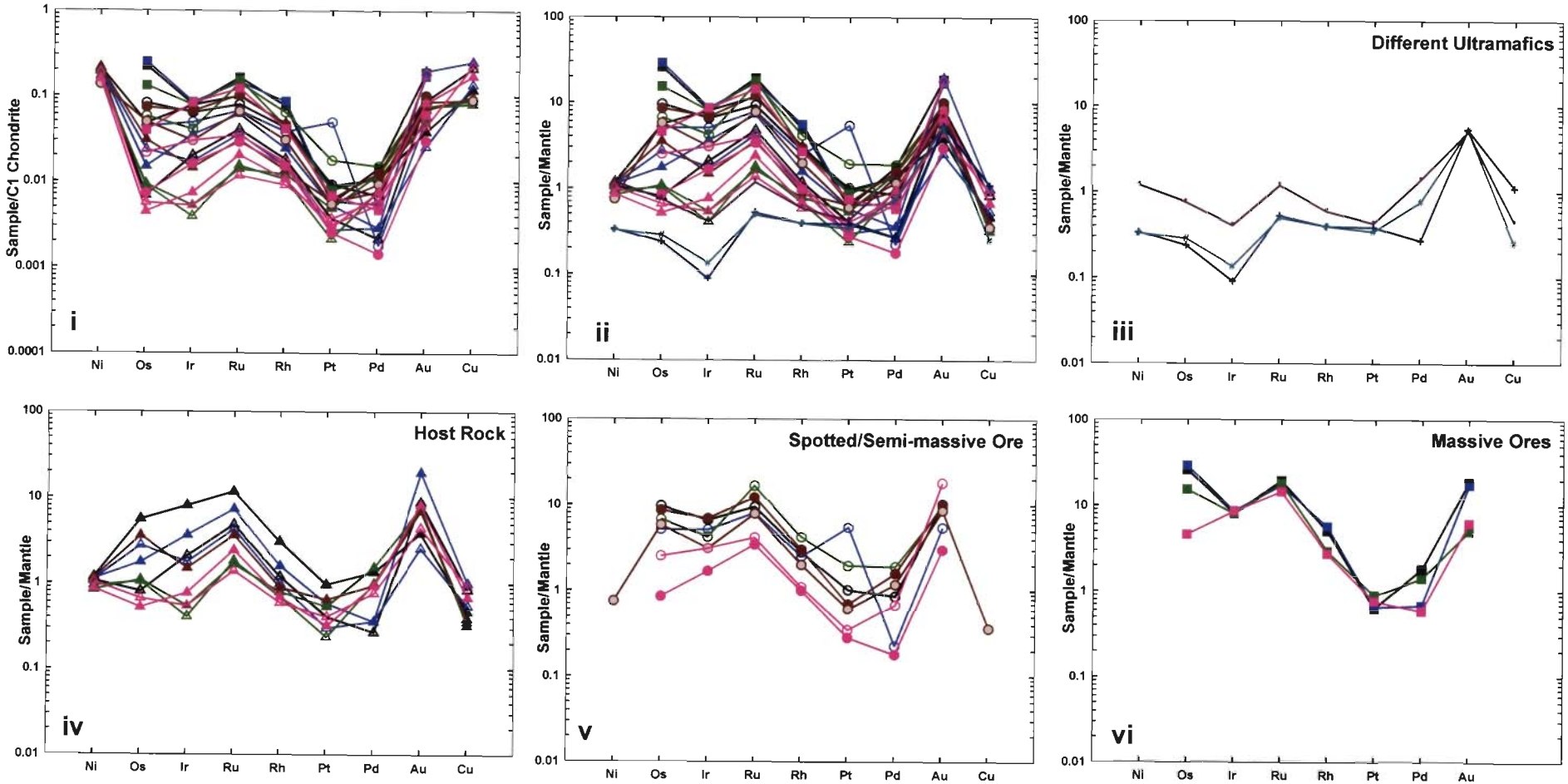

Fig.5.5 i C1 Chondrite *(after McDonough & Sun 1995)***normalized PGE plot of the host rock and chromitites, ii-vi Mantle** *(Barnes et al. 1987)* **normalized PGE plot of the all the varieties, host rock, semi-massive/ spotted ore, massive ores respectively.**

chondritic abundance and that of Pd (representing PPGE) is about 0.02 to 0.001times, in general (Fig.5.5.i). Such sub-chondritic values along with a negative slope of chondrite normalized pattern are characteristics of ophiolitic complexes (Naldrett & von Gruenewaldt 1989).

As suggested by Barnes *et al.* (1987) that majority of the alpine type peridotites are of mantle source and hence the mantle-normalized PGE plots [Mantle values of PGE are taken from Barnes *et al.* (1987) & references therein] are prepared to observe the fractionation and enrichment pattern of different PGE with respect the source melt (Fig.5.5.ii-v) (it should imitate the trace element characteristics of mantle because of its formation by high degree of partial melting). The different ultramafics, other than host rocks, show neither any clear-cut pattern in fractionation of PGE nor any enrichment (Fig.5.5.iii). An overall enrichment of IPGE is observed but PPGE values are close to one and a gradual enrichment in IPGE (Os is ~0.5 to 30 times of mantle values, Fig.5.5.ii) from massive chromite to host serpentinite (Fig.5.5.iv-vi). These evidences collectively confirm the fractionation of IPGE with chromite crystallization. A similar pattern for Cr in the primitive mantle normalized plot for host rock indicates that enrichment of IPGE is closely related to the enrichment of Cr.

Amongst other noble metals, considerable and consistent enrichment is shown for Au and Ag. Homogeneous distribution of gold in all the varieties of ore and host ultramafics might have resulted by its remobilization during late stage alteration. Ag enrichment indicates a hydrothermal origin in support of it and is discussed in the Section 5.4.

5.2 SULFIDE MINERALOGY

Although sulfide mineralization associated with other rock formations of the Indian sub-continent are well studied (Deb 2000, Sarkar 2002), the present work is one of those few studies that provides a detail account on nature of sulfide mineralization associated with the chromite bearing ultramafic rocks (Augé et al. 2002, Augé & Lerouge 2004, Sen & Mohanty *under preparation*). It has already been mentioned in Chapter-3 & 4, that the amount of sulfide minerals in the chromite ore and adjoining contact rocks is very low and normally constitutes less than one percent by volume. This is also evident from low-Ni content of the Cr-spinel and relict olivine composition. The sulfide grains are mostly fine grained and difficult to study under normal optical microscope. Based on microscopic studies the sulfide association can be divided into four categories:

i. sulfide filling interstitial spaces, ii. sulfide as micro-pit filling, iii. isolated unaltered sulfide iv. spongy altered sulfide.

The study of sulfide mineralogy is restricted to hard chromite ore and adjoining hangingwall and footwall rocks of Kathpal and Kalaringatta areas. After detailed ore microscopic studies of about 50 sections representing different varieties of ore and contact rocks, about 12 samples were chosen for EPMA studies at IIC, IIT Roorkee. About 40 sulfide grains were analyzed by EPMA and are shown in Table 5.2. The analyses overwhelmingly indicate that heazlewoodite is the most dominating sulfide species. The other important inference is the presence of As in small quantities in the sulfides. Few of the

Table 5.2 EPMA results of the sulfides of serpentinised host rocks and chromite ores

	KATHPAL									KALARANGITTA							
	DM-11		DM-13		DM-14		DM-15			DM-23					DM-24		
	1	2	3	4	5	6	7	8	9	10	11	12	13	14	15	16	17
S	26.47	33.41	34.25	23.51	28.36	27.70	27.03	26.46	26.48	26.33	26.45	26.89	27.06	26.26	26.40	26.55	26.35
Cu	0.00	0.00	0.00	0.04	0.00	0.00	0.00	-	-	-	-	-	-	-	-	-	-
Fe	1.27	0.18	0.09	0.37	0.11	0.27	1.09	0.27	0.21	0.09	0.12	0.42	1.09	0.17	0.24	1.10	1.22
Ni	68.56	66.45	66.09	67.00	71.82	71.84	69.30	70.39	71.22	73.01	73.18	71.73	67.27	71.98	72.02	71.03	70.34
Pb	0.77	0.10	0.17	6.39		0.09	0.50	0.24	0.10	0.07	0.07	-	0.12	-	0.13	0.26	-
Sb	-	-	-	-	-	-	0.00	-	-	-	-	-	-	-	-	-	-
Zn	-	-	-	-	-	-	0.00	-	-	-	-	-	-	-	-	-	-
As	0.59	0.35	0.06	2.57	0.87		0.15	0.41	-	0.43	0.03	0.50	0.33	0.83	0.34	0.28	0.18
Total	97.64	100.49	100.66	99.86	101.16	99.90	98.07	97.77	98.01	99.93	99.85	99.53	95.87	99.24	99.14	99.21	98.09
Atom	0.00	0.00	0.00	0.00	0.00	0.00	0.00										
S	40.72	47.75	48.62	37.67	41.70	41.28	41.18	40.55	40.42	39.62	39.77	40.42	41.90	39.78	39.98	40.15	40.21
Cu	-	-	-	0.03	-	-	-	-	-	-	-	-	-	-	-	-	-
Fe	1.12	0.15	0.08	0.34	0.10	0.23	0.95	0.24	0.18	0.08	0.10	0.36	0.97	0.15	0.21	0.95	1.07
Ni	57.59	51.87	51.24	58.62	57.66	58.47	57.66	58.89	59.38	60.01	60.09	58.89	56.88	59.54	59.55	58.66	58.61
Pb	0.18	0.02	0.04	1.58		0.02	0.12	0.06	0.02	0.02	0.02	-	0.03	-	0.03	0.06	-
Sb	0.00	0.00	0.00	0.00	0.00	0.00	0.00	-	-	-	-	-	-	-	-	-	-
Zn	0.00	0.00	0.00	0.00	0.00	0.00	0.00	-	-	-	-	-	-	-	-	-	-
As	0.39	0.21	0.03	1.76	0.55	-	0.09	0.27	-	0.27	0.02	0.32	0.22	0.54	0.22	0.18	0.12
Total	100.00	100.00	100.00	100.00	100.00	100.00	100.00	100.00	100.00	100.00	100.00	100.00	100.00	100.00	100.00	100.00	100.00
Min	Hz+Hm	Mil	Mil	Hz+Gal	Hz	Hz	Hz+Hm	Hz	Hz	Hz	Hz	Hz	???	Hz	Hz	Hz	Hz+Hm

Table 5.2 *Contd.*

	KALARANGITTA																				
	DM-25						DM-26						DM-27						DM-28		
	18	19	20	21	22	23	24	25	26	27	28	29	30	31	32	33	34	35	36	37	38
S	26.59	27.01	26.19	26.75	26.86	27.57	25.76	26.17	25.83	27.14	26.17	26.41	25.60	26.82	27.45	27.09	27.02	26.31	26.30	26.03	25.96
Cu	0.00	0.00	0.00	0.00	0.00	0.00	-	-	-	-	-	-	-	-	-	-	-	0.00	0.00	0.00	0.00
Fe	0.59	0.31	1.11	1.00	0.82	0.84	0.10	0.10	0.06	0.29	0.39	0.20	0.21	0.85	0.36	0.84	0.57	1.01	1.00	0.68	0.43
Ni	71.86	71.43	69.94	70.67	71.51	70.33	71.14	70.59	71.52	71.77	70.17	72.58	68.04	71.17	71.99	71.28	70.85	72.68	72.77	72.38	72.74
Pb	0.46	0.36	0.00	0.00	0.05	0.32	-	0.45	0.02	0.01	0.37	0.13	0.31	-	0.27	0.26	0.53	0.00	0.29	0.00	0.00
Sb	0.00	0.00	0.00	0.00	0.00	0.00	-	-	-	-	-	-	-	-	-	-	-	0.00	0.00	0.00	0.00
Zn	0.00	0.00	0.00	0.00	0.00	0.00	-	-	-	-	-	-	-	-	-	-	-	0.00	0.00	0.00	0.00
As	0.36	0.23	0.29	0.02	0.03	0.03	0.15	0.37	0.64	-	-	0.02	0.28	0.03	0.63	0.30	0.12	0.65	0.15	0.01	0.71
Total	99.87	99.33	97.52	98.44	99.27	99.08	97.15	97.68	98.06	99.20	97.11	99.34	94.44	98.86	100.70	99.77	99.09	100.64	100.51	99.09	99.84
Atom																					
S	40.05	40.71	40.21	40.57	40.45	41.45	39.79	40.26	39.62	40.81	40.40	39.90	40.61	40.52	40.80	40.64	40.84	39.35	39.41	39.47	39.20
Cu	-	-	-	-	-	-	-	-	-	-	-	-	-	-	-	-	-	-	-	-	-
Fe	0.51	0.27	0.98	0.87	0.70	0.73	0.09	0.09	0.06	0.25	0.35	0.17	0.19	0.74	0.31	0.72	0.50	0.87	0.86	0.59	0.37
Ni	59.10	58.80	58.63	58.54	58.82	57.73	60.02	59.30	59.90	58.93	59.16	59.89	58.93	58.72	58.43	58.39	58.47	59.37	59.56	59.94	59.97
Pb	0.11	0.08	-	-	0.01	0.07	-	0.11	0.00	0.00	0.09	0.03	0.08	-	0.06	0.06	0.12	-	0.07	-	-
Sb	-	-	-	-	-	-	-	-	-	-	-	-	-	-	-	-	-	-	-	-	-
Zn	-	-	-	-	-	-	-	-	-	-	-	-	-	-	-	-	-	-	-	-	-
As	0.23	0.14	0.19	0.02	0.02	0.02	0.10	0.25	0.42	-	-	0.01	0.19	0.02	0.40	0.19	0.07	0.41	0.10	0.00	0.46
Total	100.00	100.00	100.00	100.00	100.00	100.00	100.00	100.00	100.00	100.00	100.00	100.00	100.00	100.00	100.00	100.00	100.00	100.00	100.00	100.00	100.00
Min	Hz	Hz	Hz	Hz	Hz	Hz	Hz	Hz	Hz	Hz	Hz	Hz	???	Hz	Hz	Hz	Hz	Hz	Hz	Hz	Hz

analyses shows higher values of As and Pb and has been later confirmed from the detailed SEM-EDS studies.

A detailed and systematic study at IGEM, RAS, Moscow, especially with the aim to detect and analyze sulfide and PGE-minerals using two models of *SEM*, both *JEOL* make, *JSM-5300* with *Link ISIS* and *JSM-5610* with *JED 2300*. As the sulfides and noble metal phases are found to be very fine sized, the matrix effect has been removed in stochiometric proportion of the host silicate and/or sulfide and/or chromites depending on their association. The phase stochiometry has been recalculated to 100% making due consideration for the likely appearance of the phases and making comparisons with similar samples. The overall sulfide mineral assemblages noted in different varieties of ore and contact rocks, mainly from Kathpal area, is shown in Table 5.3.

5.2.1 Sulfides in Chromite Ore

The proportion of sulfides in spotted varieties is more compared to the massive ore. They occur both as fines and specks and confined mostly to the silicate matrix associated with chromite ore (Fig.5.6.i-ii). In some cases sulfides occur as pit fillings in chromite grains (Fig.5.6.iii). Sulfides at places developed at boundary of the chromite grains as in the case of Zone-1d (Fig.5.6.iv) whereas in Zone-2 they occur as fracture filling within chromite grains (Fig.5.6.v-vii) and in the intergranular spaces of chromite grains (Fig.5.6.viii). The relative abundance of sulfides in the spotted varieties of Zone-1d is least and is maximum in the Zone-2.

SEM study of two massive ore from Zone-1b shows occurrence of sulfides in two distinctly different modes: a) within silicates & mostly occupying the interstitial spaces between chromite grains (Fig.5.7.i-ii), b) as micro-pit filling within chromite crystals (Fig.5.7.iii-iv).

Interstitial sulfides vary in size from ~20 to ~60μm. One of the grains is sub-hedral in shape and the back scatter electron (BSE) image (Fig.5.7.i) indicates presence of two separate phases. The minor phase occupies the central part of the crystal. The major phase identified as millerite (Table 5.3, Anal.1) and the central exsolved (?) part is intermediate between nickeline (~75%) and breithauptite (~25%) in composition (Table 5.3, Anal.2).

The other two grains occur within a silicate mineral (altered olivine) and shows clear effects of alteration obliterating the original shape and composition along the periphery (Fig.5.7.ii). The unaltered part is identified as heazlewoodite with minor amount of As and Sb (representing nickeline-breithauptite?) (Table 5.3, Anal.3-4) and, is altered to millerite along the grain boundary (Table 5.3, Anal.5).

Micro-pit filling sulfides are seen within sheared massive type (Fig Ch-4) ore from Zone-1c. The pits within chromite grains are 5-20μm long but normally less than 10μm (Fig.5.7.iii). The sulfide phases occupying the space within the pits are even smaller. In most cases the pits are interconnected through a network of fine fractures along which the chromites shows alteration. Sulfide phases in four such pits are analyzed and the composition is shown in Table 5.3, Anal.6-11.

Table 5.3 SEM-EDS results of sulfides from chromitite and host rocks

	MASSIVE ORE														SPOTTED ORE								
Anal.	DM 13								DM 18						DM 14								
No.	1	2	3	4	5	6	7	8	9	10	11	12	13	14	15	16	17	18	19	20	21	22	23
	Weight Percentage (%)														Weight Percentage (%)								
Fe																							
Ni	65.09	43.74	69.57	71.73	62.62	64.22	9.80	64.67	61.07	39.68	46.04	71.46	72.32	71.88	61.71	72.49	63.52	72.13	67.69	73.77	63.47	71.67	69.85
Co											0.22				0.13							0.14	
Cu									2.42	1.82	0.57				0.41	0.26							
Pb						1.52	73.25																
Zn			0.47																				
Sn											0.75										0.40		
S	34.91	1.02	25.87	27.34	37.14	34.25	16.94	35.33			22.08	28.54	27.68	28.12	5.09	25.14		27.87	0.17	26.23	0.11	28.18	30.15
As		36.96	3.13	0.88					36.51	22.26	2.27				30.49	2.10	34.09		27.80		33.87		
Sb		18.27	0.96	0.36	0.24						19.30				2.16		2.39		4.33		2.15		
Bi										36.24	8.77												
Total	100.00	99.99	100.00	100.01	100.00	99.99	99.99	100.00	100.00	100.00	100.00	100.00	100.00	100.00	99.99	99.99	100.00	100.00	99.99	100.00	100.00	99.99	100.00
	Atomic Percentage (%)														Atomic Percentage (%)								
Fe																							
Ni	50.45	52.46	57.84	58.39	47.89	50.43	15.92	49.99	66.44	57.54	45.51	57.76	58.80	58.27	63.97	60.20	69.51	58.55	73.67	60.57	69.27	58.07	55.85
Co											0.22				0.14							0.11	
Cu									2.43	2.43	0.52				0.40	0.20							
Pb						0.34	33.71																
Zn																							
Sn											0.37										0.39		
S	49.55	2.24	39.39	40.91	52.01	49.24	50.37	50.01			39.97	42.24	41.20	41.73	9.65	38.23		41.45	0.35	39.43	0.24	41.81	44.15
As		34.73	2.04	0.56					31.13	25.28	1.76				24.76	1.37	29.24		23.71		28.97		
Sb		10.57	0.38	0.14	0.09						9.20				1.09		1.26		2.27		1.13		
Bi										14.75	2.44												
Total	100.00	100.00	99.99	100.00	99.99	100.00	100.00	100.00	100.00	100.00	99.99	100.00	100.00	100.00	100.01	100.00	100.01	100.00	100.00	100.00	100.00	99.99	100.00
Min	Hz	Nck-Brth	Hz	Hz	Mil	Mil	Gal-Mil	Mil	Orc	Mch	Mil-Hch	Hz	Hz	Hz	Orc-Hz	Hz-Orc	Orc	Hz	Orc	Hz	Orc	Hz	Hz-Mil

Table 5.3 *contd.*

	HOST ROCK																					
Anal.	C2F4				DM11									DM15					DM 20			DM11*
No.	24	25	26	27	28	29	30	31	32	33	34	35	36	37	38	39	40	41	42	43	44	45
Weight Percentage (%)																						
Fe	4.01	22.49	10.65	22.28	0.62	1.08	1.09	0.88		10.81	19.12	14.91	15.06	20.43	23.93	16.27	2.23	1.26	1.19	25.95	0.56	4.39
Ni	5.38	37.66	17.48	37.81	52.19	71.44	71.46	72.30	71.75	58.42	45.35	51.26	51.26	44.32	40.05	46.64	71.06	71.31	50.7	36.12	58.6	65.33
Co	0.66	5.33	2.67	5.08	1.22	0.20				0.68	1.48	0.96	1.10	1.37	0.82	1.36				3.39	0.73	0.45
Cu					0.39			0 31											0.29			
Pb	71 99				45.74																	
Zn																						
Sn																			17.33			
S	17.96	34.52	22.67	34.85	0.15	27.28	27.44	26.50	26.25	30.08	34.05	32.86	32.59	33.88	35.20	35.73	26.71	27.42	6.71	33.86	2.98	29.83
As					44.67														0.57	0.68	28.26	
Sb					1.15														12.83		8.86	
Bi																			10.38			
Total	100.00	100.00	99.99	100.00	100.00	100.00	99.99	99.99	100.00	99.99	100.00	99.99	100.01	100.00	99.99	100.00	100.00	99.99	100.00	100.00	99.99	100.00
Atomic Percentage (%)																						
Fe	6.65	18.21	13.15	18.01	0.73	0.93	0.93	0.75		9.05	15.55	12.24	12.37	16.63	19.28	13.10	1.91	1.08	1.51	21.10	0.65	3.70
Ni	8 47	29.02	20.15	29.06	59.07	58.22	58.16	59.24	58.11	46.53	35.07	40.03	40.09	34.31	30.70	35.73	58.11	58.04	61.38	27.94	63.83	52.26
Co	1.03	4.09	3.07	3.87	1.35	0.16				0.54	1.14	0.75	0.85	1.05	0.63	1.04				2.61	0.80	0.35
Cu			0.40					0.24											0.31			
Pb	32.10		14.94																			
Zn																						
Sn																			10.38			
S	51.76	48.68	48.26	49.04	0.29	40.70	40.91	39.76	41.89	43.68	48.24	46.98	46.68	48.02	49.39	50.13	39.98	40.88	14.86	47.95	5.94	43.66
As					38.95														0.55	0.41	24.12	
Sb					0.61														7.49		4.66	
Bi																			3.53			
Total	100.01	100.00	99.99	99.98	100.00	100.01	100 00	99.99	100.00	100.00	100.00	100.00	99.99	100.01	100.00	100.00	100.00	100.00	100.01	100.01	100.00	99.99
Min	Gal	Pn	Gal-Pn	Pn	Mch	Hz	Hz	Hz	hz	Mil	Pn	Pn	Pn	Pn	Pn	Pn	Hz	Hz	?	Pn	Mch	Hz

*PGM bearing host sulfide analysis

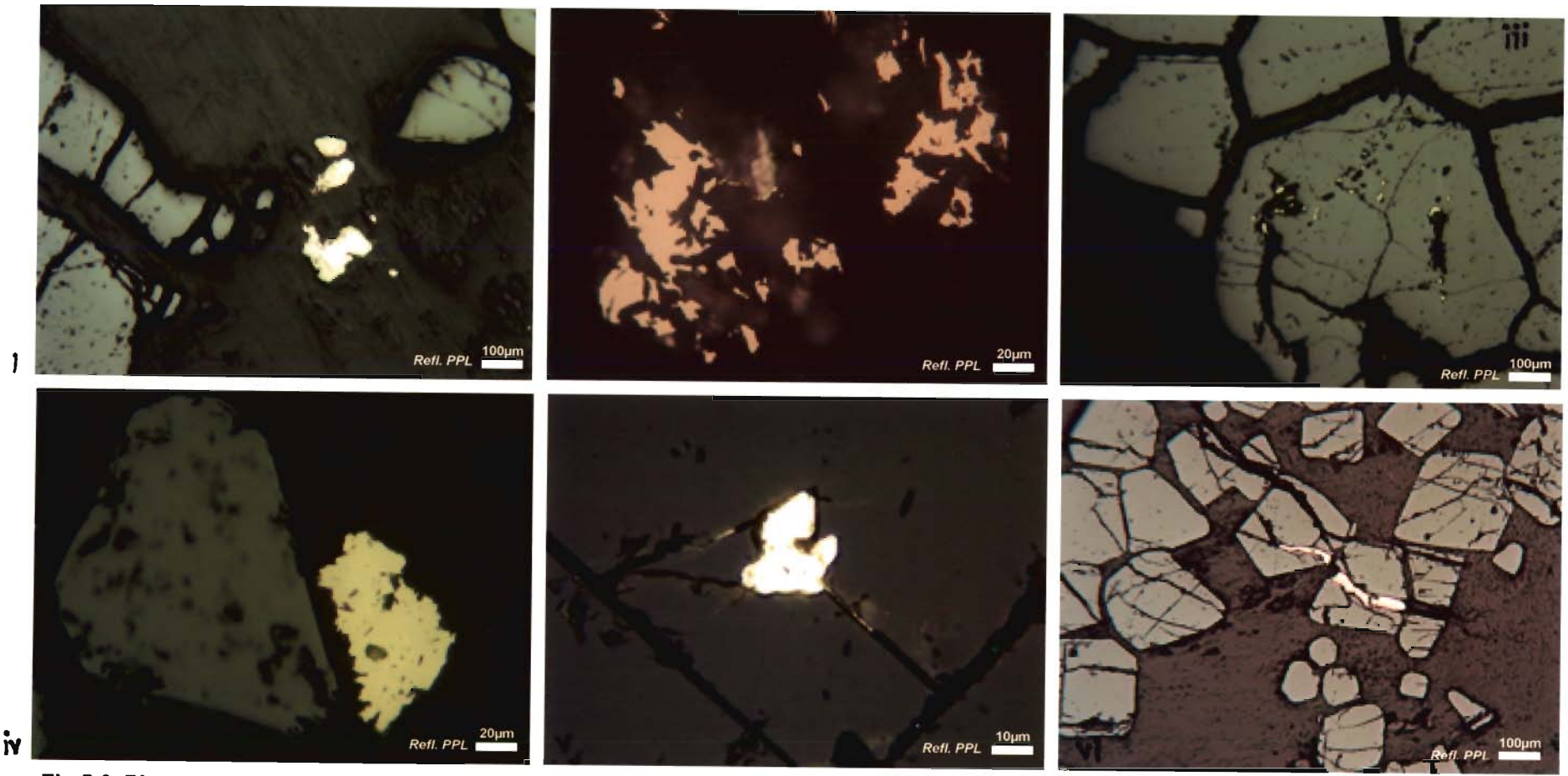

Fig.5.6. Photomicrographs showing (i-vi) i-ii sulfides as fines and specks within silicate matrix associated with chromite ore, iii sulfide as pit-filling within chromite, iv sulfide growing on chromite boundary, v-vi sulfide as fracture filling within chromite

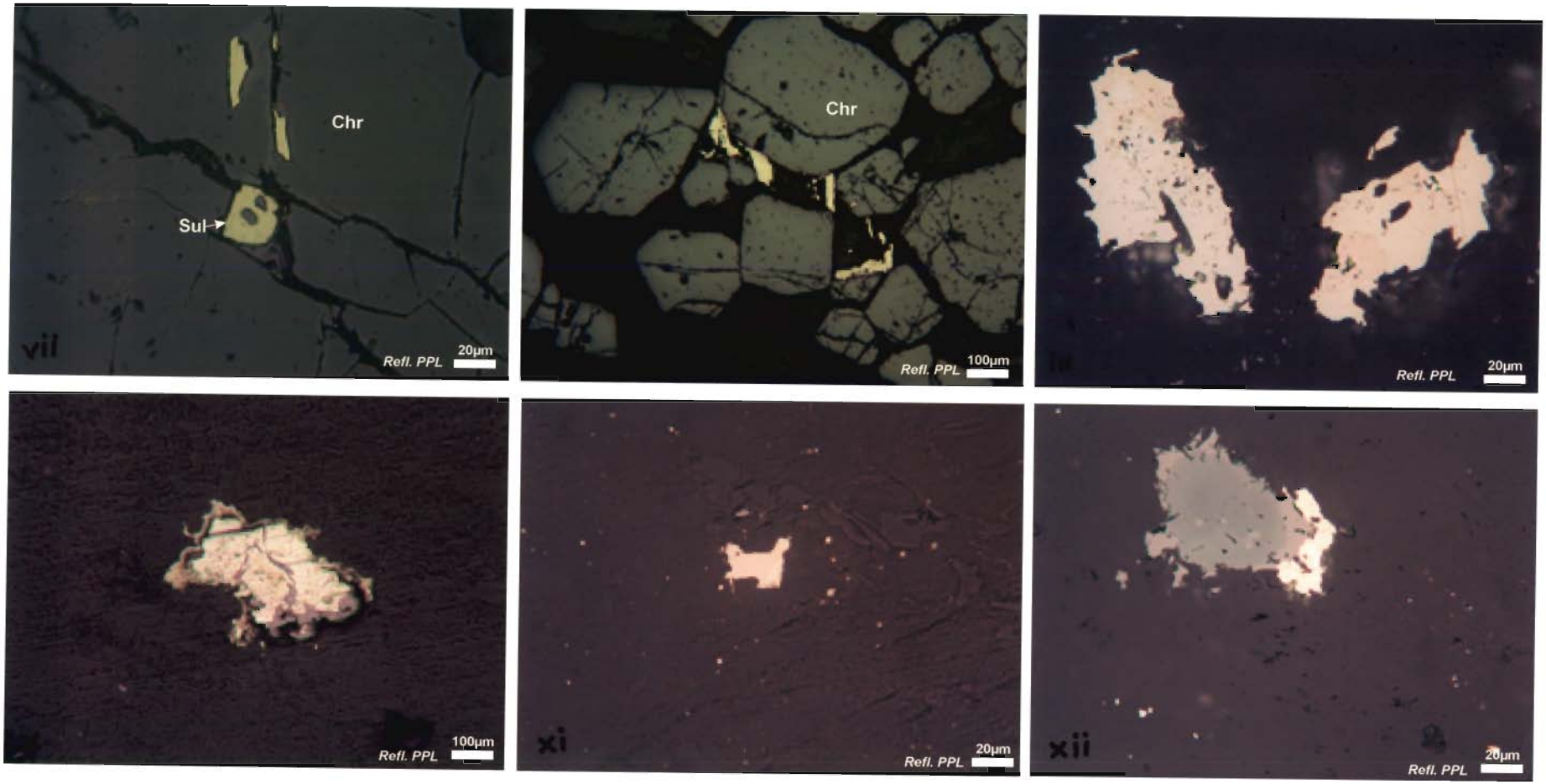

Fig.5.6. Photomicrographs showing vii sulfide as fracture filling within chromite, viii sulfides filling intergranular spaces within chromite, ix large speck of sulfide in host rock, x sulfide with spongy and colloform texture, xi specks and fines of sulfides within host rock xii alteration of chromite in contact with sulfides

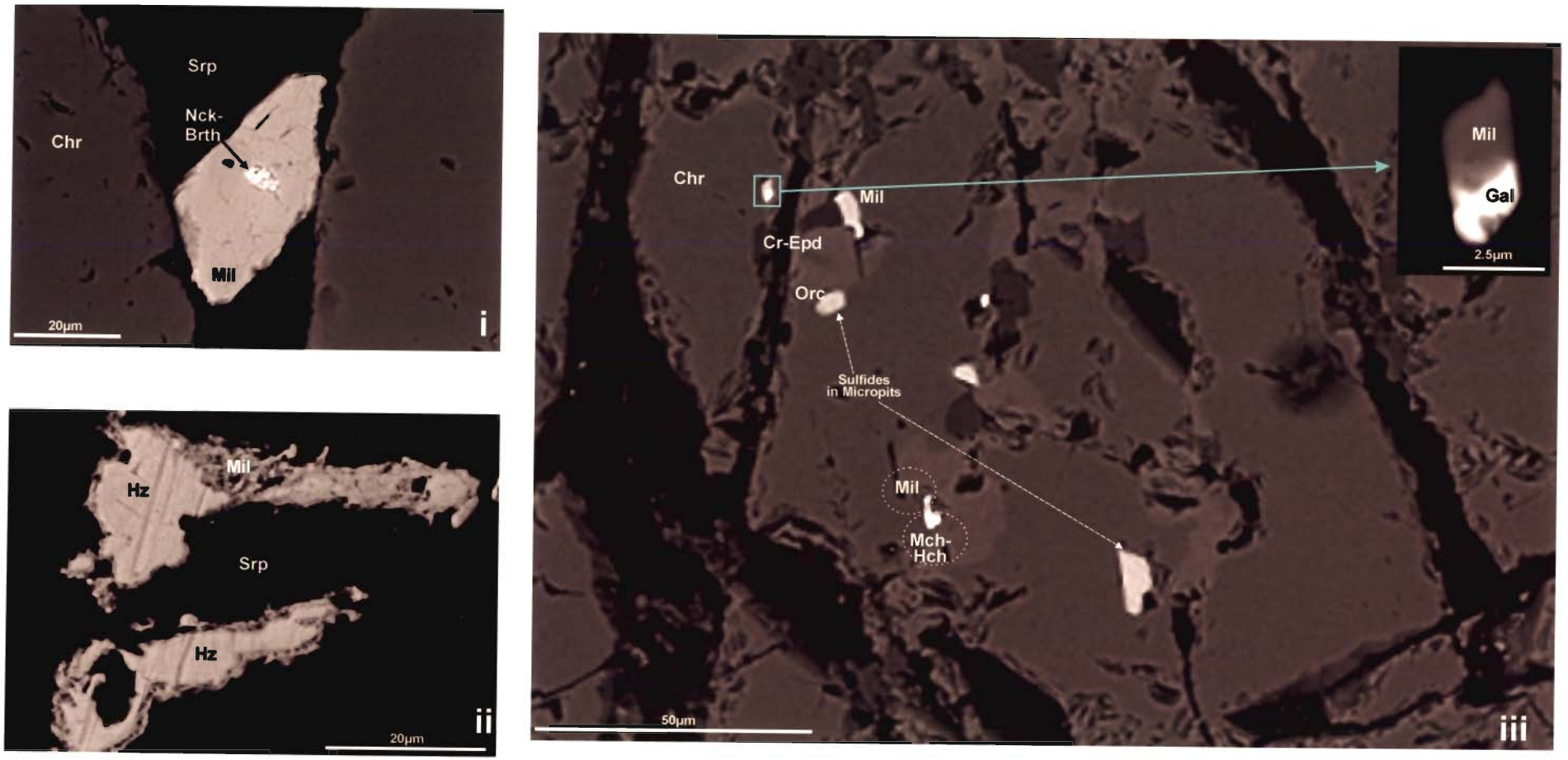

Fig.5.7. BSE images showing sulfides in i chromite, ii silicates iii. Micro-pit filling within chromite

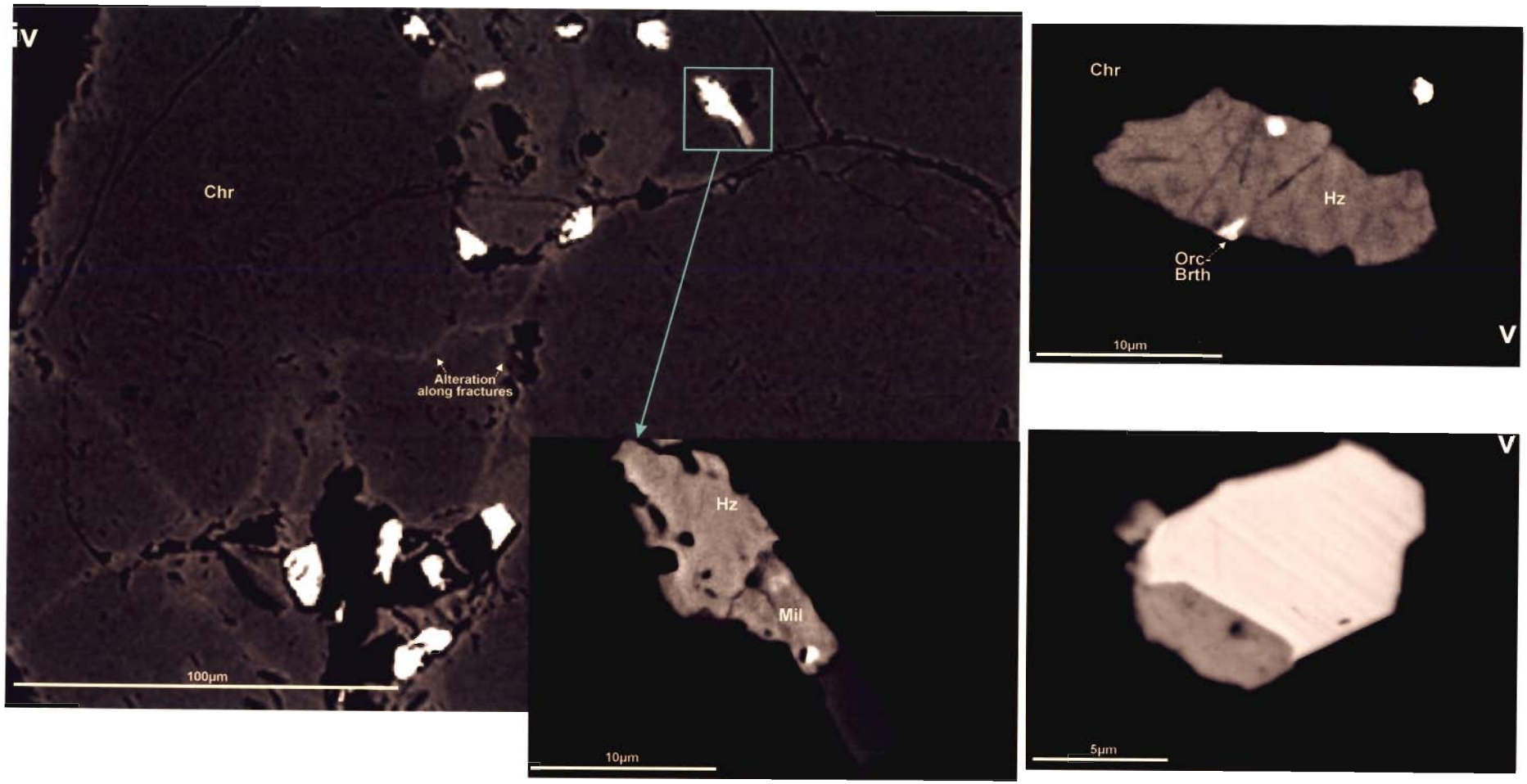

Fig.5.7 BSE images showing iv micro- pit filling within chromite, v-vi co-existing heazlwoodite-orcelite

In the first case, the minerals are millerite (NiS) and galena (PbS) (Fig.5.7.iii, inset; Table 5.3, Anal.6-7). The contact between these two mineral phases indicates simultaneous crystallization. Second pit is filled with only one phase, millerite (Table 5.3, Anal.8). Alteration of chromite is very evident. Chemical analysis of the altered part of the chromite grain is Cr-Al-bearing Ca-silicate (may be epidote?). The introduction of Ca within the chromite is possibly by the fluid moving through the very thin fracture. This is a direct evidence for hydrothermal origin of the pit filling sulfide-arsenide. Third pit is filled with a very minute grain of a rare variety of Ni-arsenide *i.e.*, orcellite ($Ni_{5-x}As_2$) with small amount of Cu (Table 5.3, Anal.9). Fourth one consists two complex sulfosalt phases, one is maucherite (Table 5.3, Anal.10) and the second one is mixture of maucherite, hauchecornite, millerite (Table 5.3, Anal.11).

5.2.2 Sulfides in Spotted Ore

In spotted ore the sulfides occur as: a) within silicates & mostly occupying the interstitial spaces between chromite grains, b) micro-pit filling within chromite crystals (Fig.5.7.iv).

The pit size of chromite grains varies from 10 to 50μm in long but normally less than 20μm and the sulfide phases within the pits are even smaller in size. Careful observation of BSE images reveals interconnectivity of the pits through a network of fine fractures and alteration of chromites along these. Sulfide phases in five pits are analyzed and the composition is shown in Table 5.3.

Micro-pit filling sulfides are mostly identified as coexisting heazlewoodite-orcelite (Fig.5.7.v, Table 5.3, Anal.12,13,14; Fig.5.7.vi, Table 5.3, Anal.16,17; Fig.5.7.vii.A, Table 5.3, Anal.18,19 and Fig.5.7.vii.B, Table 5.3, Anal.20,21) sometimes as exolved (?) phases (Fig.5.7.v, Table 5.3, Anal.12,13,14). In other cases, only heazlewoodite (Fig.5.7.iv, inset, Table 5.3, Anal.22) is found some times along with its alteration product *i.e.* millerite as minor phase (Fig.5.7.iv, inset, Table 5.3, Anal.23). Oxidation/alteration of chromite to hematite is also identified (Fig.5.7.iv, inset). The host chromite composition is $(Mg_{0.65}Fe_{0.35})(Cr_{0.78}Al_{0.17}Fe^{3+}_{0.05})_2O_4$.

5.2.3 Sulfides in Host Rock

The sulfides in the host ultramafic are present in two distinct modes: as *fine* dust homogeneously distributed in the silicate groundmass and rare relatively larger *specks* of 20-50μm size (Fig.5.6.ix). The fine dust like sulfide phases, in most likely case, developed during the serpentinization by reaction of the chalcophile elements like Ni and Fe released from olivine with the S-bearing serpentinizing fluid. The EPMA analysis confirms presence of heazlewoodite. Relatively larger sulfides are 10-30μm in size and are anhedral and highly corroded along the borders and show spongy appearance with coloform texture (Fig.5.6.x). Almost complete alteration of these sulfide grains to heazlewoodite and millerite is very common. But some remnant parts of pentlandite are still preserved in few grains. Presence of unaltered/remnant high temperature sulfide minerals may indicate formation of these grains in magmatic condition. In general, sulfide grains are relatively more abundant and coarser in the hanging wall rock compared the footwall

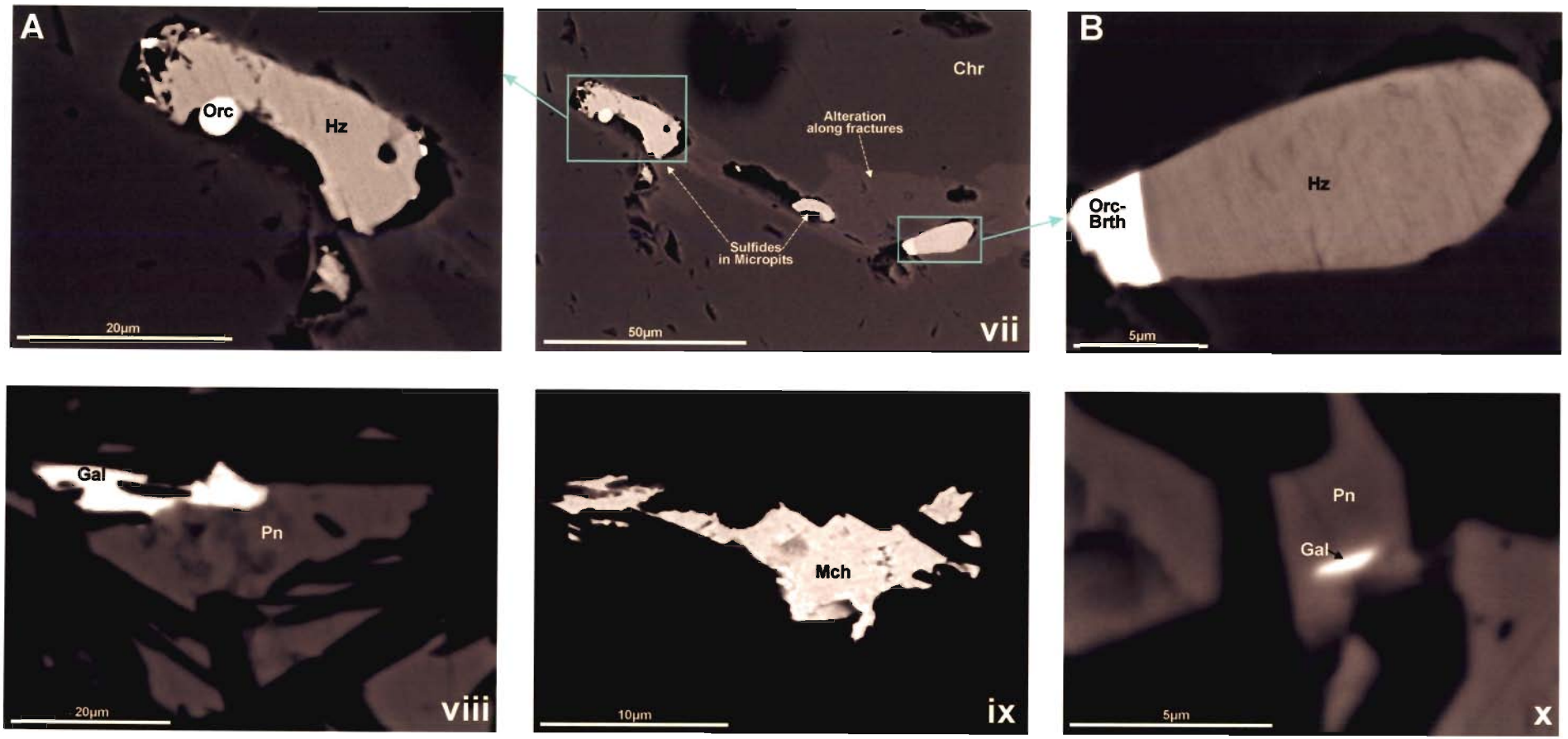

Fig.5.7 BSE images showing vii co-existing heazlwoodite-orcelite as micro-pit filling within chromite viii-x isolated grains of sulfides unaffected by alteration

rock (Fig.5.6.ix,xi). The alteration of chromites along the contacts with sulphides has also been noticed (Fig.5.6.xii). Sulfide concentration is relatively more in Zone-2 whereas variation in grain size is observed in Zone-1c.

Footwall host rock from Zone-1a (CF4) and Zone-1b (DM-11) and, hangingwall host rock from Zone-1b (DM-15) and Zone-1c (DM-20) are studied in SEM-EDS for sulfide and PGE bearing phases. Sulfides occurs as isolated grains apparently not effected by any alteration (Fig.5.7.viii-x), as a spongy looking mass of more than one phase (Fig.5.7.xi-xiii) or as fine sulfide dust of normally less than 1μm size (Fig.5.7.xiii). It may be mentioned here that both the footwall and hangingwall samples may represent contact zone between host rock and the chromite ore. At places, such contact zone is characterized by poorly developed and mostly discontinous chromite bands/laminations.

Isolated unaltered sulfide grains are fine (5-40μm) in size and consist of Ni-Fe- sulfide with galena (Fig.5.7.viii, Table 5.3, Anal.24). The host sulfide is Ni-rich pentlandite (Fig.5.7.viii, Table 5.3, Anal.25). It may possible that the pentlandite is originally separated from melt as mss. However, in few cases, the presence of galena as inclusion within the pentlandite has been observed (Fig.5.7.x, Table 5.3, Anal.26,27). One of the sulfides in interstitial space within the silicate psuedomorphs is identified to be Maucherite in composition (Fig.5.7.ix, Table 5.3, Anal.28).

Spongy altered sulfide grains appear to be severely altered during serpentinization and mostly 10-50μm in size (Fig.5.7.xi-xiii) with few exception found in hanging wall host rock of Zone-1c being coarser (~200μm).

Compositionally these are mostly having unaltered core of heazlewoodite (Table 5.3, Anal.29-32) and altered product comprising of millerite – Fe-oxide/hydroxide (haematite/goethite) phases at the periphery (Table 5.3, Anal.33). Small relict sulfide grains probably of magmatic origin (Fig.5.7.xi, Table 5.3, Anal.34-36; Fig.5.7.xii, Table 5.3, Anal.37 and Fig.5.7.xiii, Table 5.3, Anal.38,39), brighter in appearance, are found associated with these spongy type of sulfides in footwall as well as hangingwall (Fig.5.7.xiv-xv) host rocks. These are having approximate metal:sulfur ratio of 1:1 and are identified to be Ni-rich pentlandites.

Relatively coarser sulfide (>200μm) grains of hangingwall rocks of Zone-1c are similar in composition (Fig.5.7.xiv,xv) but anhedral in shape with altered border and exhibits typical colloidal texture (Fig.5.7.xiv, Table 5.3, Anal.40-41). In few cases, these sulfides are associated with flaky sulfosalts (Fig.5.7.xiv.a, Table 5.3, Anal.42). However, the Ni-content is lower for these Ni-rich pentlindite (Fig.5.7.xiv.a, Table 5.3, Anal.43) than that observed spongy type of sulfides from footwall host rocks. Millerite-maucherite (Fig.5.7.xvi, Table 5.3, Anal.44) with equilibrium texture is also noted in this sample (DM 20).

Fine dust like sulfides are less than 1μm in size and may be of varied composition as evident from BSE images but most of the ultra-fine grained sulfide may be heazlewoodite and determining their composition is limited because of their fineness.

The sulfide phases of magmatic decent are heazlewoodite and Ni-rich pentlandite (Sen & Mohanty *under preparation*) and are commonly alters to

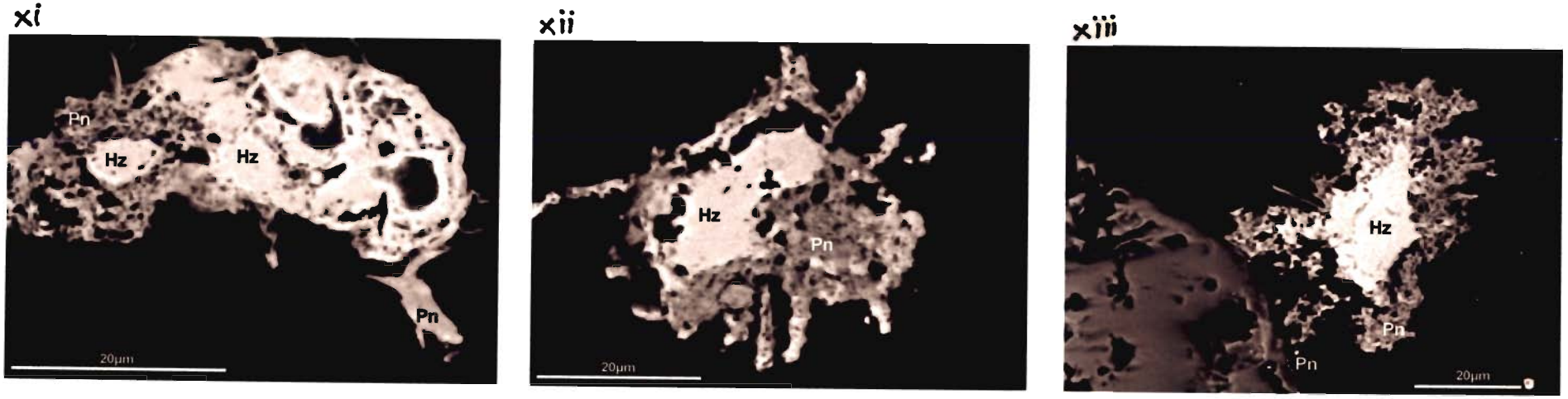

Fig.5.7 xi-xiii BSE images of spongy altered sulfide in serpentinized host

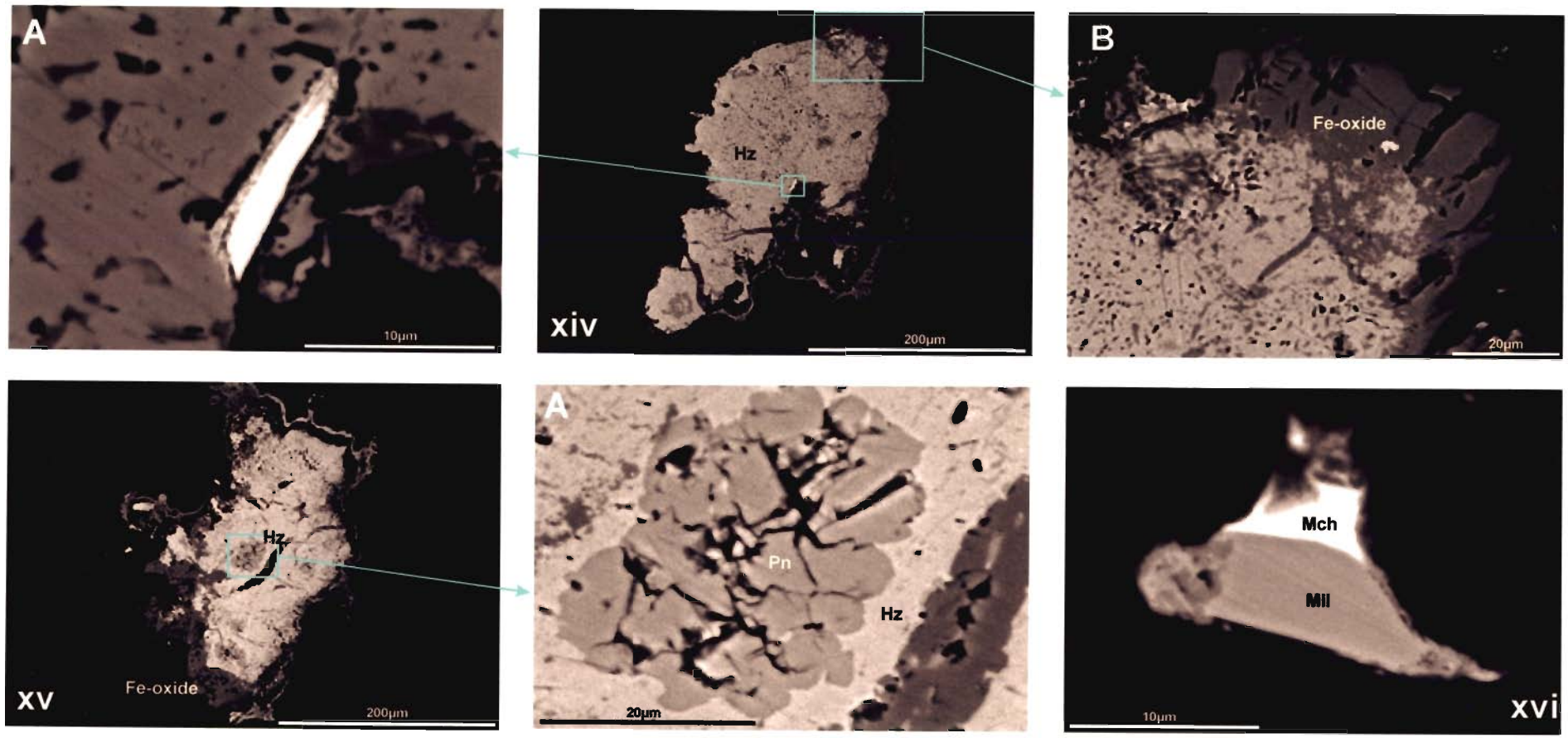

Fig.5.7 BSE image of xiv-xv coarser Ni-rich pentlandite and heazlewoodite. Heazlewoodite contains a grain of comlex sulfo-salt (xiv.A) shows and developement of Fe-oxide along the boumdar, xvi Coexisting millerite-Maucherite

millerite during serpentinization. Absence of any S-rich horizon in the chromitites and host ultramafics probably signifies their formation late in the magmatic sequence of crystallization consequent upon removal of iron by Fe-enrichment of the Cr-spinel and probably the silicates, especially in the host ultramafics. The high-Ni of pentlandite indicates crystallization from an ultramafic fraction and most of the Fe is taken off by crystallizing chromite and silicates. The serpentinization process certainly has produced low temperature heazlewoodite and also caused alteration of pre-existing magmatic sulfides. Indiscriminately, the sulfides contain very low amount of Co, As and Sb in the general structural formula of the minerals $(Ni,Co,Fe)_x$ $(As,Sb,S)_y$.

The PGM are identified in the footwall host rocks (DM-11) and is discussed in the following section (Section 5.3).

5.3 PLATINUM GROUP OF MINERAL (PGM)

The main sulfide minerals, which have been observed microscopically and by SEM, are heazlewoodite, pentlandite and also millerite. Heazlewoodite and pentlandite form massive grains and hence analyze with minimum matrix effect of other minerals, normally silicates those are associated with sulfides. Pentlandite and heazlewoodite (Table 5.3, Anal.45) are found to be in equilibrium condition (Fig.5.7.xvii), and pentlandite usually forms rim of such a bimineralic intergrowth. The evidence of equilibrium co-existence of both the minerals is that the pentlandite always occurs as a high-Ni variety with atomic ratio of Ni:Fe 1:2 to 1:3. As a rule millerite is observed under the reflected light microscope with rarely visible characteristic anisotropy. However, as it is

shown in Fig.5.7.xvii, it forms very fine and dendritic aggregates, which cannot be analyzed because of their size parameters. Based on morphological features of millerite aggregates, we consider it is possibly to be of secondary nature.

Total five PGE mineral grains could be detected. All the five PGE-mineral grains are very small and less than 0.5μm in size. All are having incipiently developed crystalline face and is subhedral to anherdal in shape. Out of total five, three grains, A, B & C, (<0.5μm) appear to be stuck on the host sulfide. The other two grains, D & E, are isolated and occur within few microns from the sulfide host of first three grains.

These five grains containing PGE is analyzed by two models of SEM, both *JEOL* make *JSM-5300* with *Link ISIS* and *JSM-5610* with *JED 2300*. As these grains are very small, it is not possible to know their exact composition. However, the composition is estimated by removing the high matrix effect from these grains. There is every chance of encountering error in estimating the exact composition of these grains. The determined minerals belong to following mineral systems:

1. The native alloys of Os-Ir-Ru system: It is Os-rich variety with varying composition ratio. The proportion of Os, Ru, Ir is approximately 11:3:1 in A and 15:1.5:1 in B ('A' & 'B' in Fig.5.7.xvii, inset-a). The approximate chemical composition of these grains (at%) is Os: 75-85%, Ru: 10-20% and Ir: 5-6%.

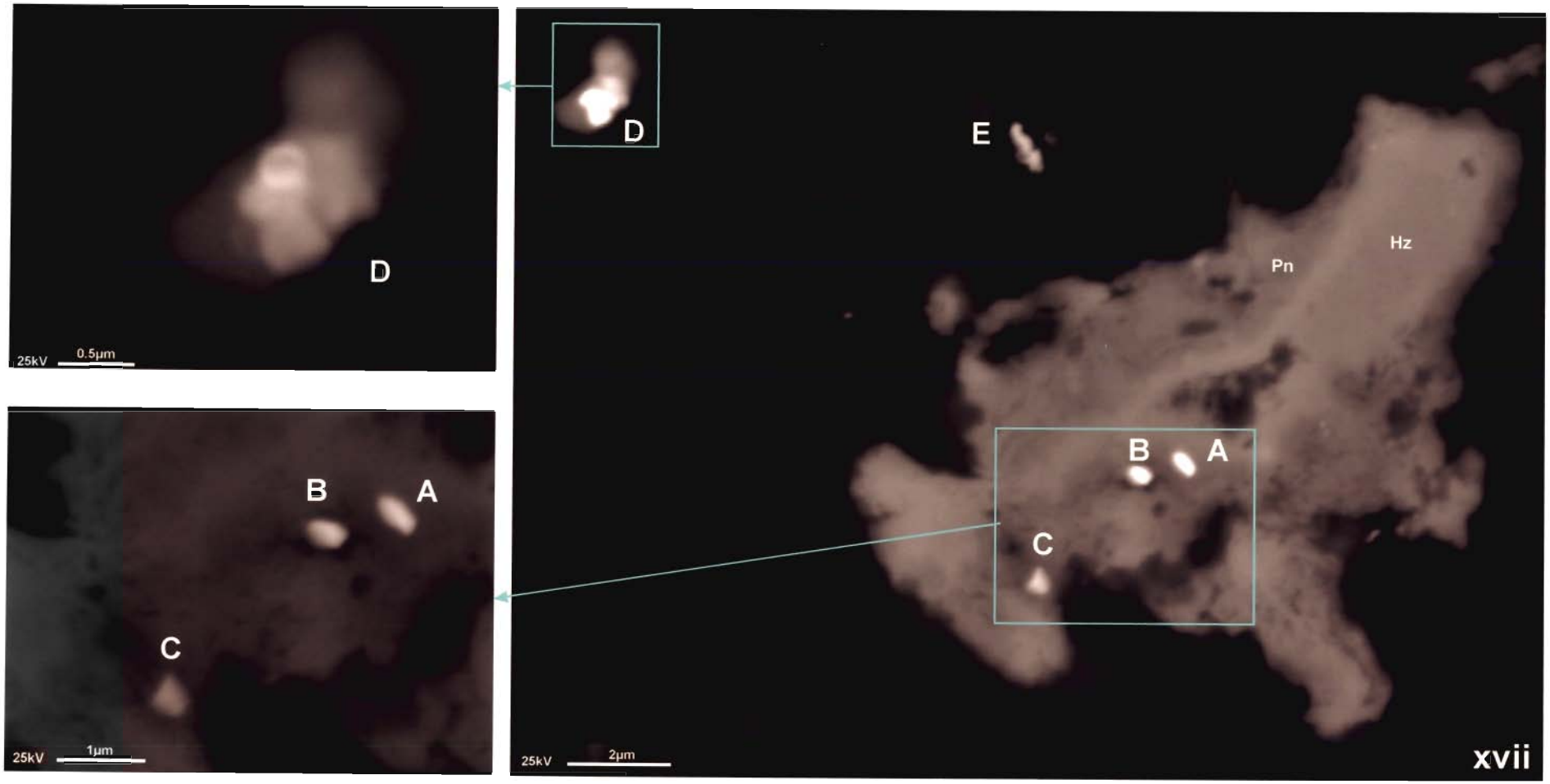

Fig.5.7.xvii BSE images showing three very minute PGM (A, B & C) occuring within Ni-rich pentlandite and heazlewoodite and two grains of PGM (D & E) within silicate matrix

2. Metallic solid solutions of Pt-Ir system: The phase composition has been only detected as an inclusion in heazlewoodite ('C' in Fig.5.7.xvii, inset-a). The brightness of 'C' in the BSE image is slightly less compared to 'A' & 'B'. The composition corresponds to ratio of Ir:Pt = 6:1., in recalculation to 100% the composition of the phase is Ir – 85.50% & Pt – 14.50% In nature minerals of such composition are known as Ir containing Pt. The findings are similar to that of Ural-Alaskan type.
3. The native alloys of Ru:Os:Ir system: It is Ru-rich variety with composition ratio close to Ru:Os:Ir = 7:6:1 (Fig.5.7.xvii, Grain-D). The chemical composition of one of such grains (at%): Ru – 50.0%, Os – 42.5% and Ir – 7.5%.
4. The BSE image of grain E (Fig.5.7.xvii, inset-b) reveals presence of three phases. The outer part is similar to that of previous host sulfide grain, whereas the phases consist of PGE may represent alloys of Os-Ir-Ru system and also sulfide of IPGE (mainly Os). The PGE-sulfides of Os-Ir-Ru-S system is dominated by Os. Therefore, such sulfides are the mineral phases of isomorphic range of laurite-erlichmanite. The ratio of the main components is close to Os: Ru:Ir = 25:8:1.

From the above observations, the PGM assemblage can broadly be grouped under three groups: Os-Ir-Ru alloys of variable ratio, Pt-Ir alloys and, sulfides of Ru and Ir *i.e.,* laurite (RuS_2)-erlichmanite (OsS_2) solid solution series. Sarkar *et al.* (2003) has also reported IPGE-rich inclusion within chromite in the breccia zone of Kathpal region. The association of Os-Ir-Ru alloys along with laurite (RuS_2)-erlichmanite (OsS_2) is an usual association of ophiolitic complexes (Melcher 2000, Malitch *et al.* 2003) and association of Pt-

Ir alloys in the similar situation are also not uncommon. However, overall IPGE dominated alloys and the direct relation of Cr-spinel with their whole rock concentration indicate that these alloys along with their sulfides are crystallized early in the fractional crystallization process. The Pt-Ir alloy perhaps represents an exolved phase from a polycomponent solid solution of the Ru-Os-Ir-Pt-Fe system late in the cooling history due to limited isomorphous mixture of Pt with the IPGE as suggested by Malich and Badanina (1998). Cr-spinel crystallization and its bearing in the fractionation IPGE rich phase assemblages can be explained well in the set of experimental studies performed by various workers. Bockrath *et al.* (2004) have shown the stability of Os-Ir-Ru enriched crystalline monosulfides in asthenospheric upper mantle conditions. The formation of laurite from a S-bearing the S-poor magma has been experimentally confirmed by Bockrath *et al.* (2004). Bockrath and Ballhaus (2002) have shown the heterogeneous nucleation of Ir (and possibly Os and Ru) on chromite surfaces while Ammossé *et al.* (2000) have shown that Rh^{3+} (as well as Ru^{3+} and Os^{3+}) in a S-poor system likely to associate with Cr^{3+} and Al^{3+} to form spinel. Again premature precipitation of IPGE may also be possible due decrease in solubility at higher fO_2 (Ammossé *et al.* 2000, Vatin-Perignon *et al.* 2000) as indicated by the precipitation of Cr-spinel composition (Chapter-4). Ammossé *et al.* 2000 have also explained that fS_2 have a similar effect on precipitation of PGE and hence explains about the least fractionation of PPGE in the present case.

The PGM detected in the sample are close to the chromitite ore contact and associated with a thin lamination of chromite indicating their formation in

the same crystallization sequence. Similar observation is also made by Bernker *et al.* (2003). However, the IPGE nuggets observed perhaps later carried out by the sulfide droplets late in the crystallization sequence and hence occur as inclusions within the BMS (Ballhaus 1998).

5.4 OTHER NOBEL METALS

In addition to analyze the sulfides and PGE-minerals in polished samples, three powdered samples of –200mesh size were prepared. The powdered samples were representative of one each from massive chromite ore, footwall host rock and hanging-wall host rock. The powder was then separated in different fractions based on specific gravity by heavy liquid separation. The main aim of this study is to know the presence of any ultra-heavy mineral (heavier than chromite) like PGM, is present or not. The overall success is limited to only two grains and is studied under *SEM JSM-5610* with *EDS JED 2300*.

The first grain (~50X~25μm^2) shows smooth appearance with small irregular pits (Fig.5.8.i.a). Fine cubic crystal growth (~1μm) with saccharoidal texture is visible on further magnification. A fibrous type mass is overgrown on the substrate (Fig.5.8.i.a *inset*). The spectral analysis of the main mass shows presence of native silver (Ag) with appreciable amount of Ni and Cu. In addition, Co and S peaks are also visible. The Si, Al, Mg, O are probably contributed by serpentine (Fig.5.8.i.b). The spectra of the fibrous mass shows presence of Ag with noticeable amount of Cu with a very prominent 'S' peak (Fig.5.8.i.c).

The second grain (Fig.5.8.ii.a) is almost double the size of first one and contains flaky overgrowth (Fig.5.8.ii.a, *inset* A & B) on the surface of the main mass which is native silver (Ag) with very small amount of Cu, Ni and S compared to Grain 1 (Fig.5.8.ii.b). The flaky overgrowth on the main ground mass is certainly composed of Ag with small amount of Cu and appreciable amount of S (Fig.5.8.ii.c). Comparison of spectral count from both the grains indicates that the main grain is composed of native silver with minor amount of Ni and Cu. The higher count of Ni and S in Grain 1 compared to Grain 2 is in all likelihood contributed by presence of Ni-sulfide, may be heazlewoodite. The fibrous or flaky overgrowth on native silver substrate is sulfide of Ag with minor amount of Cu and the mineral phase may be Jalpaite/Mckinstryite depending upon exact Ag:Cu ratio. These two grains of native silver is probably formed during serpentinization as open space filling. Rao *et al.* (2006) has also reported presence of primary gold inclusions in chromite ore from South Kaliapani Mines of main SUC.

The absence of PGM in the ultra-heavy fraction of the ore may be due to the ultra-fine size of the PGM. The PGM grains are either attached within sulfide or silicate phase. The liberation of PGM may not be achievable as the grains are less than 1μm in size.

In summary, the chromite crystallization and in turn high fO_2 condition resulted in the fractionation of the refractory IPGE and depicted well by the PGM assemblage of alloys and sulfides dominated by the IPGE. However, no mineralization of economic importance are found and is expected in a S-poor ultrabasic fraction as evident from low modal (<1 vol.%) of the sulfide phases.

Sulfides had least role in the PGE fractionation observed and only scavenged the previously formed PGE alloys and sulfides during the course of crystallization and further reworked by low temperature phenomena. The sulfides phases are dominated by heazlewoodite, Ni-pentlandite and millerite with rare arsenides i.e. orcelite and few exsolved galena. The presence of galena indicates selective assimilation of crustal material with high mobility during magmato-hydrothermal activity. The nobel metals like Au and Ag have considerable enrichment. The presence of very high Ag, not in magmatic proportion, indicates a hydrothermal source for its mineralization.

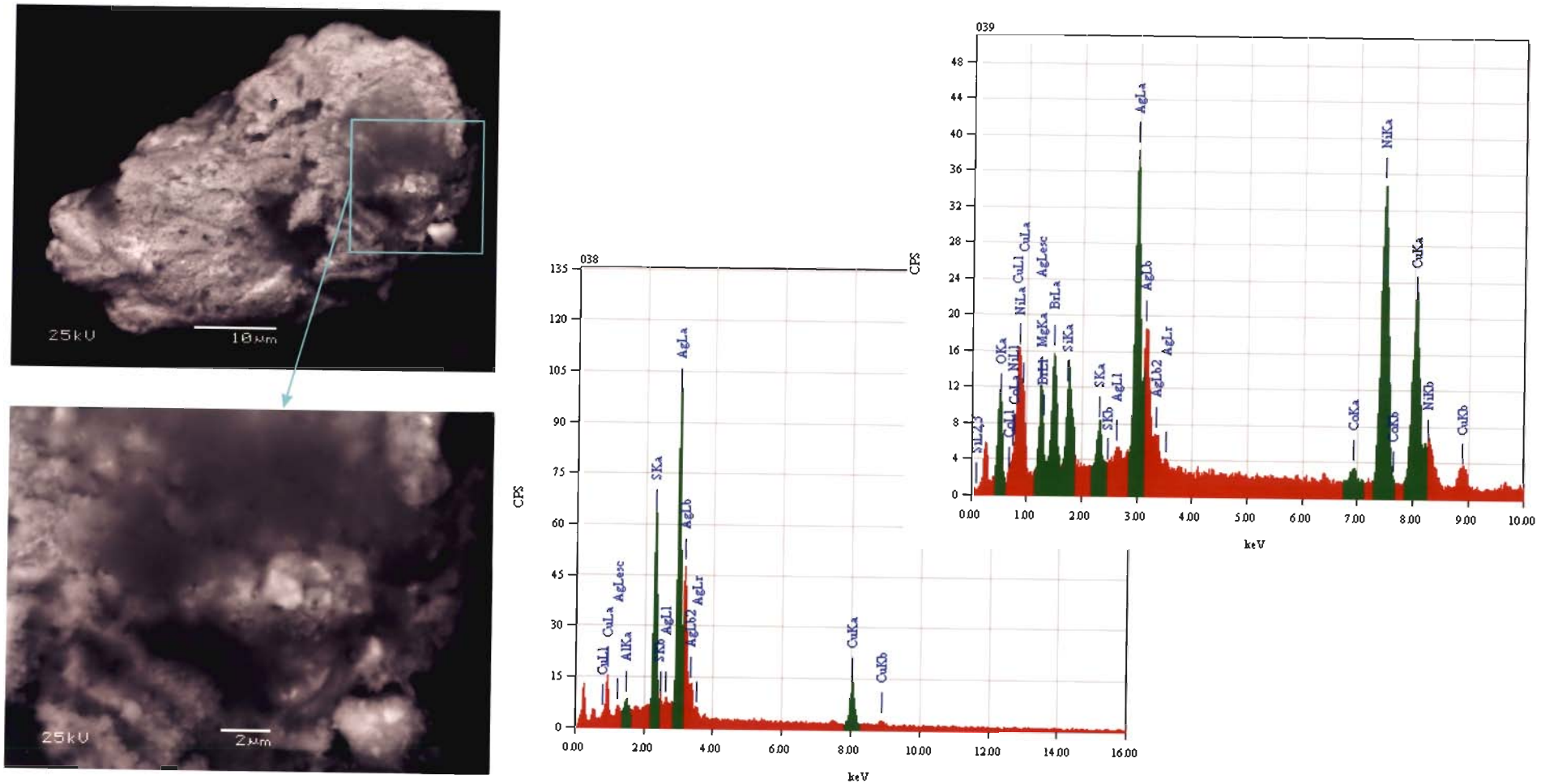

Fig.5.8.i.a BSE image of native silver with saccharoidal texture with fibrous growth of Jalpaite/Mckinstryite (*inset*), b-c their respective X-ray spectra

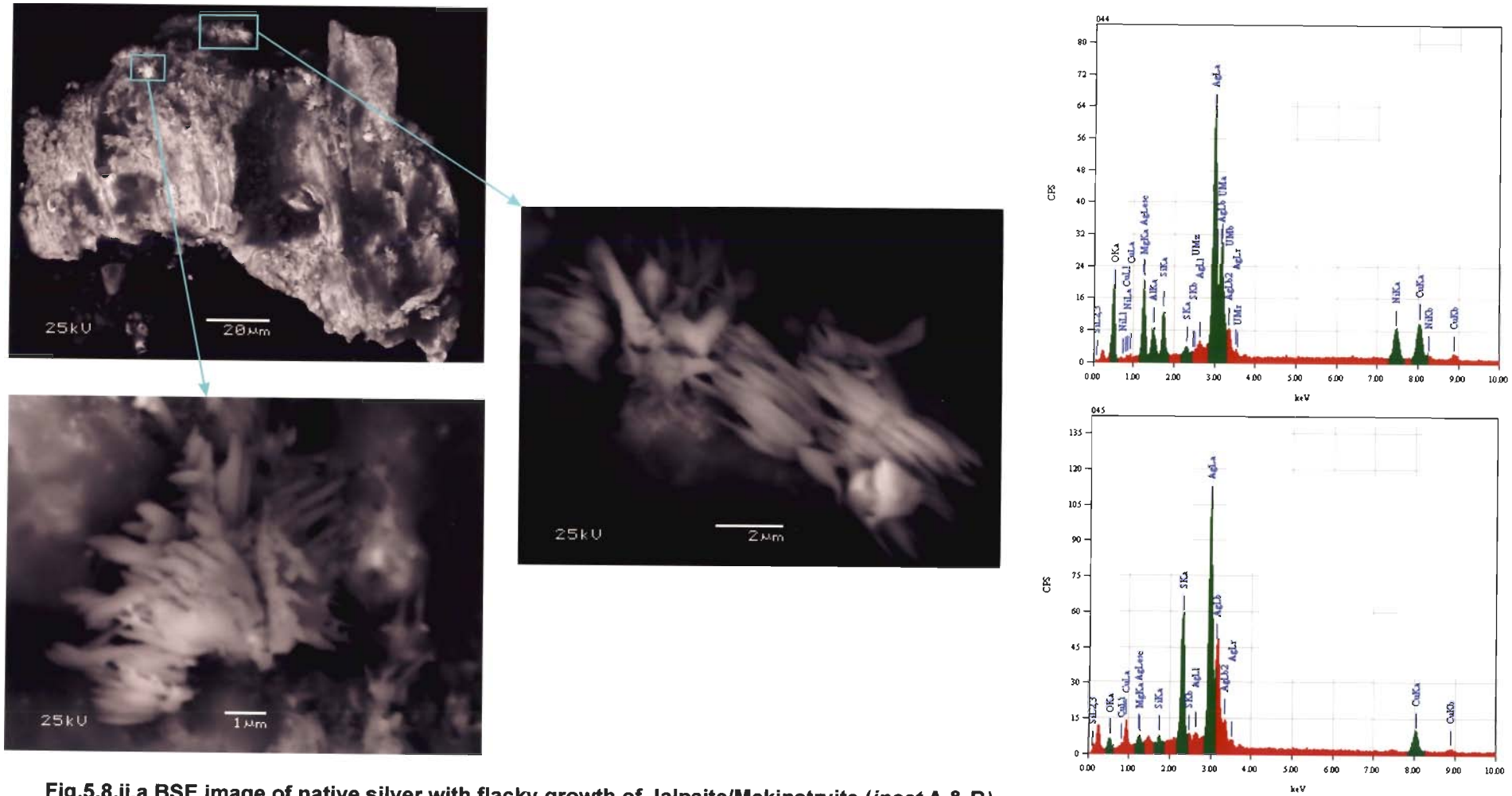

Fig.5.8.ii.a BSE image of native silver with flacky growth of Jalpaite/Mckinstryite (*inset* A & B), b-c their respective X-ray spectra

Chromitite bearing ultramafic complexes as the 'global targets' for potential PGE deposits are now an established fact (Maier 2005) and forms the central theme of the present work. The close association of chromite and PGE mineralization in such complexes indicates whatever may be the mechanism, the primary PGE mineralization had formed by the *process* similar and related to that of associated chromites (Kinnaird *et al.* 2002). Although all PGE are chalcophiles, fractionation is common between PGE but poorly understood due to their low level of concentrations (Amossé et al. 1990) and varied geological occurrences (Naldrett & Duke 1980, McCallum *et al.* 1976,, Vermaak 1976, Von Gruenewaldt 1979, Distler *et al.* 1998, Barnes & Maier 1999, Watkinson *et al.* 2002). On the other hand Cr-spinels act as a excellent petrogenetic indicator for the ultramafic complex with which it is associated (Irvine 1965, Irvine 1967, Dick & Bullen 1984, Arai 1994, Arai 1992, Coockenboo *et al.* 1997, Poustovetov & Roeder 2000, Barnes & Roeder 2001, Proenza *et al.* 2004). Hence, Cr-spinels are extensively used to evaluate the *geochemical* evolution of the parent melt to decipher the PGE mineralization pattern, if any, and to find out the role of degree of partial melting of the mantle, parent melt composition, temperature, pressure, fO_2, fS_2 *etc.* for the observed fractionation pattern of PGE (Amossé et al. 1990, Vatin-Perignon et al. 2000). Cr-spinel composition has been correlated with trace element data along with sulfide composition and their modal proportion (as they act as suitable carrier for PGE, Barnes & Maier 1999) to comment on the magmatic evolution of SUC in relation to the observed PGE mineralization

pattern. Finally, the tectonic set up for the evolution of SUC parent magma has been suggested in the light of available data set to best suit the chromite associated PGE mineralization of the SUC.

6.1 INTERPRETATION

6.2 GENETIC MODEL

6.1 INTERPRETATION

The **Landsat ETM+ image** depicts well the overall regional scale geological set up of SUC. The **geological fieldwork** confirms the intrusive relation of the Sukinda ultramafics with the IOG. Tectonically SUC suffered a relatively simple deformation phases mostly of post-emplacement and post-consolidation in nature with a broadly westerly plunging fold with steeply dipping limbs and closure towards eastern side.

The two ultramafic units of the SUC: *older* dunitic-peridotites hosting chromitites and the *younger* orthpyroxinites that is devoid of any chromitites. The cross-cutting relation (Chakraborty et al. 1980) of these suites suggests that these are perhaps two different intrusives of the same magmatic event. Here focus has been made on older ultramafics as the present study aims at the chromite associated PGE mineralization of SUC. The former has suffered through extensive serpentinization similar in nature and extent to that of the many ophiolitic complexes around the globe. This has been confirmed from the field observation, microscopic studies and XRD analysis. There are two different varieties of chromite ore:

i. *brown* (hosted in limonitized ultramafics and shows effects of serpentinization and meteoric alteration) and

ii. *grey* (hosted in serpentinized host rock and only rarely shows any effect of serpentinization especially massive ores)

Grey chromite ores are hard and compact. Alteration of these by meteoric water under surficial condition resulted in soft and friable brown varieties. The occurrence of grey variety chromite ore is restricted mostly to *two* localities of distinctly different intensities of geological disturbances *i.e.,*

i. Kathpal ultramafic suite *(Zone-1)* separated from main SUC by a concealed contact (?) and registered intense post crystallization deformation as indicated by the well preserved layers of cumulus silicate and chromites in erratically oriented lensoid chromite ore bodies representing a zone of pronounced brecciation unlike main SUC.

ii. Kalarangitta Chromitites *(Zone-2)* of main SUC with comparatively less structural deformation.

The trace element studies of **host serpentinized ultramafics** yielded trace element fractionation pattern typical of serpentinites of ophiolitic origin (Menzies 1976). Slight LILE-enrichment in PM-normalized trace element plot may be attributed to their redistribution during serpentinization (Rollinson 1993) whereas Cr-enrichment of the rock with respect to mantle indicative of crystallization of chromite from a refractory melt of *'near mantle'* composition formed from *high degree partial melting* of mantle. However, Ni and Cu do not show much fractionation as evident from mantle level of concentration of these elements in the host ultramafics. The C1-chondrite normalized REE

pattern and the concentration level of REE of the host rocks match very well with that of ultramafic rocks from ophiolite complexes (Menzies 1976). The trace element and REE composition of the host rocks of SUC points towards the oceanic mantle source for the parent magma. Such magma is likely to form at high temperature and relatively low lithostatic pressure.

Cr-spinels of grey ores (as has no or a little effect of serpentinization and lateratization) and serpentinized host rocks are treated in detail to decipher the magmatic parentage and physico-chemical condition prevalent during their formation and its relevance to the associated PGE mineralization pattern.

The variation in the range of Cr# and Mg# ratios are dependent on the subsolidus redistribution of Mg^{2+} and Fe^{2+} between olivine and Cr-spinel, and depends upon their relative proportion, the primitive composition of the parent magma can best be commented on the basis of Cr-spinel composition of the monomineralic rock *i.e.*, chromitite. They show a general high Cr# (0.71-0.79) and Mg# (0.62-0.81) with low TiO_2-content (<0.48%) indicating a high-Mg and Ti-poor parentage formed from high degree of partial melting of the mantle. The discrimination plots of Mg#~Cr# (Pober & Faupl 1988, Barnes & Roeder 2001), Cr^{3+}~Al^{3+}~Fe^{3+} (Barnes & Roeder 2001) and Cr#~TiO_2 (Arai 1992) for these spinels shows their close compositional resemblance with those of the Mg-rich magmas like komatiites and boninites, and to those from the podiform chromites and Alpine type peridotites. But the overall trend of Mg#~Cr# plot for Cr-spinels of different type ores and host rock shows gradual change and is different from that of the Alpine type peridotites.

The geothermometric calculations using the equation of Fabriès (1979) shows a temperature range of *993°C* to *760°C* for the formation of SUC chromites. These values are slightly less compared to the experimentally determined range for chromite crystallization (Murck & Campbell 1986) and may be attributed to the compositional changes during sub-solidus rediffusion between the selected pair of olivine and spinel. The selection of grains is limited by the fact that the relict olivine is very *rare* in the studied samples due to the extensive alteration of the original silicates by serpentinization. However, the values are well within the blocking temperature for diffusion between olivine-spinel pairs (Fabriès 1979). An error of 200°C in estimation of temperature yields a difference of ~0.5 log unit in fO_2 value (Murck & Campbell 1986). The fO_2 value extrapolated from Fe'''#~logfO_2 plot (Murck & Campbell 1986), assuming the chromite crystallization temperature to be 1250°C (support by the estimation of Pal & Mitra 2004) is *-9.1* to *-9.8* log units for the formation of the chromites. The Al_2O_3 of the melt calculated from the equation of Maurel & Maurel (1982) is low and varies within a smaller range (10.08 to 13.26%). Cr-spinels from different zones indicate a distinct range with some overlap in terms of their Mg# , Cr-content , TiO_2, Al_2O_3, and FeO_t. This indicates that these chromitites are formed at different crustal level from progressively evolved melt fractions during the cooling history of the parent magma most primitive being for Zone-1b.

The high degree partial melting is inferred from the Cr-spinel composition, trace element signatures and high F_O (~95%) content of the relict olivine. This implies almost complete removal of the mantle sulfides and potential of high PGE content as sulfides act as the suitable carrier phases.

So detailed examination for the sulfide phases are carried out through microscopic, EPMA and SEM-EDS studies and it is found that both chromite ores and host rocks have low modal proportion of **sulfides.** This is also evident from low-Ni content of the Cr-spinel and relict olivine composition. The sulfide phases of magmatic decent are heazlewoodite and Ni-rich-pentlandite (Sen & Mohanty *under preparation*) which commonly alters to millerite during serpentinization. Absence of any S-rich horizon in the chromitites and host ultramafics probably signifies their formation late in the magmatic sequence of crystallization consequent upon removal of iron by Fe-enrichment of the Cr-spinel and probably the silicates, especially in the host ultramafics. The high Ni of pentlandite indicates crystallization from an ultramafic fraction and most of the Fe is taken off by crystallizing chromite and silicates. The serpentinization process certainly has produced low temperature heazlewoodite and also caused alteration of pre-existing magmatic sulfide mineralogy.

The sulfides of hydrothermal (magmato-hydrothermal) are represented by Ni-sulfide with rare arsenides *i.e.* orcelite and few exsolved galena. The hydrothermal sulfide ore represent complex Ni-Co-Fe (?)-Pb-S-As-Sb system. The presence of galena may indicate selective assimilation of crustal material with high mobility during magmato-hydrothermal activity as indicated by the low Fe-content of the magmatic sulfides although the ultramafics are intrusive to the Iron Ore Group of rocks.

The base metal (Ni, Cu) and PGE (Pd, Ir) values of host ultramafics in mantle proportion indicate that there is no BMS-PGE mineralized zone

(Barnes *et al.* 1987). The sub-chondritic total **PGE concentrations** with an enrichment in IPGE with respect to the mantle coupled with the profiling for IPGE, PPGE, total PGE concentrations and IPGE/PPGE ratios that chromite crystallization had a pronounced bearing on the PGE fractionation pattern observed for the chromites and spinel-peridotitic rocks. This has been supported by the **PGE mineralogy** dominated by Os-Ir-Ru alloys of variable ratio and laurite (RuS_2)-erlichmanite (OsS_2) solid solution series (Sen *et al. under preparation*). Sarkar *et al.* (2003) has also reported the inclusion of Os-Ir-(Ru) alloys within the chromites from the Kathpal breccia zone. The determined values of whole rock IPGE may be less than actual values owing to the fact that these are determined by NiS FA ICP-MS method and oxides of Os and Ru are volatiles. Though these values of Os and Ru are semi-quantitative ones, the expected high actual values can further strengthen to the interpretation mentioned here.

Other noble metals like Au and Ag have considerable enrichment in the host rock as well as chromite ores. The presence of very high Ag, not in magmatic proportion, indicates a hydrothermal source for its mineralization. Occurrence of native silver with silver sulfides has been found from the footwall host rock representative sample from the SEM EDS studies. Sarkar *et al.* (2003) has also reported the native gold from the silicate matrix of the breccia zone of Kathpal and Rao *et al.* (2006) reported the native gold as primary inclusions within chromites from the South Kaliapani Mines of main SUC.

The questions still left unanswered are: why the sulfides are low in concentration in the ultramafics and what happened to those, as a S-rich melt is excepted with such high degree of partial melting (Barnes & Maier 1999). A review of earlier works provides some useful information aiding to the author's interpretation.

As is discussed earlier that SUC and Boula-Nausahi complex are closely related in space and time on the basis their stratigraphic position (intrusive to quartzites of IOG and hence younger than IOG but pre-Iron ore orogeny as it is co-folded with the IOG rocks), lithological association (ultramafics), magmatic differentiation trend, nature of associated mineral deposits *etc.*, and might have resulted in response of the same geologic event (Banerjee 1972, Srinivaschari 1979, Banerjee *et al.* 1987, Das *et al.* 1995).

Again Augé and Lerouge (2004) interpreted Bangur gabbro and closely associated ultramafics of Boula-Nausahi complex formed from a single protracted magmatic event. Augé *et al.* (2002) clearly shown that the emplacement of Bangur gabbro is contemporaneous with the brecciation with which it is associated. Similar kind of brecciation is also observed associated with the Kathpal chromite deposits and may be related to the same event. As a whole, ultramafics of SUC and Boula-Nausahi complex along with the brecciation event and emplacement of Bangur gabbro are broadly contemporaneous and probably formed in the response of a single but protracted tectono-magamatic event of Precambrian age. Hence, it may be expected that the primary PGE mineralization pattern associated with these complexes may also be correlated.

Bangur gabbro shows an overall enrichment of REE (Fig.6.1.i, Fig.7 of Mondal *et al.* 2001) with respect to the serpentinized host ultramafics of SUC chromites of the present study with similar C1-normalized REE patterns indicate that Bangur gabbro may represent the *residual* basic fraction of the parent melt from which Sukinda chromitites and their host ultramafics (and perhaps that of Boula-Nausahi complex) might have formed. As expected, this residual melt fraction should have been S-enriched and capable of producing PGE mineralization of economic concentration with the enrichment of PPGE. This interpretation (Mohanty & Sen 1 *under preparation*) is well supported by the findings earlier workers (Mondal & Baidya 1997, Baidya *et al.* 1999, Augé *et al.* 1999, Mondal *et al.* 2001, Augé *et al.* 2002a & b) that the Bangur PGE mineralization shows an overall PGE enrichment with an elevated PPGE concentration, and PPGE rich minerals in close associations with the base metal sulfides (Fig.6.1.ii, Fig.4 of Augé *et al.* 2002b). However, Augé *et al.* 2002b suggested that the lack of sulfides in magmatic PGE mineralization (Type-1 'contact type' of Augé *et al.* 2002b) may be due to the S-enrichment in the later volatile rich hydrothermal fluids and such an explanation also fits well in the context of present interpretation.

The nature of chromite deposits with the pattern of primary PGE mineralization observed needs to take into account the tectonic set up of the complex for the feasibility of such a hypothesis. So age relation and the field evidences are collated. Based on zircon age dating Augé *et al.* (2003) assigned a ~3.1Ga to the Bangur gabbro of Baula-Nausahi complex. Mondal *et al.* (2006) assigned an age of between 3.3-3.1Ga to is to SUC from the comparison of geochronological available data on associated litho units of the

Singhbhum craton and their field relations. All these data indicate that these related suites of ultramfics and mafics are of obvious Precambrian age. Origin of SUC variously designated as *hydrothermal* type (Varma 1953), *alpine* type (Banerjee 1972), *stratiform* type (Haldar 1969, Srinivaschari 1979, Chakroborty & Chakraborty 1984), *ophiolitic* type (Page *et al.* 1985, Banerjee *et al.* 1987), and supra-subduction zone related (Mondal *et al.* 2006) *etc.*

But if it will be considered in *stricto-sensu* the ophiolitic chromites should have other closely associated typical features *e.g.* pillow lava and is characteristic of syntectonic emplacement of Cenozoic age. On the other hand, the Layered complexes of Precambrian age should be of bulk gabbroic composition. On these qualifying grounds SUC mismatches with the respective type of ultramafic complexes. However, the *geochemical affinity* of SUC to *'ophiolites'* and emplacement features in a *stable environment* similar to *'layered complex'* may well be explained (Mohanty & Sen 2 *under preparation*) by the emplacement of a refractory *'komatiitic'* melt (Parman & Grove 2004) of *'plume'* origin those dominate (Storey *et al.* 1991) the relatively stable *Precambrian tectonics* (without much plate movements, Arndt 1983) in the oceanic *'thin spots'* (weak zones).

Based on these interpretations a model is proposed (Mohanty & Sen 2 *under preparation*) here to explain the PGE mineralization associated with the SUC of Precambrian age in the light of global Precambrian tectonics.

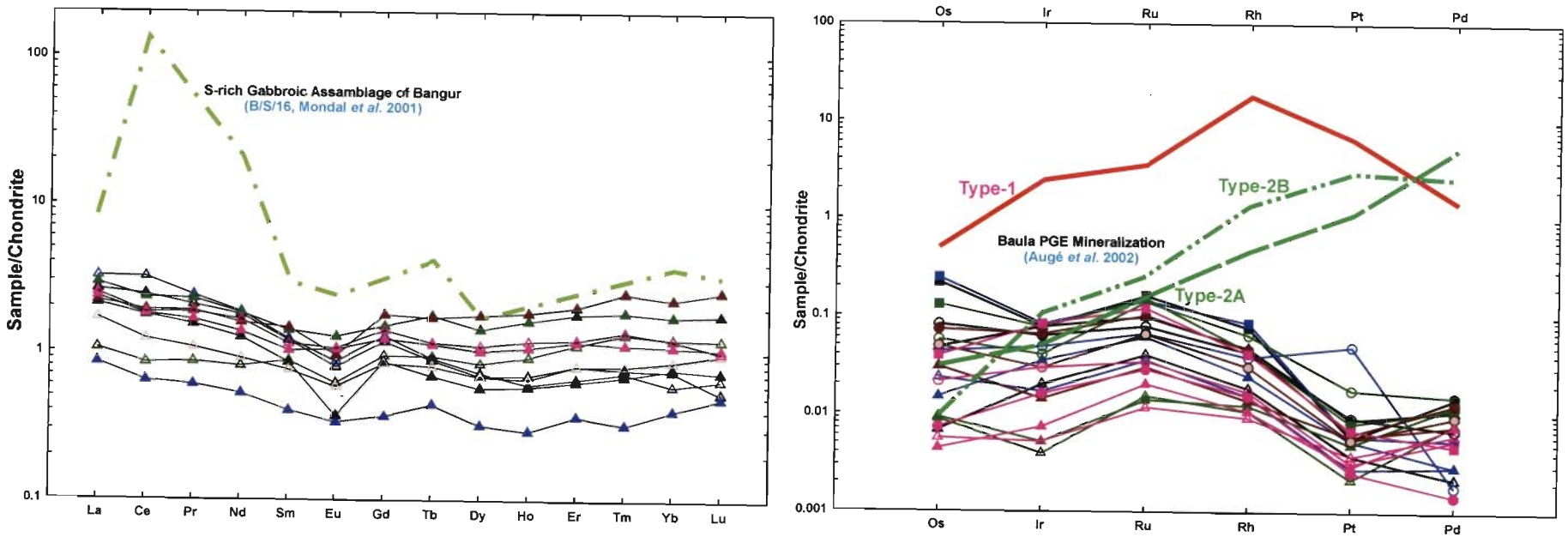

Fig.6.1 Possible genetic link between the serpentinized chromite bearing ultramafics of Sukinda with that of the Bangur gabbro of Boula-Nausahi in terms of their i REE signature *(Mondal et al. 2001)*, **ii PGE mineralization style** *(Augé et al. 2002b)*

6.2 GENETIC MODEL

Based on the above interpretation a model proposed here to explain the PGE mineralization associated with chromite hosted ultramafics of Sukinda in the light of global Precambrian tectonics and is as follows (Fig.6.2):

Stage-1: Mantle up welling as *plume* in response to the convective instabilities at the thermo-mechanical discontinuities of the Earth (~700km discontinuity for plumes of upper mantle origin) and subsequent emplacement in low pressure zone like oceanic *thin spots* or weak zones (as SUC is emplaced within IOG those were deposited in Precambrian ocean basins) (www.le.ac.uk/geology/art/gl209/lecture 7/lecture7.html).

Stage-2: High degree partial melting of the plume as a result of *decompression* with lowering of pressure to produce Mg-rich melt with high amount of sulphur removal (Barnes & Maier 1999).

Stage-3: Crystallization of IPGE rich *'micro nuggets'* similar to that of Ballhaus (1998) early in the sequence. This is supported by the IPGE-rich alloys along with the IPGE-sulfides found in the present work and IPGE-rich alloys as inclusions in chromite reported by Sarkar *et al.* 2003. This is aided by experimental data of Bockrath *et al.* (2004) that confirms the stability of the crystalline IPGE rich sulfide phases in asthenospheric mantle condition.

And/or

Chromite crystallisation with the increase in fO_2 decreases the solubility of IPGE (Amossé *et al.*1990) and subsequent nucleation of

IPGE rich on chromite surface as suggested by Bockrath & Ballhaus (2002). Evidence in support of this is the inclusions found in the present work are closely associated with the laminated chromites of the contact zone.

And/or

Fractionation of IPGE to crystallizing chromites as indicated by the consistently higher whole rock concentration of IPGE in the chromite ore along the profile of particular section in the present work. The fractionation of IPGE to chromites has been experimentally proved by Amossé *et al.* (2000). The formation of inclusion may be explained by the exsolution of IPGE during slow cooling as suggested by them. The IPGE found in the present case are in the poor grade chromite ores with laminations and but in a sulphide host indicating that the IPGE-rich alloys and sulfides released due to crushing and alteration effects and/or scavenged by Ni-sulfides of late magmatic origin as suggested by Ballhaus (1998). This provides the best explains for the mineralization found in the present study.

Stage-4: Emplacement of 1st pulse of in the *'magma mini chambers'* (similar to that of Augé 1987) at relatively deeper crustal level within IOG represented by Zone-1 ultramafics *i.e.,* Kathpal ultramafic suite in a semi-solid state as depicted by the *'within grain'* fractures.

Emplacement of 2nd pulse in the main SUC at shallower level within IOG represented by Zone-2 ultramafics *i.e.,* Kalarangitta chromitites (and probably Baula-Nausahi chromitites and host ultramafics).

The two pulses assumed here are based on very slight but consistent difference in variation in Cr-spinel compositions from both these zones.

Stage-5: Emplacement of the *basic* residual melt fraction as Bangur gabbro in Baula-Nausahi complex. This idea is supported by the REE and PGE data of the present work in combination with REE data (*source* Mondal *et al.* 2001) and PGE data (*source* Augé *et al.* 2002) of Bangur gabbro.

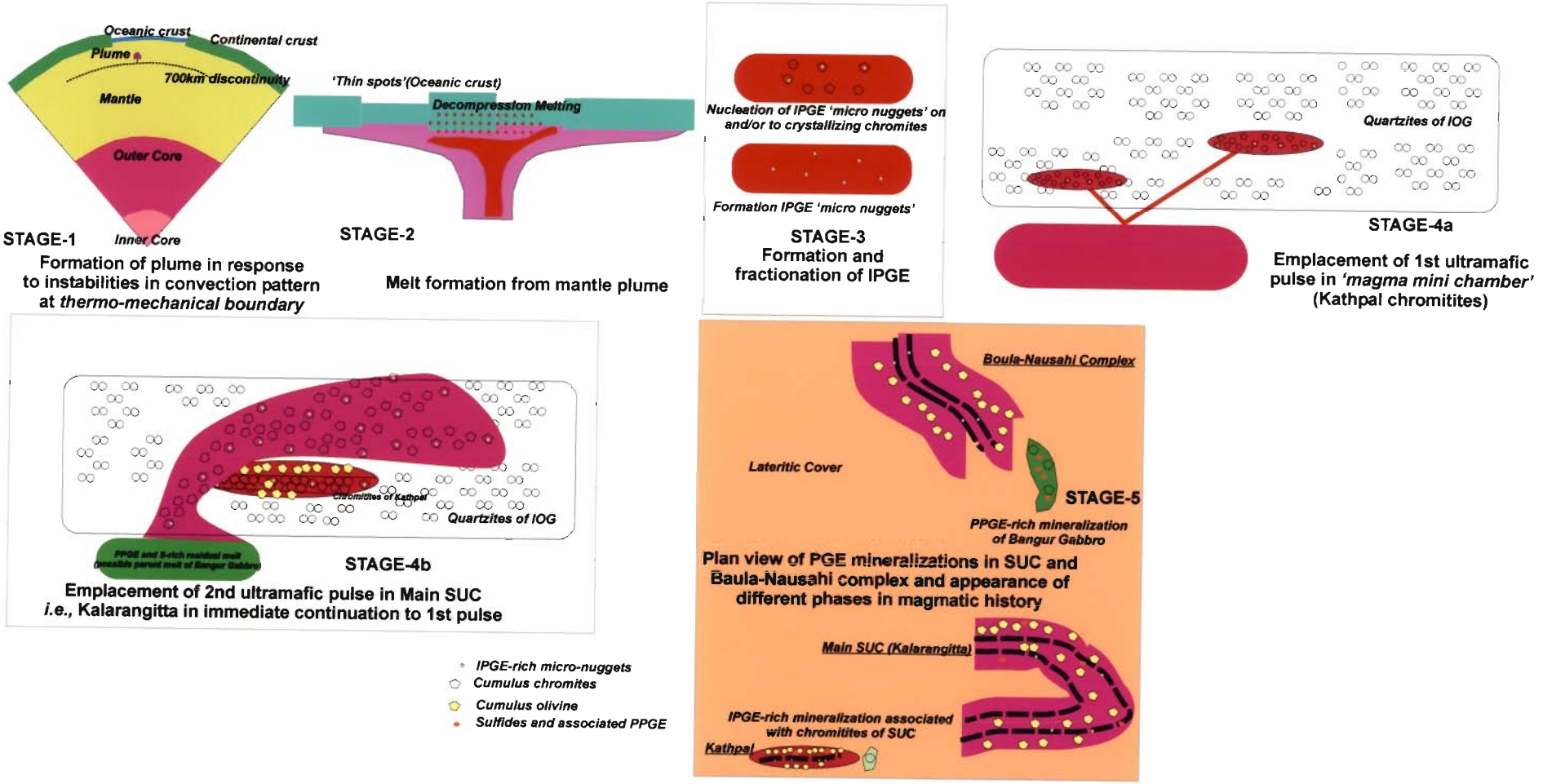

Fig.6.2 Schematic diagram of the plume model proposed for the PGE minarlization of SUC in relation to that of Baula-Nausahi complex.

Motivated by the global attractiveness for PGE values of economic importance from chromite hosted ultramafic complexes, the present work is taken up to study the primary mineralization pattern and PGE potentiality of the chromitites and the host rocks of the Sukinda ultramafic complex, if there is any. The study has suffered has the major limitation that chromitite hosted ultramafics has suffered through extensive serpentinization and limonitization. Barring few relict olivine grains, Cr-spinels of grey ore zones are the only major phases remain almost unaffected by this process and are studied extensively for evaluation of the primary magmatic conditions.

In the light of Cr-spinel composition and F_O values of relict olivines, precursor melt of these ultramafics are interpreted to be a Mg-rich melt formed by a high degree partial melting of the mantle. This is supported by the trace element studies and is expected to be S-rich melt. But the micro-scopic observations and subsequent SEM-EDS studies had shown low proportion of modal sufides. The Ni and Cu ratios with PGE confirmed that these are in mantle ratios and BMS has least role in primary PGE mineralization pattern. Profiling of PGE values along the respective section signifies that although the PGE values are subchondritic, the enrichment with respect to mantle values are related to the chromite crystallization. This has in its support a high refractory PGE (IPGE) concentration and although scanty, the alloys and sulfides of IPGE. In search for the answer that where the sulfide rich fraction has concentrated, which should be in higher concentration with such a high degree of partial melting of the mantle and should be the part of magmatic

system under consideration. The probable answer could be that it is enriched in a residual melt. The recent works have brought support to the idea that the sulpfide dominated PPGE mineralogy of magmatic origin associated with Bangur gabbro of Baula complex (geographically 70 km away from SUC) may represent the part of that expected residual melt.

Present work perhaps one of such rare work that provides the most synoptic view of Sukinda ultramafics in the light of Cr-spinel composition, relict olivine composition, trace element composition, whole rock PGE concentration and, sulphide and PGM composition. Although the data suggest chromitites and ultramafics do not contain any PGE mineralization of economic importance, as a off-shoot of this research the model proposed here explains not only the PGE mineralization pattern in Sukinda but also the origin of such complexes of Precambrian age with ophiolitic geochemical affinity but deformation history similar to that of layered complexes in terms of the *'plume'* dominated Precambrian tectonics.

Present work may act as a future exploration guide for the PGE in the Sukinda ultramafic complex. Accordingly, *three* major loci are suggested for detailed exploration: i. a probable PPGE-rich mineralization in brecciated zone in Kathpal (Zone-1), ii. IPGE-rich horizons in the nickeliferous limonites and laterites as residual and mechanical concentrations in the mere absence any chloride and bisulfide complexes as evident from the mineralogical studies, and lastly iii. placer PGE deposits along the central part of the Sukinda Valley following the course of the *Damsala nala*.

REFERENCES

Acharya S 1964. Stratigraphy of the banded iron formation of the Daitari-Tomka area, Cuttack district, Orissa, India. Proc Int Geol Cong 22nd Sess pt. X:12-21

Agiorgitis G, Wolf R 1978. Aspects of osmium, ruthenium and iridium contente in some Greek chromitite. Chem Geol 23: 267-272

Ahmed AH, Arai S 2002. Unexpectedly high-PGE chromitite from the deeper mantle section of the northern Oman ophiolite and its tectonic implications. Contrib Mineral Petrol 143: 263-278

Alapieti TT, Halkoaho TAA, Devaraju TC, Jayaraj KR 1994. Chromitite-hosted PGE mineralization in the Channagiri area, Karnataka State, India. VII. Int Plat Symp, 1-4 August 1994, Moscow (Abstract): 3-4

Amossé J, Dablé P, Allibert M, 2000. Thermochemical behaviour of Pt, Ir, Rh and Ru vs fO_2 and fS_2 in a basaltic melt. Implications for the differentiation and precipitation of these elements. Miner Petrol 68: 29-62

Arai S 1992. Chemistry of Chromium spinel in volcanic rocks as a potential guide to magma chemistry. Minerol Mag 56: 173-184

Arai S 1994. Characterization of spinel peridotites by olivine-spinel

Arndt NT 1983. Role of a thin, komatiite-rich oceanic crust in the Archean plate-tectonic process. *Geology*, 11: 372-375.

Augé T 1985. Platinum-group mineral inclusions in ophiolite chromitite from the Vourinos complex, Greece. Can Mineral 23: 163–171

Augé T 1987. Chromite deposits in the northern Oman ophiolite: mineralogical constraints. Min Deposit 22: 1–10

Augé T, Bailly L, Cocherie A, Genna A, Guerrot C, Lerouge C, Mukherjee MM, Patra RN 2002a. Magmatic and hydrothermal platinum-group-element mineralization in the Baula Area, Orissa, India. *In*: Boudreau A (ed) Proc 9th Int Platinum Symp July 2002, Billings, USA: 21–24.

Augé T, Cocherie A, Genna A, Armstrong R, Guerrot C, Mukherjee MM, Patra RN 2003. Age of the Baula PGE mineralization (Orissa, India) and its implications concerning the evolution of the Singhbhum Archaean nucleus. Precamb Res 121: 85–101

Augé T, Lerouge C 2004. Mineral-chemistry and stable-isotope constraints on the magmatism, hydrothermal alteration, and related PGE–(base-metal sulphide) mineralisation of the Mesoarchaean Baula-Nuasahi Complex, India. Mineral Depost 39: 583–607

Augé T, Maurizot P, Breton J, Eberle J-M, Gilles C, Jézéquel P, Mézière J, Robert M 1995. Magmatic and supergene platinum-group menarals in the New Caledonia ophiolite. Chron Rech Min 520: 3-26

Augé T, Salpeteur I, Bailly L, Mukherjee MM, Patra RN 2002b. Magmatic and hydrothermal platinum-group minerals and base-metal sulphides in the Baula Complex, India. Can Mineral 40: 277-309.

Augé T, Salpeteur I, Mukherjee MM, Patra RN 1999. Platinum-group element mineralisation in the breccia zone of the Baula Nuasahi Complex, Orissa, India. In: Stanley et al. (eds), Mineral Deposits: Processes to Processing, Balkema. Proc 5th Biennial SGA Meeting, London, August 1999: 701–704

Bacuta GC, Kay RW, Gibbs AK, Bruce RL 1990. Platinum-group element abundance and distribution in chromite deposits of the Acoje Block, Zambales ophiolite complex, Philippines. J Geoch Explor 37: 113–145

Bai WE, Zhou MF 1988. Variations in chemical compositions of chrome spinels from Hongguleleng ophiolites, Xianjing, China and their significance, Acta Mineral Sin 8: 313-323

Baidya TK, Mondal SK, Balaram V, Parthasarathy R, Verma R, Mathur PKK 1999. PGE-Ag-Au mineralization in a Cu-Fe-Ni sulphide-rich breccia zone of the Precambrian Nuasahi ultramafic mafic complex, Orissa, India. J Geol Soc Ind 54: 473–482

Balaram V 1995. Developments and trends in inductively coupled plasma mass spectrometry and its influence on the recent advances in trace element analysis. Curr Sci 69, 8: 640-648.

Balaram V 2001. ICP- MS: A powerful tool for geochemical and mineral exploration studies. Indian Miner 35, 1: 34-55.

Balaram V, Mathur R, Banakar VK, Hein JR, Rao CRM, Rao TG, Dasaram B 2006. Determination of platinum-group elements (PGE) and gold (Au) in

manganese nodule reference samples by nickel sulfide fire-assay and Te coprecipitation with ICP-MS. Indian J Marine Sc 35, 1: 7-16.

Balaram V, Ramesh SL, Anjaiah KV 1995. Comparative study of the sample decomposition procedures in the determination of trace and rare earth elements in anorthosites and related rocks by ICP-MS, Fresenius J Anal Chem 353: 176-182.

Balaram V, Rao TG 2003. Rapid determination of REEs and other trace elements in geological samples by microwave acid digestion and ICP-MS. Atom Spect 24, 6: 206-211.

Ballhaus CG 1998. PGE enrichment process in the Merensky reef. *In*: 8th Int Platinum Symp Abstracts, June 28- July 3: 25-28.

Ballhaus CG, Stumpfl EF 1986. Sulphide and platinum mineralization in the Merensky Reef: Evidence from hydrous silicates and fluid inclusions. Cont Miner Petrol 94: 193–204

Banerjee P K 1972. Geology and geochemistry of the Sukinda Ultramafic Field, Cuttack District, Orissa, Mem Geol Surv Ind 103: 1-171

Banerjee PK, Mahakud SP, Bhattacharyya AK, Mohanty AK (1987) On the northern margin of the Eastern Ghats in Orissa. Rec Geol Surv India 118: 1–8

Banerjee S 1960. Genesis of the chromite Oresof Jojuhat, Singhbhum district, Bihar, India With a Note on Their Mineragraphy. Proc Nat Inst Sci, India 26A, 1:31-40

Barefoot RR JCV Loon 1999.Recent advances in the determination of the platinum group elements and gold, Review article, Talanta 49: 1–14.

Barnes S-J 1990. The use of metal ratios in prospecting for platinum-group element deposits in mafic and ultramafic intrusions. J Geochem Explor 37: 91-99

Barnes SJ, Boyd R, Korneliussen A, Nillson LP, Often M, Pedersen RB, Robins B 1987. The use of mantle normalization and metal ratios in discriminating between the effects of partial melting, crystal fractionation and sulphide segregation on platinum-group elements, gold, nickel and copper: examples from Norway. *In*: Prichard HM, Potts PJ, Bowles JFW, Cribb SJ (eds) Geo-Platinum. Elsevier, Amsterdam: 113–143

Barnes SJ, Campbell IH 1988. Role of magmatic fluids in Merensky-type platinum deposits: a discussion. Geol 16: 481-491

Barnes S-J, Maier WD 2002. Platinum-group element distributions in the Rustenburg Layered Suite of the Bushveld Complex, South Africa. *In*: Cabri, L.J. (ed), Can Inst Min Metall Spec The Geology, Geochemistry, Mineralogy and Mineral Beneficiation of Platinum-group Elements 54: 431–458

Barnes S-J, Naldrett AJ 1985. Geochemistry of the J-M (Howland) Reef of the Stillwater Complex, Minneapolis Adit area. I. Sulfide chemistry and sulfide-olivine equilibrium. Econ Geol 80: 627-645

Barnes S-J, Naldrett AJ, Gorton MP 1985. The origin of the fractionation of platinum-group elements in terrestrial magmas. Chem Geol 53: 303–323

Barnes SJ, Roeder PL 2001. The range of spinel compositions in terrestrial mafic and ultramafic rocks. J Petrol 42: 2279-2302.

Barnes, S-J, Maier WD 1999. The fractionation of Ni, Cu and the noble metals in silicate and sulphide liquids. *In*: Keays, R.R., Lesher, C.M., Lightfoot, P.C., Farrow, C.E.G. (eds), Dynamic Processes in Magmatic Ore Deposits and Their Application to Mineral Exploration, Short Course Notes, Geol Assoc Can 13: 69–106

Bockrath C, Ballhaus C 2002. PGE fractionation during mantle melting. *www.crpg.cnrs-nancy.fr/NEWS/HSE-2002/HSE-PDF/bockrath.pdf*

Bockrath C, Ballhaus C, Holzheid A 2004. Fractionation of the Platinum-Group Elements During Mantle Melting. Sci 305: 1951-1953

Boudreau AE, Mathez EA, McCallum IS 1986. Halogen geochemistry of the Stillwater and Bushveld complexes: Evidence from hydrous silicates and fluid inclusions. J Petrol 27: 967– 986

Boudreau AE, McCallum IS 1986. Halogen geochemistry of the Stillwater and Bushveld complexes: evidence for transport of platinum-group elements by Cl-rich fluids, J Petrol 27: 967-986.

Boudreau AE, Meurer WP 1999. Concentration of platinum group elements by magmatic fluids in layered intrusions. Econ Geol 94: 1830–1848

Bow C, Wolfgram D, Turner A, Barnes S, Evans J, Zdepaki M, Boudreau A 1982 Investigations of the Howland reef of Stillwater complex, Minneapolis Adit area: Stratigraphy, structure, and mineralization, Econ Geol 77: 1481-1492.

Boyd FR and Nixon PH 1975. Origins of the ultramafic nodules from some kimberlites of northern Lesotho and the Monastery Mine. South Africa. Phys Chem Earth 9: 431-454

Brenker FE, Meibom A, Frei R, 2003. On the formation of peridotite-derived Os-rich PGE alloys. Ame Mineral 88: 1731–1740

Buchanan DL, Nolan J 1979. Solubility of sulfur and sulfide immiscibility in synthetic tholeiitic melts and their relevance to Bushveld Complex rocks. Can Miner 17: 483–494

Cameron EN 1977. Chromite in the central sector, eastern Bushveld Complex, South Africa. Am Mineral 62: 1082-1096

Cameron EN, Desborough GA 1969. Occurrence and characteristics of chromite deposits – eastern Bushveld Complex. Econ Geol Mon 4: 23-40

Campbell IH 1977. A study of micro-rhythmic layering and cumulate process in the Timberlana intrusion, Western Australia: I. The upper layered series, J Petrol 18: 183-215

Campbell IH, Naldrett AJ, Barnes S-J 1983. A model for the origin of the platinum-rich sulfide horizons in the Bushveld and Stillwater Complexes. Journal of Petrology, 24: 133-165

Carmichael ISE 1967. The iron-titanium oxides of salic volcanic rocks and their associated ferromagnesian silicates. Contri Miner Petrol 14: 36-64

Cawthorn RG 1999a. The platinum and palladium resources of the Bushveld Complex. S Afr J Sci 95: 481–489

Cawthorn RG 1999b. Platinum-group element mineralization in the Bushveld Complex – a critical reassessment of geochemical models. S Afr J Geol 102: 268-281

Cawthorn RG 2002. Magma mixing models for Merensky-style mineralization: The fallacy of binary diagrams. Econ Geol 97: 663-665

Cawthorn, R.G. 2005.Contrasting sulphide contents of the Bushveld and Sudbury Igneous Complexes. Mineralium Deposita 40: 231-235.

Chakraborty KL 1958. Chromite ores associated with the ultrabasic rocks of Nausahi, Keonjhar district, Orissa, India. Proc Nat Inst Sci, India 24A: 78-88

Chakraborty KL 1972. Some primary structures in the chromitite of Orissa, India, Mineral Depost 7:280-284

Chakraborty KL 1973. Some characters of the beded chromitite deposits of Kalarangi, Cuttack District, Orissa, India, Mineral Depost 8: 78-80

Chakraborty KL Chakroborty TL 1984. Geological Features and Origin of the Chromite Deposits of Sukinda Valley, Orissa, India. Mineralium Deposita, Vol. 19, pp. 256-265.

Chakraborty KL, Chakraborty TL, Majumder T 1980. Stratigraphy and Structure of the Precambrian Banded Iron Formation and Chromite bearing Ultramafic Rocks of Sukinda Valley, Orissa. J Geol Sur Ind 21: 398-404.

Chakraborty KL, Majumder T 1976. Stratigraphy and structure of the Precambrian rocks of Sukinda Valley, Orissa. Golden Jub Symp on 'Precambrian stratigraphy, tectonics and associated mineral deposits of India'. 12-13 Nov 1976, Dept App Geol, ISM Dhanbad

Chakraborty S, Mukherjee S 1971. Geology and mineralogy of chromite deposits occurring near Kondapalli, Krishna District, A.P. J Geol Soc India 12: 383-387

Chatterjee PK, Banerjee PK 1964. The early kinematic chromite deposit of Orissa, India and their bearing on the classification of the chromite deposits. Proc Int Geol Cong 22nd Sess V: 76-86

Constantinides CC, Kingston GA, Fisher PC 1979. The occurrence of platinum group minerals in the chromitites of the Kokkinorotsos chrome mine. *In*: Proc Int Ophiolite Symp, Panayiotou A (ed), Geol Sur Dept, Cyprus: 93-101

Crocket JH 1981. Geochemistry of the Platinum-group elements. *In:* Cabri L (ed) Platinum Elements: Mineralogy, Geology, Recovery, CIM Spec 23: 47-63

Das SK, Mohanty JK, Sahoo RK, Paul AK, Mukherji S 1995. Ore mineralization in the mafic-ultramafic plutons of southern and eastern parts of the Singhbhum granitic platform. VISTAS in Geol Research, Prof. S. Acharya Felicitation Vol U. U. Spec Pub in Geol-1: 65-83.

Dasgupta S 1959. Chromite Deposits near Sukinda, Cuttack District, Orissa. Quat J Geol Min Metall Soc Ind 31: 227-232

Davies G, Tredoux M 1985. The platinum-group element and gold contents of the marginal rocks and sills of the Bushveld Complex. Econ Geol 80: 838-848

Deb M 2000. Crustal evolution and metallogeny in the northwestern Indian Sheild. 515pp.

Deb S, Chakraborty KL 1962. Origin chromite deposits associated with the ultrabasic rocks of eastern part of the Indian Peninsula. Proc Nat Inst Sci, India 27A: 503-519

Deekshitulu MN 1955. On the emplacement of chromite in quartzite near Ghotringa, Dhenkanal District, Orissa. Proc Ind Sci Cong 42nd Sess, pt.3 (Abst): 204p

Devaraju TC, Alapieti TT, Halkoaho TAA, Jayaraj KR Khanadali KD 1994. Evidence of PGE mineralization in the Channagiri mafic complex, Shimoga District, Karnataka, J Geol Soc India 43: 317-318

Devaraju TC, Alapieti TT, Kaukonen RJ 2005. SEM-EDS study of Platinum Group Minerals in the PGE Mineralized Hanumalapura Segment of Layered Mafic-Ultramafic Complex of Channagiri, Davangere District, Karnataka. J Geol Soc Ind, 65: 745-752

Dick HJB, Bullen T 1984. Chromian spinel as a petrogenetic indicator in abyssal and alpine-type peridotites and spatially associated lavas. Contri Miner Petrol 86: 54-76

Distler VV, Mitrofanov GL, Nemerov VK, Kovalenker VA, Mokhov AV, Semeikina LK, Yudovskaya MA 1998. The platinum mineralization of the gold deposit Sukhoi Log, Russia. *In*: Laverov NP, Distler VV (eds), International Platinum. Theophrastus Publications, St. Petersburg–Athens, Russia: 178–194

Dunn JA 1940. Stratigraphy of South Singhbhum. Geol Surv Ind Mem 59 pt.3: 303-369

Eales HV 2000. Implications of the chromium budget of the Western Limb of the Bushveld Complex. *S A J G* 103: 141-150

Economou-Eliopoulos M 1996. Platinum-group element distribution in chromite ores from ophiolite complexes: implications for their exploration. Ore Geol Rev 11: 363-381

Economou-Eliopoulos M, Vacondios I 1995. Geochemistry of chromitites and host rocks from the Pindos ophiolite complex, northwestern Greece. Chem Geol 122: 99-108

Enzweiler J, Potts PJ, Jarvis KE 1995. Determination of platinum, palladium, ruthenium and iridium in geological samples by isotope dilution inductively coupled plasma mass spectrometry using a sodium peroxide fusion and tellurium coprecipitation, Analyst 120:1391-1396

Fabriès J 1979. Spinel-olivine geothermometry in peridotites from ultramafic complex. Contributions to Mineralogy and Petrology 69: 329–336.

Frey FA 1969. Rare earth abundances in a high-temperature peridotite intrusion. Geochim Cosmochim Acta 33: 1429-1447

Fuchs WA, Rose AW 1974. *The geochemical behavior of platinum and palladium in the weathering cycle in the Stillwater complex, Montana*, Econ Geol 69: 332-346.

Gammons CH, Bloom MS 1993. Experimental investuigations of the hydrothermal geochemistry of Pt and Pd. II. The solubility of PtS and PdS in aqueous sulfide solutions at 300°C. Geochim Cosmochim Acta 57: 2451-2467

Gammons CH, Bloom MS, Yu Y 1992. Experimental investigations of the hydrothermal geochemistry of Pt and Pd. I. Solubility of Pt and Pd sulfide minerals in NaCl/HCl solution at 300^0C, Geochim Cosmochim Acta 56: 3881-3894.

Gros M, Lorand J-P, Luguet A 2002. Analysis of platinum group elements and gold in geological materials using NiS fire assay and Te coprecipitation; the NiS dissolution step revisited; Chem Geol 185: 179-190.

Gunn AG 1989. Drainage and overburden geochemistry in exploration of platinum-group-element in the Unst ophiolite, Shetland, UK. J Geochem Explor 31: 209-236

Gupta RP 2003. Remote Sensing Geology. 2nd edn., Springer-Verlag, Heidelberg.

Haughton DR, Roeder PL, Skinner BJ 1974. The solubility of sulfur in mafic magmas. Econ Geol 69: 451–462

Henderson P 1989. Rare earth element geochemistry. 1st edn, Elsevier 510p.

Hervig RL, Smith JV, Steele IM, Dawson JB 1980. Fertile and barren A1-Cr-spinel harzburgites the upper mantle: ion and electron probe analyses of trace elements in olivine and orthopyroxene: relation to lherzolites. Earth Planet Sci Lett 50: 41-58

Hulbert LJ, Gregoire CD, Paktunc D 1992. Sedimentary nickel, zinc, and platinum-group-element mineralization in Devonian black shales at the Nick property, Yukon, Canada: A new deposit type. Expl Min Geol 1: 39–62

Irvine TN 1965. Chromian spinel as a petrogenetic indicator; Part 1, Theory. Can J Earth Sci 2: 648-671

Irvine TN 1974. Petrology of the Duke Island Ultramafic Complex, Southeastern Alaska. Geol Soc Am Mem 138 : 240

Irvine TN 1975. Crystallization sequences in the Muskox intrusion and other layered intrusions-II. Origin of chromitite layers and similar deposits of other magmatic ores. Geochim Cosmochim Acta 39: 991–1020

Irvine TN 1977. Origin of chromitite layers in the Muskox intrusion and other stratiform intrusions: a new interpretation. Geol 5: 273-277

Irvine TN, Keith DW, Todd SG 1983. The J-M platinum-palladium Reef of the Stillwater Complex, Montana: II. Origin by double diffusive convective magma mixing and implications for the Bushveld Complex. Econ Geol 78: 1287-1334

Jarvis I, Gray AL, Houk RS 1992. Handbook of Inductively Coupled Plasma Mass Spectrometry. Blackie and Son, Glasgow

Johan, Z., Bel, L., Robert, J.L., Volfinger, M., 1982. Role of reducing fluid in the origin of chromite deposits from ophiolitic complexes. Geological Association of Canada/ Mineralogical Association of Canada program with Abstracts 7, 58.

Keays RR, Lightfoot PC 2000. Exploration for platinum-group of element (PGE) deposits in mafic and ultramafic rocks. *In:* 9th Int Plat Symp Abst, June 28-July 3, 2000.

Kinloch ED, Peyerl W 1990: Platinum-group minerals in various rock types of the Merensky Reef: genetic implications, Econ Geol 85: 537-555.

Kinnaird JA, Kruger FJ, Nex PAM, Cawthorn RG 2002. Chromitites of the Bushveld Complex –Processes of formation and PGE enrichment. Econ Geol Resear Inst, Univ Witwatersrand, Inform Cir 369: 28p

Konstantopoulou UG, Economou M 1991. Distribution of platinum-group elements and gold within the Vourinos chromite ores, Greece. Econ Geol 86: 672-1682

Kruger FJ, Marsh J 1982. Significance of $^{87}Sr/^{86}Sr$ ratios in the Merensky cyclic unit of the Bushveld Complex. Nature 298: 53-55

Kucha H 1982. Platinum-group metals in the Zechstein copper deposits, Poland Econ Geol 77: 1578-1594.

Leblanc M 1991. Platinum-group elements and gold in ophiolite genesis and evolution of the oceanic lithosphere ophiolitic complexes: Distribution and fractionation from mantle to oceanic floor. *In*: Peters TJ, Nicolas A, Coleman RG (eds) Ophiolite genesis and evolution of the oceanic lithosphere (Dordrecht: Kluwer) 231–260

Lee YI 1999. Geotectonic significance of detrital chromium spinel: a review. GeoSci J 3: 23-29

Leelanandam C 1997. The Kondapalli Layered Complex, Andhra Pradesh, India : A Synoptic Overview. Gond Resear, V.1, 1: 95-114

Lehmann J 1983. Diffusion between olivine and spinel: application to geothermometry. Earth Planet Sci Lett 64:123-138

Lesher CM, Campbell IH 1993. Geochemical and fluid-dynamic modelling of compositional variations in Archean komatiite-hosted nickel sulfide ores in Western Australia. Econ Geol 88: 804–816

Li C, Naldrett AJ 1993. Sulfide capacity of magma: A quantitative model and its application to the formation of the sulfide ores at Sudbury. Econ Geol 88: 1253-1260

Maier WD 2005. Platinum-group element (PGE) deposits and occurrences: Mineralization styles, genetic concepts, and exploration criteria. Geol Soc Afri Presidential Rev 9, J Afri Earth Sci 41, 9: 165-191

Maier WD, Barnes S-J 1999. Platinum-group elements in silicate rocks of the Lower, Critical and Main Zones at Union section, western Bushveld Complex. J Petrol 40: 1647-1671

Malich, K.N., and I.Y. Badanina (1998): Natural Polycomponent Solid Solutions of the System Ru–Os–Ir–Pt–Fe and Their Genetic and Applied Significance; Doklady Earth Sciences, Interperiodica; v. 363; no. 8; p. 1089-1092.

Malitch KN, Badanina IY 1998. Natural Polycomponent Solid Solutions of the System Ru–Os–Ir–Pt–Fe and Their Genetic and Applied Significance; Doklady Earth Sciences, Interperiodica 363, 8: 1089-1092

Malitch KN, Thalhammer OAR, Knauf VV, Melcher F 2003. Diversity of platinum-group mineral assemblages in banded and podiform chromitite from the Kraubath ultramafic massif, Austria: Evidence for an ophiolitic transition zone? Mineral Depos 38: 282–297

Mathez EA 1995. Magmatic metasomatism and formation of the Merensky Reef, Bushveld Complex. Cont Miner Petrol 119: 277– 286

Mathez EA, Agriner P, Hutchinson R 1994. Hydrogen isotope composition of the Merensky reef and related rocks, Atok section, Bushveld complex, Econ Geol 89: 791-802

Mathur R, Balaram V, Rao CRM, Rao TG, Ramesh SL, Charan SN, Dasaram B, Anjaiah KV, Rajashekhar VB 2003. Fire-assay methods in combination with ICP-MS for determination of PGE and Au in geological materials. In: National training course on "Inductively coupled plasma mass spectrometry and associated analytical techniques for geochemical, mineral exploration and environmental studies & Workshop VI- "Trends in Geochemistry", NGRI, India: 81-94.

Maurel C 1984. Etude expdrimentale de l'rquilibre spinelle chromifére liquide silicat6 basique. SFMC Meet. "Les spinelles", Lille.

Maurel C, Maurel P 1982. Etude exprrimentale de la distribution de l'aluminium entre bain silicat6 basique et spinelle chromifrre. Implications prtrogrnrtiques: teneur en chrome des spinelles. Bull Minrral 105:197-202

Mavrogenes JA, O'Neill HC 1999. The relative effects of pressure, temperature and oxygen fugacity on the solubility of sulfide in mafic magmas. Geochim Cosmo 63: 1173-1180

McCallum ME, Loucks RR, Carlson RR, Cooley EF, Doerge TA, 1976. Platinum metals associated with hydrothermal Cu ores of the New Rambler Mine, Medicine Bow Mountains, Wyoming. Econ Geol 71: 1429–1450

McDonald D 1960. A History of Platinum. Johnson Matthey and Co Ltd, London. 254p

McDonald I, Vaughan DJ, Tredoux M 1995. Platinum mineralization in quartz veins near Naboomspruit, central Transvaal. S Afr J Geol 98: 168–175

McDonough WF, Sun S-s 1995. The composition of the Earth. Chem Geol 120: 223-253

Melcher F 2000. Base metal - platinum-group element sulfides from the Urals and the eastern Alps: Characterization and significance for mineral systematics. Miner Petrol 68: 177-211

Menzies M 1976. rare earth geochemistry of fused ophiolitic and alpine lherzolites, I. Othris, Lanzoand Troodos. Geochim Cosmochim Acta 40: 645-656

Misra KC 1998. Platinum-Group Element (PGE) Deposits. *In*: Understanding Mineral Deposits, 1st ed, Kluwer Acad Pub: 845p

Mitra S 1962. Iron Ore deposits of Daitari Range, Cuttack District, Orissa. Quart J Geol Min Met Soc Ind 34: 27-32

Mitra S 1973. Olivines from Sukinda ultramafites and the nature of the parental magma. N J Min Mh 2: 177-189

Mitra S, Bidyananda M 2003. Evaluation of metallogenic potential of the Nuggihalli greenstone belt, south India. Geomaterials, Comptes Rendus Geosci, 335: 185–192

Mitra, S., and M. Bidyananda (2003): Evaluation of metallogenic potential of the Nuggihalli greenstone belt, south India; Geomaterials, Comptes Rendus Geoscience, Elsevier; v. 335; p. 185–192.

Mogessie A, Stumpfl EF, Weiblen PW 1991. The role of fluids in the formation of platinum-group minerals, Duluth complex, Minnesota: mineralogic, textural, and chemical evidence, Econ Geol 86: 1506-1518

Mohanty JK, Sahoo RK 1995. Mineralogical and chemical characteristics of chromite from Boula-Nausahi igneous complex, Orissa. VISTAS in

Geological Research. Prof. S. Acharaya felicitation Volume, U.U. Spl Publ Geol 1: 50-64

Mondal SK, Baidya TK 1997. Platinum-group minerals from the Nuasahi ultramafic-mafic complex, Orissa, India. Mineral Mag 61: 902–906

Mondal SK, Baidya TK, Rao KNG, Glascock MD 2001. PGE and Ag mineralization in a breccia zone of the Precambrian Nuasahi ultrama.c-ma.c complex, Orissa, India. Can Mineral 39:979–996

Mondal SK, Ripley EM, Li C, Frei R 2006. The genesis of Archaean chromitites from the Nuasahi and Sukinda massifs in the Singhbhum Craton, India. Precamb Resear 148: 45-66

Mukherjee MM (1998) Platinum Group Elements. In: Acharya S, Mahalik NK, Mohapatra S (eds) 2nd edn Geology and Mineral Resources of Orissa. Soc Geoscientists Allied Technologists, Bhubaneswar: 339-346

Mukherjee S 1962. Geology, mineralogy and geochemistry of the chromite deposits of Nausahi, Keonjhar District, Orissa, India. Quart J Geol Min Met Soc India 34, 1: 29-45

Mukherjee S, Haldar D, 1975. Sedimentary structures displayed by the ultramafic rocks of Nuasahi, Keonjhar district, Orissa, India. Miner Dep 10: 109-119

Murck BW, Campbell IH 1986. The effect of temperature, oxygen fugacity and melt composition on the behaviour of chromium in basic and ultrabasic melts. Geoch et Cosmo Acta 50: 1871–1887

Naldrett AJ 1981. Platinum-group element deposits. *In*: Cabri LJ (ed) Platinum-group Elements: Mineralogy, Geology, Recovery. Can Inst Min Metall Spec 23: 197–232

Naldrett AJ 1989. Magmatic sulphide deposits. Oxford Monogr Geol Geophy 14: 186p

Naldrett AJ, von Gruenewaldt G 1988. The upper Critical Zone Bushveld Complex and the origin of Merensky-type ores – a reply. Econ Geol 83: 1085-1091

Naldrett AJ, von Gruenewaldt G 1989. Association of platinum-group elements with chromitite in layered intrusions and ophiolite complexes. Econ Geol 84: 180-187

Naldrett, AJ, Duke JM 1980. *Platinum metals in magmatic sulfide ores*, Science, 208: 1417-1428.

Nanda JK, Patra RN, Mishra R 1996. Petrogenetic history of the platiniferous magmatic breccia zone in Baula Igneous Complex: a conceptual model for PGM localisation. *In*: Proc Worksh Geology and Exploration of Platinum Group, Rare Metal and Rare Earth Elements, April 1996, Calcutta, Geol Sur Ind:17–19

Narayanswamy S 1966. tectonic problems of the Precambrian rocks of Penninsular India. Symp Tectonics Bull Nat Inst Sci Ind 32: 77-94

Oshin IO, Crocket JH 1982. Noble metals in Thetford Mines ophiolites, Quebec, Canada, Part I: distribution of gold, iridium, platinum, and palladium in the ultramafic and gabbroic rocks. Econ Geol 77: 1556

Page NJ, Banerji PK, Hafety J 1985. Characterization of the Sukinda and Nausahi ultramafic complexes, Orissa, India by Platinum-Group element geochemistry. Precamb Res 30: 27-41

Page NJ, Cassard D, Haffty J 1982a. Palladium, platinum, rhodium, ruthenium, and iridium in chromitites from the Massif du Sud and Tiebaghi massif, New Caledonia. Econ Geol 77: 1571–1577

Page NJ, Engin T, Singer DA, Haffty J 1984. Distribution of platinum-group elements in the Bati Kel chromite deposits, Guleman-Elazig area, Eastern Turkey. Econ Geol 79: 177–184

Page NJ, Pallister JS, Brown MA, Smewing JD, Haffty J 1982b. Palladium, platinum, rhodium, ruthenium, and iridium in chromite-rich rocks from the Samail ophiolite, Oman. Can Mineral 20: 537–548

Pal T, Mitra S 2004. P–T–fO_2 controls on a partly inverse chromite bearing ultramafic intrusive: an evaluation from the Sukinda Massif, India. J Asian Earth Sci 22: 483-493.

Pan P, Wood SA 1994. Solubility of Pt and Pd sulfide and Au metal in aqueous bisulfide solutions. II. Results at 200°C to 350°C and saturated vapour pressure. Mineral deposita 29: 373-390

Pasava J 1993. Anoxic sediments–an important environment for PGE: An overview. Ore Geol Rev 8: 425–445

Patra RN, Mukherjee MM 1996. Exploration for PGE in Baula-Nuasahi-Bangur ultrama.c complex, Keonjhar District, Orissa. *In*: Workshop on Geology and

Exploration of Platinum Group, Rare Metal and Rare Earth Elements, Calcutta. Geol Sur Ind: 7–9

Peach CL, Mathez EA 1996. Constraints on the formation of platinum-group element deposits in igneous rocks. Econ Geol 91: 439-450

Peach CL, Mathez EA, Keays RR, Reeves SJ 1994. Experimentally determined sulfide melt-silicate melt partitioning coefficient for iridium and palladium. Chem Geol 117: 361-377.

Peck DC, Keays RR 1990. Geology, geochemistry and origin of platinum-group element chromitite occurrences in the Haezlewood River Complex, Tasmania. Econ Geol 85: 765–793

Pedersen T, Johannesen GM, Boyd R 1993 Stratiform platinum-group element mineralization in the ultramafic cumulates of the Leka ophiolite complex, central Norway. Econ Geol 88: 782-803

Perignon NV-, Amossé J, Radelli L, Keller F, Leyva TC 2000. Platinum group element behaviour and thermochemical constraints in the ultrabasic–basic complex of the Vizcaino peninsula, Baja California Sur, Mexico. Lithos, 53: 59-80.

Philpotts AR 1994. Principles of igneous and metamorphic petrology. Prentice-Hall: 498p.

Pober E, Faupl P 1988. The chemistry of detrital chromian spinels and its implications for the geodynamic evolution of the Eastern Alps. Geologische Rundschau 77: 641-670

Potts P J 1987: A Handbook of Silicate Rock Analysis, Blackie, 1st edn: 622p

Prasad Rao GHSV, Murty JGK, Deekhsitulu MN 1964. Stratigraphic relationship of Precambrian iron formation and associated sedimentary sequence in part of Keonjhar, Dhenkanal and Sundargarh Districts of Orissa, India. Proc Int Geol Cong 22nd Sess pt.X: 72-87

Prichard HM, Lord RA 1990. Platinum and palladium in the Troodos ophiolite complex, Cyprus. Can Mineral 28: 607-617

Prichard HM, Potts PJ, Neary CR (1981) Platinum group element minerals in Unst chromite, Shetland Isles. Trans Inst Min Metall 90: B186-B188

Prichard HM, Potts PJ, Neary CR 1981. Platinum group element minerals in Unst chromite, Shetland Isles. Trans Inst Min Metall 90: B186-B188

Rao NVC, Ram M, Sutaone AT, Gundewar CS 2006. Gold in chromite ore of South Kaliapani Mines, Sukinda Ultramafic Belt, Jajpur District, Orissa. J Geol Soc Ind 68: 171-175

Rao P. 1950. Report on Systematic Mapping in Cuttack District, Orissa. Geol. Surv. Ind. (F.S. 1949-50).

Ripley EM 1999. Systematics of sulphur and oxygen isotopes in mafic igneous rocks and related Cu-Ni-PGE mineralization. *In*: Keays RR, Lesher CM, Lightfoot PC, Farrow CEG (eds), Dynamic Processes in Magmatic Ore Deposits and their Application to Mineral Exploration: Geol Asso Can, Short Course Notes 13: 133-158

Rollinson H 1993. Using geochemical data: evaluation, presentation, interpretation. 1st edn, Longman Scientific & Technical: 352p.

Ross JR, Keays RR 1979. Precious metals in volcanic-type nickel sulfide deposits in Western Australia. Part I: Relationship with composition of the ores and their host rocks. Can Mineral 17: 417-436.

Rowell WF, Edgar AD 1986. Platinum-group element mineralization in a hydrothermal Cu–Ni sulphide occurrence, Rathbun Lake, northeastern Ontario. Econ Geol 81: 1272–1277

Saha AK, Sankaran AB, Bhattacharya TK 1973. Geochemistry of newer dolerite suite of intrusion within the Singhbhum granite-Preliminary study. J Geol Soc Ind 14: 329-346

Sahoo RK, Kaaden GV 1976. Chemistry of the Sukinda Chromites, Orissa, India and its Petrogenetic significance. N Jb Miner Mh 11: 484-494

Sahu BK, Bagchi TC 1959. Chromite deposits of Saruabil area, District Cuttack, Orissa. East Met Rev 12, 29: 781-793

Sampson E 1932. Magmatic chromitite deposits in Southern Africa. Econ Geol 27: 113-144

Sarkar NK, Panigrahi D, Ghosh SN, Mallik AK, Shome S 2003. A note on the incidence of gold-PGM in the breccia zone of Katpal chromite quarry, Sukinda ultramafic Complex, Dhenkanal District, Orissa. Ind Min 57: 85-92

Sarkar SC 2002. Carbonate hosted lead-zinc deposits of Rajasthan, India, in the context of the world scenario. In: Deb M, Goodfellow WD (eds), Sediment-

hosted lead-zinc sulfide deposits in the northwestern Indian Sheild, Deposit Modelling Program, Delhi-Udaipur, Dec 10th -17th 2001, Proc: 189-195

Sarkar SN, Saha AK, Miller JA 1969. Geochronology of the Precambrian rocks of Singhbhum and adjacent regions, Eastern India. Geol Mag 106: 13-45.

Sen AK, Mohanty D 2004. Techniques for quantitative determination of Platinum Group of Elements: A Review, In: Proc Int Sem "Mineral Business Development", Nagpur, India, Org Indian Bureau of Mines, 16th–17th January 2004: 59.

Sen AK, Mohanty D 2005. PGE Mineralization Associated with Sukinda Chromite Deposit, Orissa, India - An Ore Genetic Model. In: 10th Int Platinum Symp Platinum-Group Elements - from Genesis to Beneficiation and Environmental Impact, Finland, August 2005: 566-569

Sen AK, Sharma PK, Mohanty D, Ghosh TK 2005. Composition of Cr-Spinel – An Ore Genetic Indicator of Kathpal Chromite Deposit, Sukinda Ultramafic Complex, Orissa, India. Curr Sci 88,10: 1547-1550

Sharpe MR 1982. Nobel metals in the marginal rocks of the Bushveld complex, Econ Geol 77: 1286-1295

Shima H, Naldrett AJ 1975. Solubility of sulfur in an ultramafic melt and the relevance of the system Fe–S–O. Econ Geol 70: 960–967

Singh KK 1971. Tectonic setting and emplacement of the ultramafic rocks of Jojuhta, Singhbhum, Bihar. J Inst Geol, Vikram Univ: 8

Srinivasachari K (1984) Correlation of Chromite Lodes in Sukinda-Nausahi Ultramafic Belt, Orissa. Ind Min: 26-33.

Srinivasachari, K. 1979. Stratiform Chromite Deposits of Sukinda-Nausahi Ultramafic Belt, Orissa, India. GSI. Misc. Pub. No. 34, Part II, pp. 151-160.

Stevens RE 1944. Composition of some chromites of the western hemisphere. Am Mineral 29:1-34

Stone WE, Crocket JH, Fleet ME 1993. Sulfide-poor platinum-group mineralization in komatiitic systems: Boston Creek Flow, Late basaltic komatiite, Abitibi belt, Ontario. Econ Geol 88: 817-836

Storey M, Mahoney JJ, Kroenke LW, Saunders AD 1991. Are oceanic plateaus sites of komatiite formation? *Geology,* 19: 376-379.

Subramanium AP 1956. Mineralogy and Petrology of Sittampundi Complex, Salem district, Madras State, India. Bull Geol Soc Am 67: 317-390

Suen CJ, Frey FA, Malpas J 1979. Bay of Islands Ophiolite Suite, Newfoundland: petrologic and geochemical characteristics with emphasis on rare earth element geochemistry. Earth Planet Sci Lett 45:337-348

Sun S-s, McDonough WF 1989. Chemical and isotopic systematics of oceanic basalts: implications for mantle composition and processes. In: 4. Saunders D, Norry MJ eds. Magmatism in the Ocean Basins. Geol Soc Lond 3: 13-345

Takahashi E 1990. Speculations on the Archean mantle: missing link between komatiite and depleted garnet peridotite. J Geophys Res 95:15,941-15,954.

Talkington RW, Watkinson DH 1986. Whole rock Platinum-group elemwnt trends in chromite-rich rocks in ophiolitic and stratiform igneous copmplexes. *In*: Metallogeny of basic and ultrabasic rocks, Gallaher MJ, Ixer RA, Neary CR, Prichard HM (eds) London. Inst Mining Metall: 427-440.

Talkington RW, Watkinson DH, Whittaker PJ, Jones PC 1984. Platinum group minerals and other solid inclusions in chromite of ophiolite complexes: occurrence and petrological significance. Tschermaks Mineral Petrol Mitteilungen, 32: 285-301

Thiagarajan TA, Thothathiri G, Rao MS, Ramachandrarao MN 1989. A report on the investigation for PGM in the Nuasahi chromite belt, Orissa and Sindhuvalli-Talur ultramafic belt, Karnataka. Bangalore, GSI/AMSE Open File Rep

Todd SG, Keith DW, Schissel DJ, Leroy LL, Mann EL, Irvine TN 1982: the J-M platinum-palladium reef of the Stillwater complex, Montana: I. Stratigraphy and petrology, Econ Geol 77: 1454-1480.

Tucker CJ 1979. Red and Photographic Infrared Linear Combinations for Monitoring Vegetation. Rem Sen Envir 8, 2: 127-150

Varma OP 1953. Geology of the Chromite Deposits of Nausahi Area, Koeonjhar District, Orissa. Econ Geol 50: 799-825

Varma OP 1964. Chromite deposits of Keonjhar District, Orissa, India. Econ Geol 59: 799-825

Varma OP 1965. Periods of crystallization and alteration of chromite from Keonjhar, Orissa. Proc Min Geol Met Inst, India 62: 67-79

Vermaak CF 1976. The Merensky Reef–thoughts on its environment and genesis. Econ Geol 71: 1270-1298

Vlassopoulos D, Wood SA 1990. Gold speciation in natural waters. I. Solubility and hydrolysis reactions of gold in aqueous solution. Geochim Cosmochim Acta 54: 3-12

Volborth AM, Tarkian M, Stumpfl, Housley RM 1986. A survey of the Pd-Pt mineralization along the 35-km strike of the J-M reef, Stillwater complex, Montana, Can Mineral 24: 329-346.

Von Grunewaldt G 1979. A review of some recent concepts of the Bushveld Complex with particular reference to the sulfide mineralization. Can Min 17: 235-256

Wager LR, Brown GM 1968. *Layered igneous rocks*. Oliver and Boyd, Edinburgh: 588p

Watkinson DH, Lavigne MJ, Fox PE 2002. Magmatic-hydrothermal Cu- and Pd-rich deposits in gabbroic rocks from North America. *In*: Cabri, L.J. (ed), Can Inst Min Metall, Spec. The Geology, Geochemistry, Mineralogy and Mineral Beneficiation of Platinum-group Elements 54: 299–319

Wendlandt RF 1982. Sulfur saturation of basalt and andesite melts at high pressures and temperatures. Am Min 67: 877–885

White WM 2000. Trace elements in Igneous Process. www.geo.cornwell.edu/geology/classes/chapter/chapterof.pdf

Willmore CC, Boudreau AE, Kruger FJ 2000. The halogen geochemistry of he Bushveld Complex, Republic of South Africa: Implications for chalcophile element distribution in the Lower and Critical Zones. J Petrol 41: 1517–1539

Wood SA, Sampson IM 1998. Solubility of ore minerals and complexation of ore metals in hydrothermal solutions. Rev Econ Geol 10: 33-80.